UNIVERSITE LOUIS PASTEUR DE STRASBOURG I
ECOLE DOCTORALE SCIENCES DE LA VIE ET DE LA SANTE

THESE

pour obtenir le grade de

DOCTEUR DE L'UNIVERSITE LOUIS PASTEUR DE STRASBOURG

Discipline : Sciences du Vivant
Spécialité : Aspects moléculaires et cellulaires de la biologie

Soutenue le 12 septembre 2005 et présentée par

Anne ANSTETT

APPROACH OF COMBINED CANCER GENE THERAPY AND RADIATION: RESPONSE OF PROMOTERS TO IONIZING RADIATION

devant le jury composé de :

Pr. Kurt BALLMER-HOFER	Rapporteur
Dr. Pierre BISCHOFF	Rapporteur
Pr. Josef JIRICNY	Examinateur
Pr. Jean-Pierre CAZENAVE	Directeur de thèse

UNIVERSITE LOUIS PASTEUR DE STRASBOURG I
ECOLE DOCTORALE SCIENCES DE LA VIE ET DE LA SANTE

THESE

pour obtenir le grade de

DOCTEUR DE L'UNIVERSITE LOUIS PASTEUR DE STRASBOURG

Discipline : Sciences du Vivant
Spécialité : Aspects moléculaires et cellulaires de la biologie

Soutenue le 12 septembre 2005 et présentée par

Anne ANSTETT

APPROCHE DE THERAPIE GENIQUE ANTI-CANCEREUSE COMBINEE A L'IRRADIATION : ETUDE DE LA REPONSE DE PROMOTEURS AUX RADIATIONS IONISANTES

devant le jury composé de :

Pr. Kurt BALLMER-HOFER	Rapporteur
Dr. Pierre BISCHOFF	Rapporteur
Pr. Josef JIRICNY	Examinateur
Pr. Jean-Pierre CAZENAVE	Directeur de thèse

TABLE OF CONTENTS

SUMMARY

Gene therapy is an emerging cancer treatment modality. We are interested in developing a radiation-inducible gene therapy system to sensitize the tumor vasculature to the effects of ionizing radiation (IR) treatment. An expression system based on irradiation-inducible promoters will drive the expression of anti-tumor genes in the tumor vasculature. Solid tumors are dependent on angiogenesis, a process in which new blood vessels are formed from the pre-existing vasculature. Vascular endothelial cells are untransformed and genetically stable, thus avoiding the problem of resistance to the treatments. Vascular endothelial cells may therefore represent a suitable target for this therapeutic gene therapy strategy.

The identification of IR-inducible promoters native to endothelial cells was performed by gene expression profiling using cDNA microarray technology. We describe the genes modified by clinically relevant doses of IR. The extension to high doses aimed at studying the effects of total radiation delivery to the tumor. The radio-inducibility of the genes selected for promoter study was confirmed by RT-PCR. Analysis of the activity of promoters in response to IR was also assessed in a reporter plasmid. We found that authentic promoters cloned onto a plasmid are not suitable for cancer gene therapy due to their low induction after IR. In contrast, synthetic promoters containing repeated sequence-specific binding sites for IR-activated transcription factors such as NF-κB are potential candidates for gene therapy. The activity of five tandemly repeated TGGGGACTTTCCGC elements for NF-κB binding in a luciferase reporter was increased in a dose-dependent manner. Interestingly, the response to fractionated low doses was improved in comparison to the total single dose. Thus, we put present evidence that a synthetic promoter for NF-κB specific binding may have application in the radio-therapeutic treatment of cancer.

Keywords: gene therapy, cancer, ionizing radiation, endothelial cells, native promoters, synthetic promoters, transcription factor, NF-κB

RÉSUMÉ

La thérapie génique est un moyen de traitement du cancer en voie de développement. Cette étude s'intéresse au développement d'un système de thérapie génique induit par les radiations ionisantes (RI) dans le but de radiosensibiliser les cellules vasculaires. Un système d'expression basé sur l'utilisation de promoteurs induits par les irradiations va permettre l'expression de gènes anti-tumoraux dans le réseau vasculaire tumoral. Le développement des tumeurs solides est dépendant de l'angiogénèse, un processus dans lequel de nouveaux vaisseaux sanguins sont générés à partir d'une vascularisation pré-existante. Les cellules endothéliales vasculaires ne sont pas transformées et sont génétiquement stables, ainsi évitant le problème de résistance aux traitements. Pour ces raisons, les cellules endothéliales représentent une cible efficace pour l'introduction de tels vecteurs géniques thérapeutiques.
L'identification de promoteurs induits par les RI, endogènes aux cellules endothéliales, a été menée suite à une étude des profils d'expression utilisant la technologie des puces à ADN. Les gènes modulés par des doses de RI, utilisées en clinique, ont été décrits. L'utilisation de fortes doses de RI a pour but d'étudier l'effet d'une dose totale d'irradiation délivrée dans les tumeurs. La radio-induction de gènes sélectionnés pour l'étude de promoteurs a été confirmée par RT-PCR. L'analyse de l'activité des promoteurs en réponses aux RI a été testée dans un plasmide rapporteur. Cette étude a montré que des promoteurs natifs clonés dans des plasmides ne sont pas utilisables en tant que tels en thérapie génique du cancer, limités par leur trop faibles inductions en réponses aux RI. A l'opposé, des promoteurs synthétiques contenant des sites répétés spécifiques pour la fixation de facteurs de transcriptions tels que NF-κB sont de bons candidats en vue d'une utilisation en thérapie génique. L'activité de cinq éléments TGGGGACTTTCCGC placés en tandem dans un système rapporteur luciferase a été augmentée d'une manière dose-dépendente. De plus, la réponse à de faibles doses thérapeutiques fractionnées a été augmentée en comparaison à une même dose unique. Une application du promoteur synthétique de fixation pour NF-κB est envisageable dans le traitement radio-thérapeutique du cancer.

Mots clefs : thérapie génique, cancer, radiations ionisantes, cellules endothéliales, promoteurs natifs, promoteurs synthétiques, facteur de transcription, NF-κB

SYNTHÈSE DE LA THÈSE

APPROCHE DE THERAPIE GENIQUE ANTI-CANCEREUSE COMBINEE A L'IRRADIATION : ETUDE DE LA REPONSE DE PROMOTEURS AUX RADIATIONS IONISANTES

1 INTRODUCTION

Le cancer est encore de nos jours une cause majeure de décès. C'est pourquoi, un intérêt primordial de la recherche sur le cancer consiste à trouver et à améliorer de nouvelles stratégies de traitement. Les radiations ionisantes (RI) font partie avec la chirurgie et la chimiothérapie des trois traitements principaux du cancer. La radiothérapie peut être appliquée seule, en combinaison avec la chimiothérapie ou en tant que thérapie palliative. Elle est également utilisée comme thérapie adjuvante pré- ou postopératoire, afin de prévenir le développement de nouveaux tissus tumoraux à partir de sites résiduels (récidive).

La radiothérapie possède l'avantage de pouvoir être appliquée de façon très ciblée empêchant ainsi une toxicité systématique. Cependant, tout comme les substances chimiothérapeutiques, les radiations affectent toutes les cellules qu'elles atteignent, pouvant provoquer des effets secondaires sévères. De surcroît, de nombreuses tumeurs malignes ne répondent aux radiations que très faiblement. La dose applicable à une certaine tumeur est limitée par la sensibilité des tissus et organes normaux avoisinants se trouvant dans le champ des radiations. Pour ces différentes raisons, un défi majeur de la recherche sur le cancer consiste à approfondir les connaissances des processus moléculaires induits par les radiations. Ceci permettrait d'améliorer les thérapies et de surmonter les défaillances des traitements.

Le degré de résistance aux radiations (radiorésistance) des cellules tumorales est non seulement dépendant de leur patrimoine génétique mais est également influencé par le microenvironnement dans lequel elles se trouvent. En particulier, les tumeurs solides sont dépendantes de l'angiogénèse, un processus dans lequel de nouveaux vaisseaux sanguins sont générés à partir du réseau vasculaire pré-existant. L'approvisonnement en oxygène et en nutriments par les vaisseaux sanguins assure le développement des tumeurs. Une thérapie

anti-angiogénique visant à inhiber ou détruire le réseau vasculaire tumoral par l'utilisation d'inhibiteurs d'angiogénèse ou d'agents chimiothérapeutiques est une avancée dans le traitement des cancers. De plus, les cellules endothéliales formant les vaisseaux sanguins représentent des cibles importantes dans la thérapie anti-angiogénique du cancer. Contrairement aux cellules tumorales qui mutent rapidement et sont génétiquement instables, les cellules endothéliales sont génétiquement stables évitant ainsi le problème de résistance aux substances anti-cancéreuses.
L'utilisation de la thérapie anti-angiogénique en complément de la radiothérapie a pour but de rendre les cellules endothéliales et tumorales plus radiosensibles. Une réduction notable dans la taille des tumeurs a été observée dans les essais cliniques combinant thérapie anti-angiogénique et radiothérapie.

Les lésions de l'ADN qu'elles soient des doubles ou simples ruptures des filaments d'ADN représentent les dommages cellulaires centraux induits par les radiations ionisantes. En réaction, une multitude de processus moléculaires et cellulaires est activée pouvant conduire à l'arrêt du cycle cellulaire, à l'induction de l'appareil de réparation de l'ADN ou encore à la mort cellulaire (post-mitotique ou par apoptose) lorsque les dommages causés sont trop importants. De plus, les radiations ionisantes induisent également un réseau de signaux complexes indépendants des dégâts produits sur l'ADN induits au niveau de la membrane cellulaire ou du cytoplasme. L'activation de l'ensemble des processus cellulaires suite à l'exposition aux RI mène à une altération de l'expression d'une batterie de gènes.

2 BUT DE CE TRAVAIL

Dans une optique de développer un nouveau système de thérapie génique combiné aux radiations ionisantes, les objectifs de ce travail ont été les suivants :

1) Etudier les profils d'expression génique de cellules endothéliales exposées à de faibles, hautes et doses fractionnées de radiations ionisantes.
2) Evaluer et identifier de potentiels promoteurs induits par radiations ionisantes à partir des études de profils d'expression génique.
3) Etudier la réponse de promoteurs artificiels aux radiations ionisantes.
4) Exprimer un gène toxique sous le contrôle de promoteurs induits par radiations ionisantes dans des cellules endothéliales.

3 REPONSES TRANSCRIPTIONNELLES DE CELLULES ENDOTHELIALES EXPOSEES AUX RADIATIONS IONISANTES

Les outils de l'ère post-génomique tels que la technologie des puces à ADN permettent d'analyser et comparer le niveau relatif de milliers d'ARN messagers simultanément dans une seule expérience d'hybridation. L'étude de ces profils d'expression génique est très prometteuse en terme de compréhension des mécanismes moléculaires associés aux radiations ionisantes.

L'objectif de ce travail a été d'analyser les effets des radiations ionisantes dans les cellules endothéliales. Nous avons utilisé des puces à ADN contenant 12625 gènes humains pour identifier les gènes modulés par RI dans les cellules endothéliales humaines nommées EA.hy 926. L'ARN des cellules EA.hy 926 a été isolé à 1, 6 et 12 h après expositions à 3 Gy et 20 Gy.

En réponse à une dose thérapeutique de 3 Gy, 24, 30 et 72 gènes signifiants ont été induits et 10, 18 et 18 gènes signifiants ont été réprimés respectivement à 1h, 6h et 12h après exposition à 3 Gy. Dans une perspective d'identification de gènes répondant fortement aux RI, nous avons également analysé l'expression des gènes des cellules endothéliales exposées à 20 Gy. L'exposition des cellules à 20 Gy a permis d'identifier 9, 147 et 92 gènes induits et 8, 143 et 88 gènes significativement réprimés respectivement à 1h, 6h et 12h post 20 Gy. Les figures 1 et 2 montrent les profils des gènes exprimés parmi l'ensemble des différents échantillons (Figure 1 et 2, gauche) et les profils des gènes modulés significativement suite aux expositions respectives de 3 Gy et 20 Gy (Figure 1 et 2, droite). La comparaison des profils d'expression génique de cellules EA.hy 926 exposées à 3 Gy et 20 Gy révèle différent motifs de modulation par les RI dépendants de la dose de RI et du temps d'expression (Figure 1, droite et Figure 2, droite). Les résultats montrent une faible réponse à des faibles et fortes doses de RI après 1 h d'exposition. Les réponses aux RI deviennent apparentes dans les temps plus tardifs (6 h et 12 h). Un changement considérable du transcriptome des cellules EA.hy 926 après exposition à 20 Gy contraste avec les cellules exposées à 3 Gy. En effet, une plus grande magnitude des modulations ainsi qu'un plus grand nombre de gènes modulés par les RI (voir ci-dessus) a été observé après 20 Gy en comparaison à 3 Gy. Ceci est probablement dû à plus de dommages de l'ADN causés par les RI, engendrant ainsi des réponses plus

intenses aux fortes doses. Puisque les RI causent des cassures doubles brins dans l'ADN, un large nombre de gènes répondant aux RI a été trouvé après 3 Gy et 20 Gy. Ils sont pour la plupart impliqués dans les processus de la régulation du cycle cellulaire, de la réparation de l'ADN or de l'apoptose. Parmi les quelques gènes induits dans ces processus nous avons identifiés, plusieurs gènes dépendants de la protéine p53. Ces gènes comprennent par exemple parmi les gènes induits p21 $^{Cip1/WAF1}$ (CDKN1A) et GADD45, impliqués dans la régulation du cycle cellulaire, les gènes impliqués dans les processus d'apoptose tels que TNFRF6/Fas/Apo-1, TNFRSF10B/KILLER/DR5, le gène de translocation cellulaire BTG2 ou encore le gène de la serine/thréonine phosphatase PPM1D/Wip1. Parmi les gènes réprimés, nous avons identifié par exemple des gènes impliqués dans la régulation du cycle cellulaire tels que E2F1, B-MYB, cyclin A2, B2, D3, E1, F ou CDC25C.

L'induction de certains des gènes a été vérifiée par RT-PCR quantitative: BTG2, NK4, 4-1BB, RANTES, Fas/Apo1 et le sous-unité p50 de NF-κB. Le gène tueur naturel 4 (NK4), dû à ses fortes amplitudes de 85.4 et 92.1 aux temps de 6 h et 12 h après exposition à 20 Gy, a un intérêt particulier dans la découverte de son rôle en réponses aux RI.

En conclusion, une partie des réseaux de gènes impliqués dans les réponses aux RI a été décrite dans cette étude. Elle permet de contribuer à la compréhension des conséquences des radiations dans le but ultime d'aider au développement de nouvelles stratégies de lutte contre le cancer.

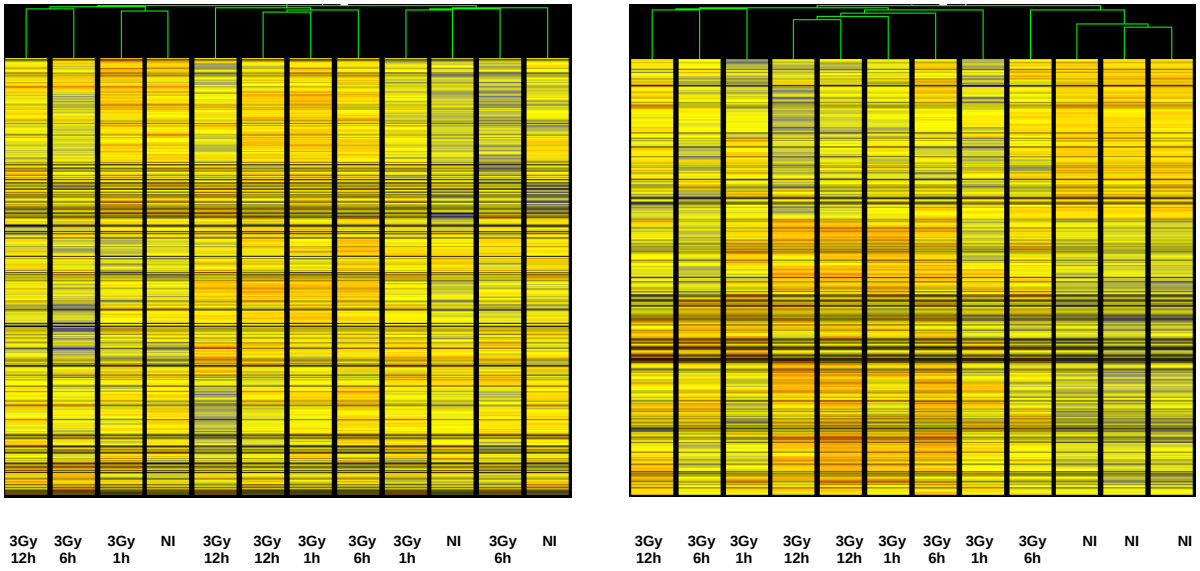

Figure 1 *Regroupements hiérarchiques de 9 échantillons irradiés (1, 6 et 12 h post 3 Gy) et 3 échantillons non irradiés (0 h) dans les cellules EA.hy 926. Les regroupement des échantillons (axe Y) est basé sur 5909 gènes exprimés (à gauche)et sur 349 gènes significativement exprimés (à droite) représentés sur l'axe X. Le regroupement des gènes est basé sur le degré de similarité des gènes. Le code couleur indique l'expression relative des gènes (en bleu : faible expression, rouge : expression élevée, jaune : pas de changement d'expression). NI : non-irradiés. Un total de 12625 gènes sur chaque puce à ADN a été testé. La procédure statistique est décrite dans la partie matériel et méthode du chapitre 3.*

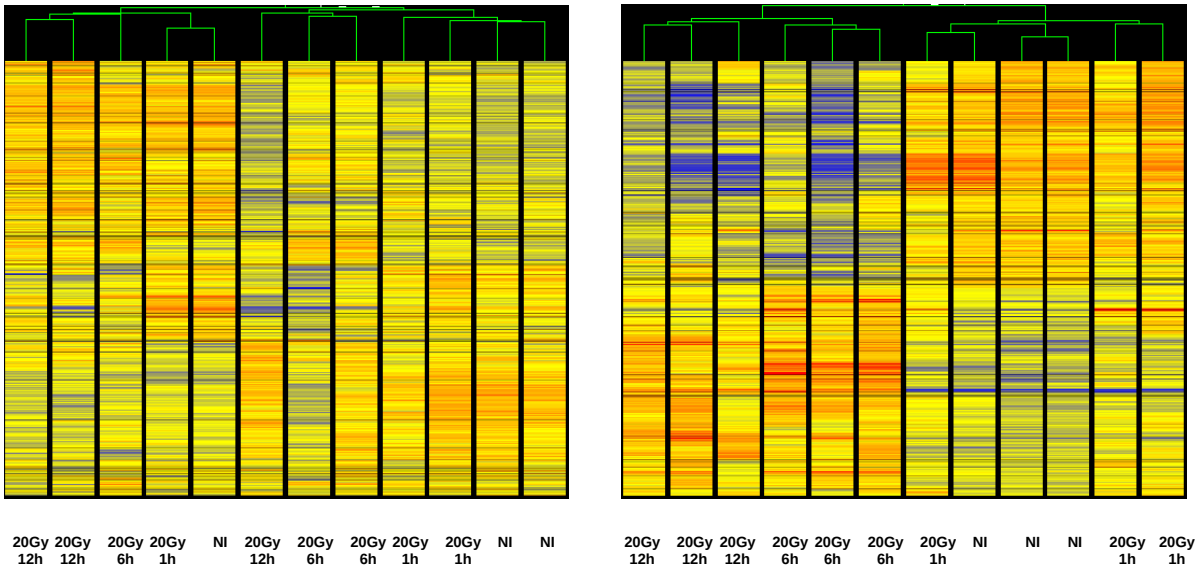

Figure 2 *Même description que dans la Figure 1, mais après 20 Gy. Les regroupement des échantillons (axe Y) est basé sur 5988 gènes exprimés (à gauche) et sur 424 gènes significativement exprimés (à droite) représentés sur l'axe X.*

4 ETUDE DE PROMOTEURS EN REPONSE AUX RADIATIONS IONISANTES

Le second objectif de ce travail a été d'identifier des promoteurs induits par les radiations ionisantes et pouvant être utilisés en thérapie génique suicide. Le principe de la thérapie génique suicide induits par RI est basé sur l'utilisation d'un promoteur répondant aux RI qui contrôle l'expression d'un gène codant une toxine dans la région de la tumeur.

Pour identifier de tels promoteurs, nous nous sommes basés sur les résulats des puces à ADN (voir description précédente). Nous avons clonés des promoteurs dans un vecteur rapporteur. L'activité des promoteurs a été mesurée en suivant l'activité luciférase dans des expériences de transfections transitoires et stables et après exposition de cellules aux rayons X.
Nous avons testé les promoteurs de gènes induits par RI, le gène B de translocation du gène 2 (BTG2) et le membre de la super-famille du facteur de nécrose de tumeur 4-1BB. Des études ont été conduites en vue de la caractérisation du promoteur du gène tueur naturel 4 (NK4). Nous avons montré que le promoteur du gène BTG2 a été activé dans des doses thérapeutiques de 3 Gy. Cependant, sa trop faible induction (3-3.5 fois) et son expression basale dans les cellules non-irradiées ne permettraient pas son utilisation thérapie génique. Aucune activité promotrice en réponse aux RI n'a pu être détecté pour le promoteur du récepteur 4-1BB. Le gène NK4 présentant de très bons critères en vue de la thérapie génique : gène le plus fortement induit après 20 Gy dans les puces à ADN, expression transitoire, non-expression dans les cellules non-irradiées ainsi que d'inducibilité du gène à doses fractionnées. Des investigations supplémentaires sont nécessaires quant à la caractérisation et localisation du promoteur.

Dans ce travail, nous avons montré que l'utilisation d'un site de fixation artificiel pour un facteur de transcription a été une approche réussie pour contrôler la réponse aux RI. Cette stratégie a été basée sur l'utilisation d'un plasmide contenant des éléments cis-régulateurs T GGGGACTTTCCGC du facteur nucléaire NF-κB, répétés cinq fois et placés en tandem (pNF-κB-Luciférase). NF-κB est un facteur de transcription connu pour être induit par RI et les résultats des puces à ADN ont montré des inductions de NF-κB au niveau transcriptionnel. Dans les cellules non-irradiées, NF-κB est retenu dans le cytoplasme par la protéine inhibitrice IκB. Les RI engendrent un signal intracellulaire résultant en une phosphorylation

de IκB, son ubiquitination et sa dégradation. NF-κB est alors libre de transloquer dans le noyau et d'activer la transcription des gènes.

Nous avons montré que le système pNF-κB-Luciférase répond aux RI dans des essais transfections transientes et de mesure de l'activité de la luciférase (Figure 3). L'activité du plasmide rapporteur a été testé après des doses de 3 Gy, 9 Gy et 20 Gy. La réponse à 9 Gy a permis l'induction du système de 4-fois dans les cellules endothéliales EA.hy 926. Ceci est particulièrement encourageant puisque les cellules endothéliales sont difficiles à transfecter par des méthodes standard. Une induction de 10-fois après 9 Gy a été observée dans les cellules 293-T, facilement transfectable.

La Figure 4 montre une réponse du système pNF-κB-Luciférase de manière dose-dépendente aux RI dans des cellules 293-T, transfectées de manière stable. Une induction de 16-fois a été observée avec la dose de 20 Gy. Après des doses thérapeutiques, le système a été induit de 1.5-fois et de 3-fois respectivement après 1 Gy et 3 Gy. De plus, l'application des doses thérapeutiques fractionnées à intervalles de 24 h d'application a résulté en une induction bien supérieure à l'application de la dose totale. L'application de 3 x 3 Gy a donné une induction du système de 12-fois alors que l'application d'une dose singulière de 9 Gy a résulté en une induction de seulement 6-fois. La même observation a été faite dans le fractionnement de doses de RI de 2 x 3 Gy.

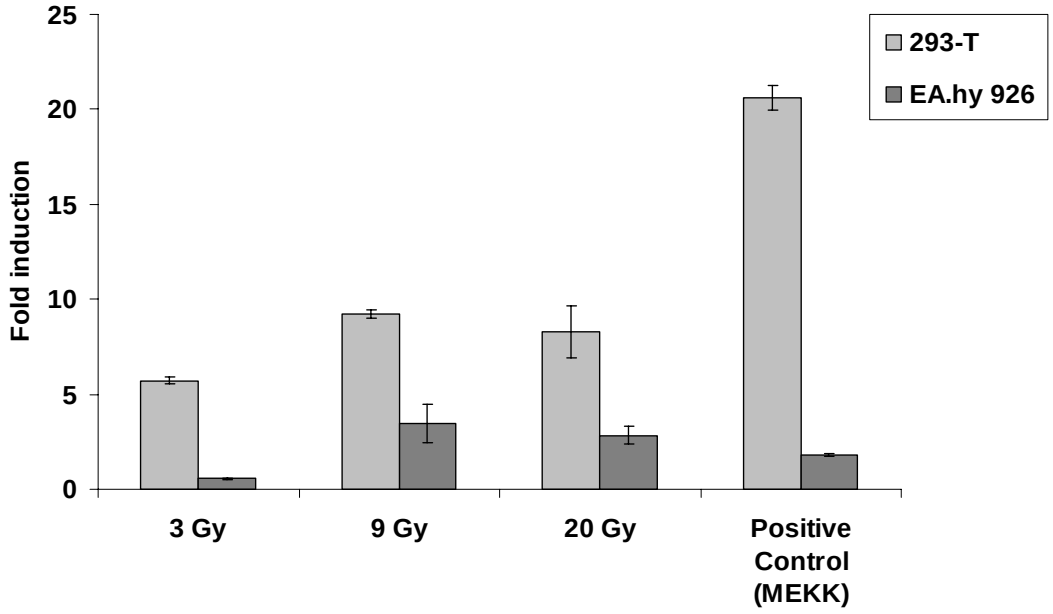

Figure 3 *Induction relative de l'expression de la luciférase dans un système pNF-κB-Luciférase après RI dans les cellules EA.hy 926 et 293-T. Les cellules ont été transfectées de manière transiente avec le rapporteur pNF-κB-Luciférase et 24 heures après transfection, les cellules ont été exposées ou non au traitement d'irradiation. 24 heures après RI, les cellules ont été récoltées, lysées dans du PBL et l'activité de la luciférase a été mesurée. Une cotransfection de pNF-κB-Luciférase avec pFC-MEKK est montré ici comme un contrôle positive.*

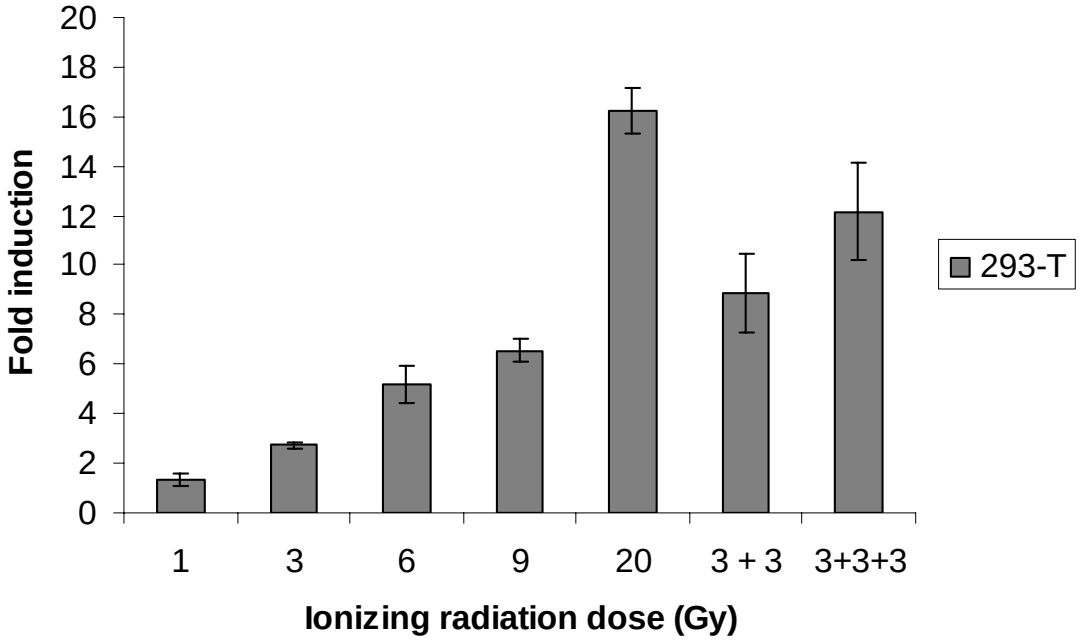

Figure 4 *Induction relative de l'expression de la luciférase dans un système pNF-κB-Luciférase après RI dans les cellules 293-T. Les cellules ont été transfectées de manière stable avec le plasmide rapporteur pNF-κB-Luciférase. 24 heures après traitement par les RI ou non irradiées, les cellules ont été récoltées, lysées dans du PLB et l'activité de la luciférase a été mesurée.*

5 CONCLUSIONS ET PERSPECTIVES

En conclusion, ces études ont démontré que l'utilisation des promoteurs artificiels représente une approche prometteuse afin d'améliorer la cytotoxicité des radiations ionisantes. Les éléments cis-régulateurs TGGGGACTTTCCGC pour NF-κB répondent de manière dose-dépendente aux RI. Le fractionnement des doses de RI rend ce système particulièrement intéressant pour des applications cliniques.

Des études supplémentaires de cytotoxicité du système NF-κB/toxine et de transduction de ce sytème, à l'aide de lentivirus, dans des cellules endothéliales sont envisagées et en cours. Ceci nous apportera la réponse quant à une possible utilisation d'un promoteur artificiel pour la fixation du facteur de transcription NF-κB dans un but thérapeutique.

ABBREVIATIONS

293-T	human embryonic kidney 293 cells expressing the adenovirus large T antigen
4-1BB	member of the tumor necrosis factor receptor superfamily
AIF	apoptosis-inducing factor
AIP1	apoptosis-inducing protein 1
Ang2	angiopoietin 2
AP-1	activating protein-1
AT	ataxia telangiectasia
ATF	activating transcription factor
ATM	ataxia telangiectasia-mutated gene
ATR	ataxia telangiectasia-mutated gene Rad3-related
BAC	bacterial artificial chromosome
BAX	Bcl2-associated X protein
bFGF	basic Fibroblast Growth Factor
bFGFR	basic fibroblast growth factor receptor
BSA	bovine serum albumin
BTG2	B cell translocation gene 2
bZIP	basic region-leucine zipper
cAMP	cyclic adenosine 5'-monophosphate
CAT	chloramphenicol acetyl transferase
CBP	CREB binding protein
CDK	cycling dependent kinases
CDKN1	cyclin-dependent kinase inhibitor 1
cDNA	complementary deoxyribonucleic acid
CMV	cytomegalovirus
CRE	cyclic AMP response element
CREB	CRE binding protein
DAG	diacylglycerol
DAPI	4'-6-Diamidino-2-phenylindole
DIABOLO	direct IAP-binding protein with low pI
DMEM	Dulbecco's modified Eagle medium
DNA	deoxyribonucleic acid
DNA-PK	DNA-dependent protein kinase
DSB	double strand breaks
EA.hy 926	HUVEC immortalized with a human lung carcinoma cell line
EC	endothelial cells
EDTA	ethylenediaminetetraacetic acid
EGF	epidermal growth factor
EGFR	epidermal growth factor receptor
EGR-1	early growth response 1
ELISA	Enzyme-Linked Immunosorbent Assay
EMSA	electrophoretic mobility shift assay
ERK	extracellular signal regulated kinase
FACS	Fluorescence activated cell sorting
FADD	Fas-associated death domain protein
FBS	Fetal bovine serum

FITC	fluorescein-5-isothiocyanate
GADD45	growth arrest and DNA damage inducible gene 45
GAPDH	glyceraldehyde-3-phosphate dehydrogenase
GATA-1	globin transcription factor 1
GDP	guanosine di-phosphate
GRB2	growth factor receptor-bound protein 2
GTP	guanosine tri-phosphate
HCT116	human colorectal carcinoma cell line
HeLa	malignant cell line, derived from the cervical carcinoma of Henrietta Lacks
HGF	hepatocyte growth factor
HIF-1α	hypoxic induced factor
HMEC	human microvascular endothelial cells
HRE	hypoxic response element
HSV-TK	herpes simplex virus-thymidine kinase
HUVEC	human umbilical vein endothelial cells
IAP	inhibitors-of-apoptosis proteins
IKK	IκB kinase kinase
IL2	interleukin 2
IL-6	interleukin 6
IMRT	intensity modulated radiation therapy
IP3	inositol triphosphate
IR	ionizing radiation
JNK/SAPK	c-Jun NH2-terminal/stress-activated protein kinase
MAPK	mitogen activated protein kinase
MEKK	mitogen-activated protein/ERK kinase kinases
NADH	nicotianamide adenine dinucleotide
NF-κB	nuclear factor-κB
NK4	natural killer transcript 4
NLS	nuclear localization sequence
NO	nitric oxid
$OH^{\bullet}$	hydroxyl radical
PBS	phosphate-buffered saline
PCR	polymerase chain reaction
PDGF-α	platelet Derived Growth Factor α
PI3K	phosphoinositide-3-kinase
PIP2	phosphatidylinositol-4,5-biphosphate
PKB (Akt)	protein kinase B
PKC	protein kinase C
PLCγ	phospholipase Cγ
PlGF	placental growth factor
PMSF	phenylmethylsulphonylfluoride
PS	penicillin and streptomycin
Pu	purine
Py	pyrimidine
RB	retinoblastoma
RNA	ribonucleic acid
ROS	reactive oxygen species
RT-PCR	reverse transcription-polymerase chain reaction
SDS-PAGE	sodium dodecyl sulfate polyacrylamide gel electrophoresis

Smac	second mitochondria-derived activator of caspases
SOS	guanine nucleotide exchange factor
SRE	serum-response element
TBST	tween 20 in Tris-buffered saline
TGF-α	transforming growth factor-α
TK	thymidine kinase gene
TNF-α	tumor necrosis factor alpha
TRAF	TNF receptor associated factor family
TRAIL	tumor necrosis factor-related apoptosis-inducing ligand
TRE	12-O-tetradecanoylphorbol-b-acetate response element
VEGF	vascular endothelial growth factor
VEGFR	vascular endothelial growth factor receptor

1 INTRODUCTION

1.1 Cancer and cancer treatments

Each year, more than 10 million people worldwide are diagnosed with cancer, which results in 6 million cancer-related deaths. Thus, cancer is among the leading causes of death, occupying the second position after heart disease. The most common cancers expected to occur in women are breast and cervical cancers, whereas in men cancers of prostate and lung are the most common. It is estimated that there will be 15 million new cases every year by 2020 (World Health Organization, 2004).

Ionizing radiation (IR) used as a therapy (radiotherapy) belongs, besides surgery and conventional cytotoxic chemotherapy, to the three major cancer treatment modalities. More than half of the patients receive radiotherapy during their treatment and more than one third of cancers are cured with this technique. IR is given for curative treatment usually as a stand-alone therapy or in combination with chemotherapy. Radiotherapy can also be delivered as a therapy after surgical removal of a tumor to prevent the growth of new tumor tissue from residual sites. In cases of non-curable cancer, radiotherapy is also applied as a palliative treatment to reduce or eliminate symptoms caused by tumors.

A benefit of ionizing radiation as a therapeutic tool is the possibility to apply it locally to solid tumors, which prevents systemic toxicity. However, a need remains to improve the cure rate by radiation therapy. In common with conventional chemotherapeutics, IR also affects the adjacent normal tissues, which leads to severe cytotoxic side effects. Furthermore, there is a large number of malignant tumor cells that show poor response to IR and the doses applied to the tumor cannot be increased arbitrarily because of the neighboring tissues and sensitive organs located in the vicinity of the tumor.

The efficacy of radiotherapy could be substantially improved through the development of more efficient IR-delivery techniques, acquisition of more knowledge of the mechanisms of the cellular and molecular responses to IR and further novel IR-based anti-cancer therapies.

1.2 Ionizing radiation as a cancer treatment modality

Radiotherapy (also called radiation therapy, X-ray therapy or irradiation) uses ionizing radiation to kill cancer cells and shrink tumors. Ionizing radiation includes electromagnetic radiation forms such as X-rays and gamma rays, as well as subatomic particles such as protons, neutrons and heavy ions. Standard radiotherapy uses mainly high radiation energy photons such as X-rays and gamma rays generated by radiation from linear accelerators and Cobalt 60 isotopic sources, respectively. The absorbed IR dose is measured in Gray (Gy). By definition, 1 Gy corresponds to the transfer of 1 joule of energy absorbed by 1 kilogram of material. In the biological target material, IR causes excitation or ionization of atoms by electron transfer or by electron(s) ejection respectively, thus causing secondary biological effects. The consequences of IR in the human body are mainly induction of DNA damage either by direct ionization of DNA or indirectly by the generation of free radicals. The free radicals due to their unpaired electron are highly unstable and reactive. Since 80 % of the cell is constituted from water, free radicals induced by IR are produced predominantly by the degradation of water molecules. As a consequence, reactive oxygen species (ROS) such as $OH^{\bullet}$, H_2O_2 or $O_2^{\bullet-}$ are generated. These free oxygenated radicals are strong oxidants that damage macromolecules such as DNA, but also cellular proteins and lipids.

Already at the end of the 19th century, shortly after Wilhelm Konrad Roentgen's description of X-rays in 1895 and the discovery of radium by Marie and Pierre Curie in 1898, ionizing radiation was applied for cancer treatment as an alternative to surgery. The earliest irradiation treatments were delivered as single large exposures, by placing low energy cathode ray tubes or radium glass tubes close to tumors. This approach fell out of favor, as tumors could only rarely be cured, and the method caused extensive damage to normal tissues. From these early days of radiotherapy, it was recognized that damage to normal tissue was less severe when the total dose was delivered in fractions within one or more days compared to one single dose. Claude Regaud demonstrated that repeated small doses of radiation could sterilize a ram's testicle without creating extensive skin damage. Coutard applied this concept of fractionated radiotherapy to cure patients with laryngeal tumors from 1920 to 1926.

As used nowadays, fractionation and hyperfractionation reduce radiation side effects. Fractionation allows the delivery of a larger total dose of radiation to the cancer that would not have been possible as a single dose. Currently, most radiation treatments are applied daily with a frequency of 5 days a week. The 24-hour interval and the two-day interval between doses allow for recovery of normal tissues between doses, while cancer cells, in general, are

less capable of recovery. Recent findings indicate that some cancers are best treated by reducing the 24-hour interval doses to 6-8 hours interval doses in order to enhance the toxic effects on cancer cells. This method, widely used to treat a variety of cancer is called hyperfractionation.

However, even with all the precautions taken to reduce the damage to normal cells to IR, it is impossible to have an absolutely safe radiation treatment. Indeed, the invasive nature of cancer growth means that IR must also be delivered to the areas that immediately surround the tumor. For this reason, technical progress has focused on improved radiation energy sources, better diagnostic localization of solid tumors and better restriction of applied radiation to the tumor site. This concept culminates nowadays in the development of intensity modulated radiation therapy (IMRT). IMRT is an advanced mode of high-precision radiotherapy that utilizes computer-controlled X-ray accelerators to deliver precise radiation doses to specific areas within the tumor. This technology allows a more targeted therapeutic dose delivery to the tumor, while sparing the surrounding normal tissue.

1.3 The cellular and molecular response to ionizing radiation

During the last century, research in radiotherapy focused mainly on the improvement of IR delivery techniques. In parallel, radiobiological concepts were developed in an attempt to understand the clinical response to IR on the cellular and molecular level. For example, concepts of radiosensitivity and radioresistance were developed more than 30 years ago. Radiosensitivity varies during different cell cycle stages, showing the highest sensitivity in G2 and M phase, intermediate sensitivity in G1 and early S-phase and rather low sensitivity in late S phase. An apparent increase of radioresistance after treatment could have been observed with fractionated irradiation doses due to the enrichment of cell populations in the resistant cell cycle phases, thus introducing the notion of acquired radioresistance. Further analyses introduced the concept of radiation-induced repair and intrinsic radiosensitivity. Inactivation of the cell cycle checkpoints involved in the repair was shown to increase cell radiosensitivity (for further details see (Hall, 1994)). Nowadays, modern research in the radiation biology domain aims at understanding these concepts at the molecular level. A better comprehension of the mechanisms of IR-induced cellular response can further allow the improvement of existing treatments and the development of new medical applications using IR.

The response of mammalian cells to ionizing radiation at the cellular and molecular level is a complex and active process, involving numerous gene products. Signaling responses to IR emanate from the alteration of the macromolecules in the plasma membrane and cytoplasm and from lesions produced in the DNA. An overview of the cellular events following IR described in this Chapter is shown in Figure 1.11 at page 28.

1.3.1 Plasma membrane damage signaling to ionizing radiation

At the cellular plasma membrane, IR exerts its effects on proteins or lipids that constitute the membrane. The consequences can be the modification of the function or even the degradation of the membrane (Somosy, 2000).

Peroxidation of the lipid bilayer by ROS and protein activation/inactivation are the main effects occurring at the plasma membrane. Activation of some proteins, such as membrane receptors, triggers specific signaling pathways. Membrane receptors, such as epidermal growth factor (EGF) and tumor necrosis factor (TNF), have been reported to be activated by precise IR stimuli. Activation can be driven by IR-induced binding of a ligand itself, by

nuclear signals emanating from DNA lesions or directly by IR via mechanisms that are still to be elucidated. The main cellular signaling IR-induced processes occurring at the plasma membrane are described in the following Sections.

1.3.1.1 The EGF receptor signaling

Ionizing radiation activates the epidermal growth factor receptor (EGFR) present on the plasma membrane. Schmidt-Ullrich and colleagues reported that therapeutically relevant exposure in the 0.5-5 Gy range activates the EGFR in various carcinomas (Schmidt-Ullrich *et al*, 1997). They showed that proliferative response is linked to the activation of EGFR after single and repeated radiation exposure. The blockage of radiation-induced EGFR function by overexpression of a dominant negative form of EGFR or treatment with antibodies against EGFR or small tyrosine kinase inhibitor molecules sensitizes the tumors cells to IR (Contessa *et al*, 1999; Mendelsohn and Baselga, 2000).

IR directly induces tyrosine phosphorylation of EGFR to a similar extent as its ligands, EGF or transforming growth factor-α (TGF-α) (Schmidt-Ullrich *et al*, 1997). It leads to EGFR dimerization and its autophosphorylation at tyrosine residues. Signaling mainly involves the mitogen-activated protein kinases/extracellular signal regulated kinase (MAPK/ERK) and the phosphoinositide-3-kinase (PI3K).

Signaling to MAPK includes the intermediates PLCγ, PKC, Ras and Raf. Activation of EGFR by IR promotes the stimulation of the small G-protein Ras, the growth factor receptor-bound protein 2 (GRB2) and the guanine nucleotide exchange factor (SOS). In turn, GRB2 and SOS activate the proto-oncogene Ras by exchanging GDP for GTP. Radiation-induced activation of EGFR results in the oxidative stimulation of phospholipase Cγ (PLCγ), with the production of diacylglycerol (DAG) and inositol triphosphate (IP3). Diacylglycerol activates protein kinase C (PKC) and IP3 induces the release of Ca^{2+} from the endoplasmic reticulum. Other studies suggested that PKC can directly regulate Raf-1, a member of the serine-threonine Raf family kinases (Cai *et al*, 1997). Subsequent events include the Ca^{2+}-dependent recruitment of Raf-1 to the plasma membrane by Ras-GTP. Activated Raf-1 phosphorylates and activates the MAPK that promotes cell proliferation.

The PI3K signaling network involves the PI3K, PIP2, IP3 and Akt. The phosphatidylionositol 3-kinase (PI3K), composed of a catalytic subunit p110 and a regulatory subunit p85, mainly converts phosphatidylinositol-4,5-biphosphate (PIP2) into inositol 3,4,5-triphosphate (IP3). IP3 acts as a second messenger. It activates the phosphoinositide-dependent kinases, which in

turn activate Akt also known as protein kinase B (PKB). Several Akt substrates such as Bad, through direct interaction (Zundel and Giaccia, 1998) or nuclear factor κB (NF-κB) through indirect interaction (Guo *et al*, 2004) have been identified to inhibit apoptosis and promote cell cycle progression respectively.

1.3.1.2 The death receptor signaling

Ionizing radiation can activate death receptors of the tumor necrosis factor alpha receptor family, such as TNFR, Fas/APO1/CD95 or TRAIL from the plasma membrane and trigger apoptosis (Embree-Ku *et al*, 2002; Gong and Almasan, 2000; Kim *et al*, 2001; Marini *et al*, 2005; Reap *et al*, 1997). The apoptotic pathway triggered by death receptors is described on page 18.

1.3.1.3 The ceramide signaling pathway

Ionizing radiation targets the plasma membrane and activates sphingomyelinases. These enzymes hydrolyse sphingomyelin and produce ceramides. Investigations by Haimovitz-Friedman and colleagues revealed that IR acts on the cellular membrane to generate ceramide (Haimovitz-Friedman *et al*, 1994). They reported that IR, similar to the TNFR ligands, induces rapid release of ceramide and subsequent apoptosis in bovine aortic endothelial cells. They also showed that ceramide is generated after IR of DNA/nuclei-free membrane preparations illustrating that apoptotic signaling is induced by interaction of IR with cellular membranes.

The mechanisms leading to the activation of sphingomyelinases by IR and the subsequent apoptosis are still unknown. Vit & Rosselli showed that two ceramide pathways are triggered in response to IR-induced cell damage. A transitory increase of ceramide is observed within minutes after IR exposure due to hydrolysis of sphingomyelin from membranes. Several hours after IR, a second *de novo* ceramide synthesis occurs, following DNA damage, which requires the ATM (Ataxia telangiectasia-mutated gene) protein. The late ceramide accumulation is dependent on the first and is rate limiting for the apoptotic process induced by IR (Vit and Rosselli, 2003).

The radiation-induced ceramides also lead to the activation of the main class of MAPK, the c-Jun NH2-terminal/stress-activated protein kinase (JNK/SAPK) (Verheij *et al*, 1996). Activation of the JNK pathway via sphingomyelinase enzymes was shown to act through the

upstream activators of the low-molecular weight GTP-binding proteins of the Rho family, in particular Cdc42 and Rac1 (Dent *et al*, 2003; Lu and Settleman, 1999). The JNK/SAPK pathway has been proposed to play a major role in the initiation of apoptosis by IR (Chmura *et al*, 1997; Kyriakis and Avruch, 1996; Santana *et al*, 1996; Verheij *et al*, 1996).

1.3.2 DNA damage signaling to ionizing radiation

Besides damage at the plasma membrane, IR exposure of higher eukaryotic cells causes a large spectrum of lesions at the DNA level. These lesions include alterations of nucleotide bases, single and double strand breaks, cross linking between DNA and proteins as well as chromosomal aberrations. The most prominent lesions caused by IR are DNA double strand breaks (DSB). The consequences of IR damage at the DNA level have larger impact compared to the IR-damaged plasma membrane, since the DNA contains the genetic information that can be transmitted to daughter cells. To cope with the damaged DNA, cells have evolved signaling pathway checkpoints that promote cycle delay or arrest to provide time for repair. Data show that these checkpoints are involved in DNA repair pathways, chromatin remodeling, activation of transcription and induction of cell death by apoptosis. The checkpoints can be implicated either in response to DNA damage or in response to replicative stress. The signal transduction cascades that respond to DNA damage consist of sensors, transducers and effectors and shown in Figure 1.1.

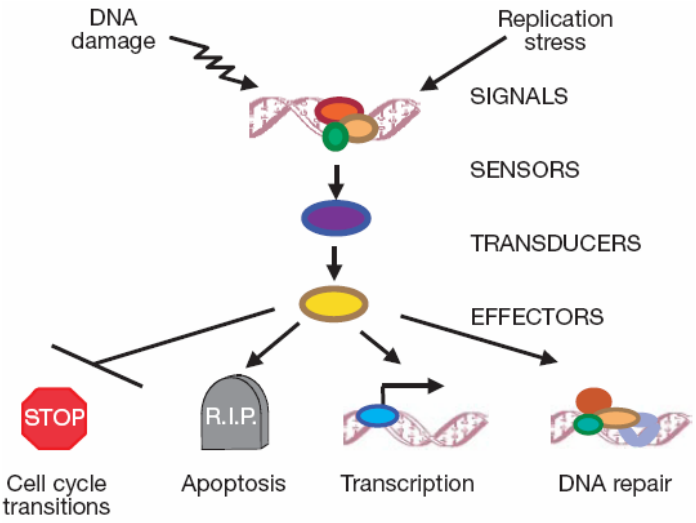

Figure 1.1 *General view of the DNA damage response signal transduction pathway (Zhou and Elledge, 2000).*

1.3.2.1 DNA damage signal transduction

The recognition of the damaged DNA is ensured by the sensors (not described here, for further details see (Zhou and Elledge, 2000)) that transduce the signal to downstream factors. Two related and conserved proteins, ATM (Ataxia telangiectasia-mutated gene) and ATR

(Ataxia telangiectasia-mutated gene Rad3-related) are central signal transducers in the response to DNA damage. ATM and ATR are both activated by DNA damage and play a role in cell cycle checkpoint signaling (Abraham, 2001). They belong to the family of phosphatidylinositol 3-kinase-like (PI3K-like) proteins. Despite similarities, important differences distinguish ATM and ATR, the most prevalent being the kinetics of activation and the types of damage. In response to IR, evidence suggests that ATM is the main determinant of the early checkpoint response, while ATR responds later to process IR-induced lesions and responds to stalled DNA replication forkes (Zhou and Bartek, 2004; Zhou and Elledge, 2000). ATM plays an important part in the response to DSB due to its rapid activation in all cell cycle phases. The implication of ATM in cell cycle transition in response to DNA damage was first observed in ataxia telangiectasia (AT) cells, which are defective for the ATM gene (Painter and Young, 1980). The deficiency of ATM proteins in AT patients is characterized by high sensitivity to IR and is responsible for neurodegeneration, immunodeficiency and predisposition to cancer.

ATM and ATR transduce the DNA damage signal and activate the downstream effectors kinases Chk2 and Chk1. Chk2 and Chk1 are structurally and functionally overlapping serine/threonine kinases activated in response to diverse genotoxic insults (reviewed in (Bartek *et al*, 2001; McGowan, 2002). In response to DSB, Chk2 is phosphorylated on threonine 68 (T68, see Figure 1.5) by ATM (Matsuoka *et al*, 1998; Matsuoka *et al*, 2000) and Chk1 is phosphorylated on serine 345 by ATR (Liu *et al*, 2000; Sanchez *et al*, 1997). The original concept of rather strict dependency of Chk1 on ATR and Chk2 on ATM has been recently softened by reports of various crosstalks among these kinases. For example, novel checkpoint cascade signaling via ATM-Chk1 (Groth *et al*, 2003), and ATM-independent activation of Chk2 (Hirao *et al*, 2002) were identified. The roles of Chk2 and Chk1 are the implication in DNA replication, chromatin restructuring, apoptosis and cell cycle progression.

1.3.2.2 The cell cycle arrest in response to DNA double strand breaks

To protect themselves against the IR damage, cells arrest temporarily in progression through the cell cycle to permit repair prior to DNA replication or cell division. Cell cycle checkpoints are activated to prevent progression of cells in the G1 and G2 phases and to delay the progression of cells through S phase. A simplified scheme of the DNA-integrity checkpoints by DNA damage is shown in Figure 1.2. The molecular organization of the checkpoint control players in cells exposed to ionizing radiation is reviewed by Iliakis *et al* (Iliakis *et al*, 2003).

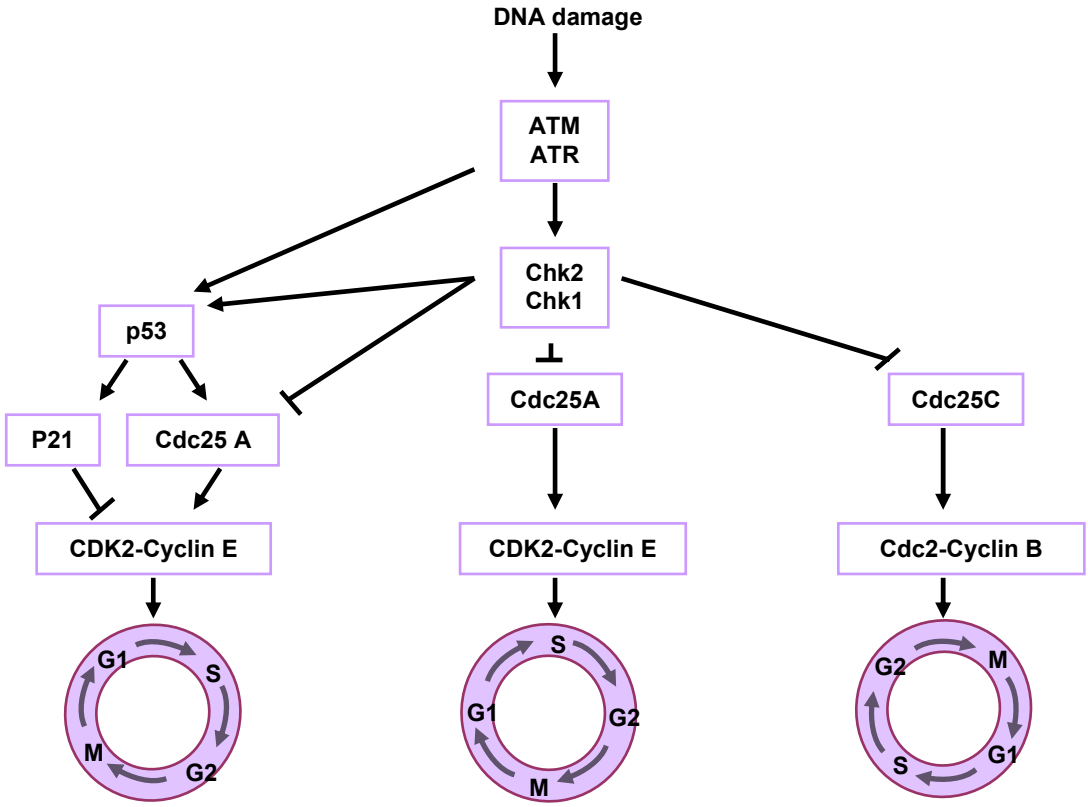

Figure 1.2 *A simplified scheme of cell-cycle checkpoint pathways induced in response to DNA damage.*

The G1/S checkpoint

Ionizing radiation induces the G1/S checkpoint to prevent the cells from entering the S phase when the DNA is damaged. The dominant checkpoint response to IR in cells is through the ATM network. As discussed in the previous section, ATM phosphorylates Chk2 and p53, leading to the activation of two pathways. One involves ATM-Chk2-Cdc25A and the second the p53-P21$^{/CIP1/WAF1}$ pathway. Kastan described the importance of Chk2 for the IR-induced phosphorylation and degradation of Cdc25A (Kastan, 2001). Lack of active Cdc25A leads to accumulation of inactive cyclin dependent kinases (CDK), in particular CDK2. The role of CDK2 is to phosphorylate the RB (retinoblastoma) protein, which results in the dissociation of the RB/E2F complex. The released E2F transcription factor can then help activate the S-phase entry. The second pathway activates p21$^{/CIP1/WAF1}$ that stabilizes the RB/E2F complex, and thus prevents S-phase entry and causes a G1 arrest.

The S checkpoint

The intra-S-phase checkpoint is activated when DNA is damaged in the early part of the DNA synthesis phase. Studies have shown down-regulation of DNA replication in response to radiation damage (Kastan *et al*, 1991; Waldman *et al*, 1996). The exact mechanisms responsible for this cell cycle arrest are poorly understood. The transient reduction in the rate of DNA synthesis most likely allows repair of damage before the lesions would be permanently fixed by DNA replication into irreparable chromosomal breaks. ATM could play a central role in this pathway, since AT cells display relative resistance to radiation-induced inhibition of DNA replication. Several ATM substrates, including Chk2, are required for repression of DNA synthesis after IR and act cooperatively with other signaling pathways downstream of ATM. One of the direct downstream effectors of the ATM-Chk2 pathway is the phosphatase Cdc25A. Cdc25A is phosphorylated by Chk2. In turn, Cdc25A dephosphorylates and activates the Cdk2-CyclinE and leads to a delay in S phase progression.

The G2/M checkpoint

The G2/M checkpoint prevents cells from initiating mitosis and thus from segregating damaged DNA into daughter cells.

ATM and ATR pathways are both involved in the G2/M arrest and involve ATM-Chk2-Cdc25 and ATR-Chk1-Cdc25. Activated Chk2 and Chk1 phosphorylate the Cdc25 phosphatase. The binding of 14-3-3 proteins to the phosphorylated Cdc25 results in nuclear export and cytoplasmic sequestration of Cdc25. This leads to the inhibition of Cdc2 activity and arrest of G2 to M progression.

Other studies suggest that p53 may also play a role in the G2/M transition, involving downstream target genes such as $p21^{/CIP1/WAF1}$ (Dulic *et al*, 1998), 14-3-3 σ (Hermeking *et al*, 1997) and growth arrest and DNA damage inducible gene 45 (GADD45) (Wang *et al*, 1999).

1.3.2.3 The p53 protein

The tumor suppressor p53 plays a key role in response to ionizing radiation. The p53 protein was discovered in 1979. It has been named the guardian of the genome (Lane, 1992). It leads to cell cycle arrest and coordinates DNA repair and/or the initiation of apoptosis (Fei and El-Deiry, 2003). The function of p53 is supported by the findings that p53 knockout mice show a high incidence of tumor development (Donehower, 1996) and a germline mutation of one p53 allele in humans gives rise to the Li-Fraumeni cancer-susceptibility syndrome. More than 50% of tumors have a p53 gene mutation (Vogelstein *et al*, 2000).

The p53 structure and activation mechanism

The human p53 is a nuclear phosphoprotein of 393 amino acids. It is commonly divided into three functional domains (Figure 1.3): an N-terminal transactivating domain and proline-rich region, a central conserved DNA-binding domain and a complex C-terminal domain (Bode and Dong, 2004; Wang *et al*, 1994). The transcriptional function of p53 is conferred by its N-terminal transactivation domain that spans amino acids 1 to 42. The proline-rich domain was shown to be important for growth arrest after damage. The central core is the DNA-binding domain. After stress-induced stabilization, p53 forms tetramers that bind to two copies of a 10 base pair motif 5'-PuPuPuC(A/T)(T/A)GPyPyPy-3' separated by 0-13 base pairs (el-Deiry *et al*, 1992). The majority of mutations found in human tumors are missense mutations clustered into the central DNA-binding domain (Greenblatt *et al*, 1994). The C-terminal domain contains the nuclear localization sequence (NLS) region, the tetramerization domain and the domain regulating the DNA binding. The tetramerization domain permits p53 to form transcriptionnally active tetrameric forms. Tetramerization of p53 masks the nuclear export signal, thus retaining active p53 in the nucleus. The C-terminal domains contain several acetylation and phosphorylation sites. These post-translational modifications may further contribute to the ability of p53 to function as a transcription factor.

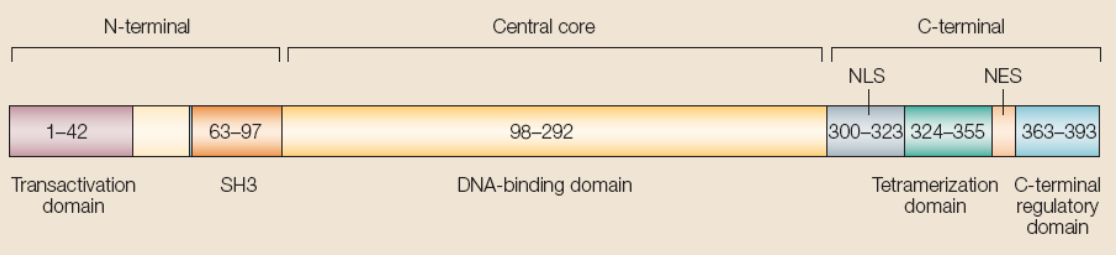

Figure 1.3 *Three functional domains of the human p53: the N-terminal domain (1-97) for transactivation, the DNA-binding domain (98-292) for DNA binding and the C-terminal domain (300-393) for its activity regulation (Bode and Dong, 2004).*

Under normal conditions, p53 is maintained at low levels in unstressed cells. Its half-life is short (5-20 min) and p53 is rapidly degraded. Its degradation is under the control of the protein Mdm2 (Mouse double minute 2). The interaction of Mdm2 with p53 stimulates the degradation of p53 by continuous ubiquitylation and subsequent degradation by the 26S proteasome. This degradation by the 26S proteasome is responsible for the rapid turnover of p53. In addition, Mdm2 binds the N-terminal transactivation domain of p53, inhibiting thus its transactivation activity. A graphical overview of p53 degradation/activation is given in Figure 1.4.

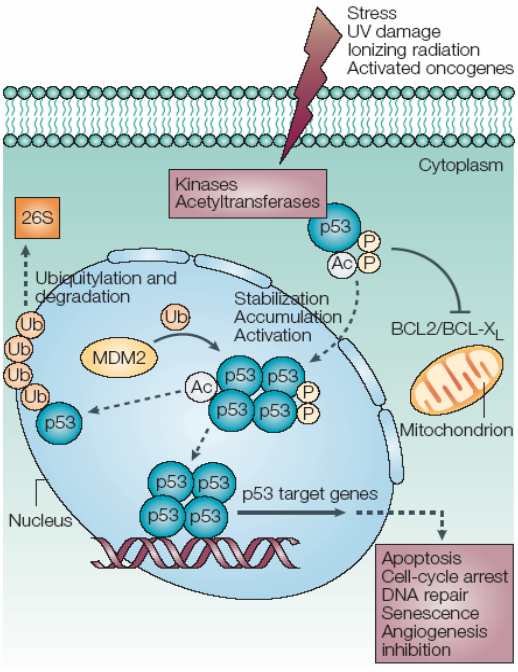

Figure 1.4 *Activation of the p53 and cellular response (Bode and Dong, 2004).*

Following genotoxic stress such as IR, p53 is activated. Its interaction with Mdm2 is blocked by phosphorylation (Shieh *et al*, 1999), thus leading to the suppression of its ubiquitination. p53 is stabilized and accumulates in the nucleus. The level of p53 protein thus increases several fold. To become transcriptionally active, a change in p53 conformation is necessary. This change results from a series of post-translational modifications of this molecule, including phosphorylation or dephosphorylation and acetylation of various residues.

p53 is phosphorylated by ATM or Chk1/Chk2 in response to DSB in DNA. ATM was found to bind p53 *in vivo*, and to directly phosphorylate serine 15 (S15, see Figure 1.5) *in vitro*. The rapid *de novo* phosphorylation of serine 15 in response to IR is ATM dependent (Banin *et al*, 1998; Siliciano *et al*, 1997). Chk1 and Chk2 have been shown to also activate p53. p53 is phosphorylated by these kinases on serine 20 (S20, see Figure 1.5) in its N-terminal transactivation domain (Shieh *et al*, 2000). In the same way, Mdm2 is phosphorylated on serine 395 (S395, see Figure 1.5) by ATM, thus disrupting the binding of Mdm2 with p53 (Maya *et al*, 2001). ATM thus promotes p53 activation and stabilization by mediating simultaneous phosphorylation of p53 and Mdm2 (Khosravi *et al*, 1999) (Figure 1.5).

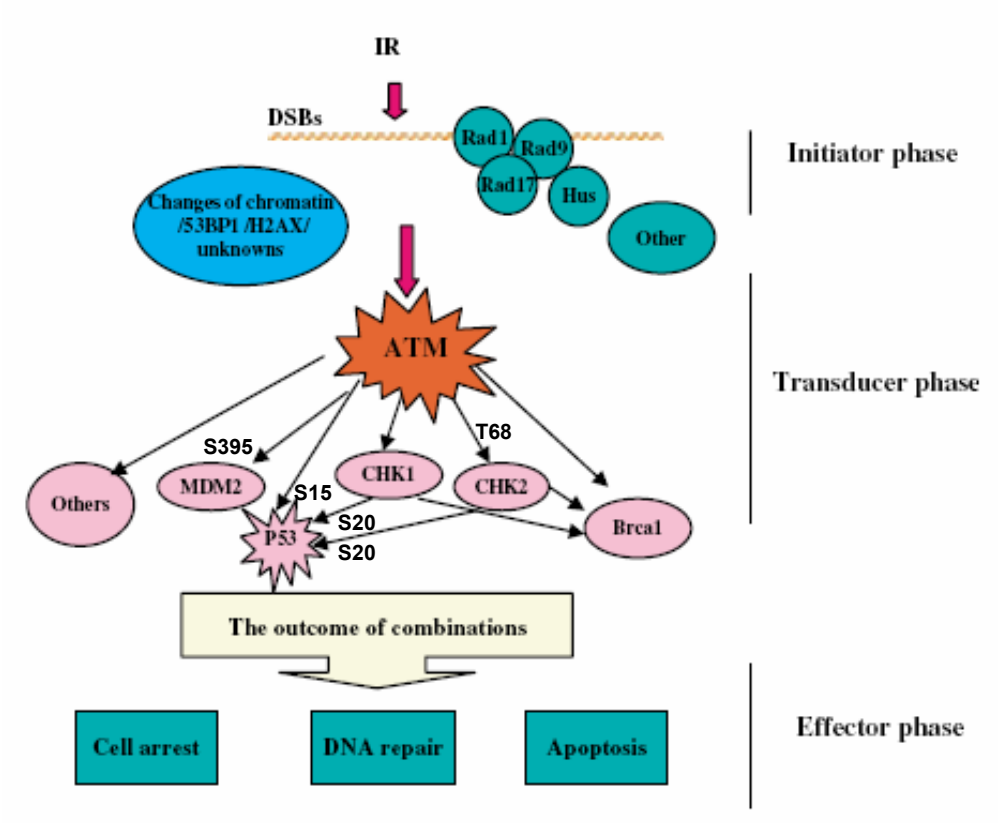

Figure 1.5 *General cascade of IR responses and phophorylation sites of p53 (adapted from Fei and El-Deiry (Fei and El-Deiry, 2003)).*

The p53 target genes and the cellular outcome decisions

Once active, p53 acts as a transcription factor *via* its DNA-binding domain to activate or repress various target genes (Figure 1.6). More than 150 genes targeted by p53 are associated with regulation of cell cycle arrest, apoptosis and DNA repair ((Stewart and Pietenpol, 2001), see Figure 1.6).

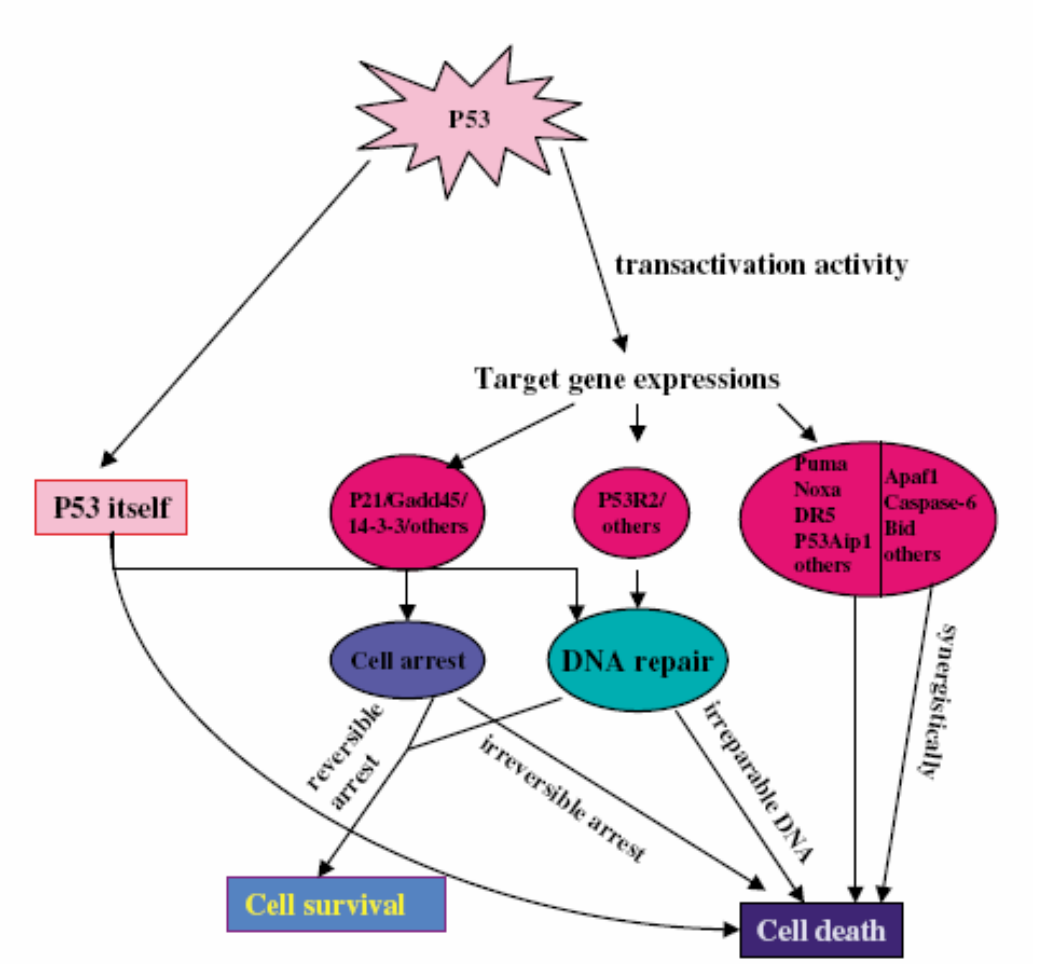

Figure 1.6 *Schematic presentation of roles of p53 in radiation responses (Fei and El-Deiry, 2003).*

The cellular response to IR depends on the types of activated or repressed genes or following factors: First, the cellular response depends on the concentration of p53 present in the cell. Indeed, Chen *et al* showed that a weak p53 increase leads to cell cycle arrest and that a strong p53 increase leads to apoptosis (Chen *et al*, 1996). The affinities for promoters may be responsible for this difference: an elevated concentration of p53 leads to the interaction with promoters of pro-apoptotic genes and a low concentration leads to the interaction with more

specific promoters of cell cycle regulation genes. Second, the affinity of p53 for promoters also depends on the interaction with co-factors present in the cell. For example, CBP/P300 was shown to increase the activity of all target genes and other proteins to induce apoptosis such as the apoptosis stimulating of p53 proteins (ASPP) (Slee and Lu, 2003). Third, the response to IR is variable depending on the tissues. Different gene expression profiles were observed in various tissues (Burns and El-Deiry, 2003; Fei *et al*, 2002). For example, the bowel is sensitive to apoptosis induced by p53 following IR exposure, whereas p53 increase after irradiation of the liver induces a cell cycle arrest. In the bowel, IR activates pro-apoptotic genes whereas in the liver it induces the expression of p21. These factors as well as additional factors, such as alterations of p53 or IR doses, influence the cellular fate (Offer *et al*, 2002; Oren *et al*, 2002).

The p53 apoptotic target genes

Among p53 targets, some of the genes have been shown to be involved in the process of apoptosis. These genes can be divided into groups based on their subcellular location.

The first group of p53-target genes encodes proteins that localize to the cell membrane and are involved in the extrinsic pathway (Section 1.3.3.1). Activation of the death receptor Fas/Apo1/CD95, a TNF-α receptor superfamily member has been shown to trigger p53-dependent apoptosis (Owen-Schaub *et al*, 1995). A substractive hybridization screen for p53 target genes led to the identification of KILLER/DR5, another member of the TNFR family (Wu *et al*, 1997). Takimoto and El-Deiry identified three p53 DNA-binding sites in the human KILLER/DR5 gene, suggesting a p53-dependent transactivation of KILLER/DR5 (Takimoto and El-Deiry, 2000). Indeed, expression of the KILLER/DR5 appears to be increased following exposure of wild-type p53-expressing cells to cytotoxic DNA-damaging agents such as IR (Wu *et al*, 1997).

The second group of genes encodes proteins that localize to the mitochondria and is involved in the intrinsic pathway (Section 1.3.3.2). p53 activation by DNA damage is associated with the mitochondrial apoptotic cascade. p53 leads to the transactivation of several pro-apoptotic genes including Bcl2 family members. Bax, a pro-apoptotic member of the Bcl-2 family has been shown to be induced by p53. Indeed, the promoter of the human BAX gene contains typical p53-binding sites and the gene has been shown to be transcriptionally activated by IR (Zhan *et al*, 1994). Other targets of p53 that are likely to contribute to apoptosis through

mitochondria include p53-regulated apoptosis-inducing protein 1 (p53-AIP1) (Oda *et al*, 2000), NADH oxidase A (NOXA) (Shibue *et al*, 2003) and p53-upregulated modulator of apoptosis (PUMA) (Nakano and Vousden, 2001).

1.3.3 Apoptosis following DNA damage

Apoptosis is a well defined and regulated process leading to cellular death, which may be activated in diverse stress situations. Apoptosis induction is characterized by distinct systematic morphological changes, including a decrease in cell volume, chromatin condensation, DNA fragmentation, cell surface blebbing and the formation of membrane-bound apoptotic bodies. This process protects multicellular organisms from genomic instability and neoplastic transformation. Apoptosis is ultimately caused by the activation of caspases. Caspases are cysteine proteases that are synthesized as inactive proenzymes and, after activation, cleave specific substrates at aspartic acid residues. Three main mechanisms resulting in apoptosis by IR are described in the following Sections and in Section 1.3.1.3. The first mechanism depends on the death-receptor pathway and the second mechanism operates through the mitochondrial pathway (Figure 1.7). These two pathways are mainly mediated through p53 and its ability to activate the transcription of its target genes (Haupt *et al*, 2003). The third pathway involves the ceramide accumulation that results from sphingomyelinase activation (see Section 1.3.1.3).

1.3.3.1 The death receptor apoptotic pathway

This extrinsic pathway is triggered by death receptors of the tumor necrosis factor alpha receptor family, such as TNFR, Fas/APO1/CD95 or TRAIL (Budihardjo *et al*, 1999). This complex recruits *via* the adaptor molecule FADD (Fas-associated death domain protein) multiple procaspase 8 molecules. Following procaspase-8 cleavage and subsequent activation, caspase 8 can then initiate the proteolytic cascade through caspase-3 that leads to apoptosis. The extrinsic pathway is also regulated by factors that repress the apoptotic signaling such as C-FLIP interfes with recruitement and activation of caspase-8. This pathway can branch to the mitochondrial pathway through caspase 8-mediated cleavage of the proapoptotic member of the Bcl-2 family, Bid, which can trigger the release of cytochrome c from mitochondria.

1.3.3.2 The mitochondrial apoptotic pathway

This intrinsic pathway leads to caspase activation and induction of apoptosis *via* the mitochondria (Budihardjo *et al*, 1999). It can be initiated by DNA damage, often in a p53-dependent manner. Responses to DNA insults converge to the mitochondria *via* the activation

of a pro-apoptotic member of the Bcl-2 family. Members of the Bcl-2 family such as Bax, Bad, Bim and Bid can shuttle between cytosol and organelles, whereas Bcl-2 is attached to the inner mitochondrial membrane. The mitochondria ultimately induce apoptosis through a reduction in the inner mitochondrial membrane potential and the release of a number of small molecules including apoptosis-inducing factor (AIF), Smac/DIABOLO and cytochrome c. Cytochrome c normally resides in the space between the inner and outer mitochondrial membranes, where it functions in oxidative phosphorylation. Cytochrome c release from the mitochondria is controlled by the Bcl-2 family. Once released, the cytochrome c participates in the proteolytic activation by caspase-9 and caspase-3. These events enable the assembly of a cytoplasmic multiprotein complex, the apoptosome. Apoptotic protease activation factor-1 (Apaf-1) forms the central core component of the apoptosome. Apaf-1 is a caspase activating protein which upon binding to cytochrome c associates with procaspase-9. Consequently, caspase 9 is activated, which in turn leads to the activation of effector caspases such as caspase 3. Caspase-3 activation and activity is antagonized by the inhibitors-of-apoptosis proteins (IAP), which themselves are antagonized by the Smac/DIABOLO protein released from the mitochondria. Downstream of caspase-3, the apoptotic programme leads to cell death.

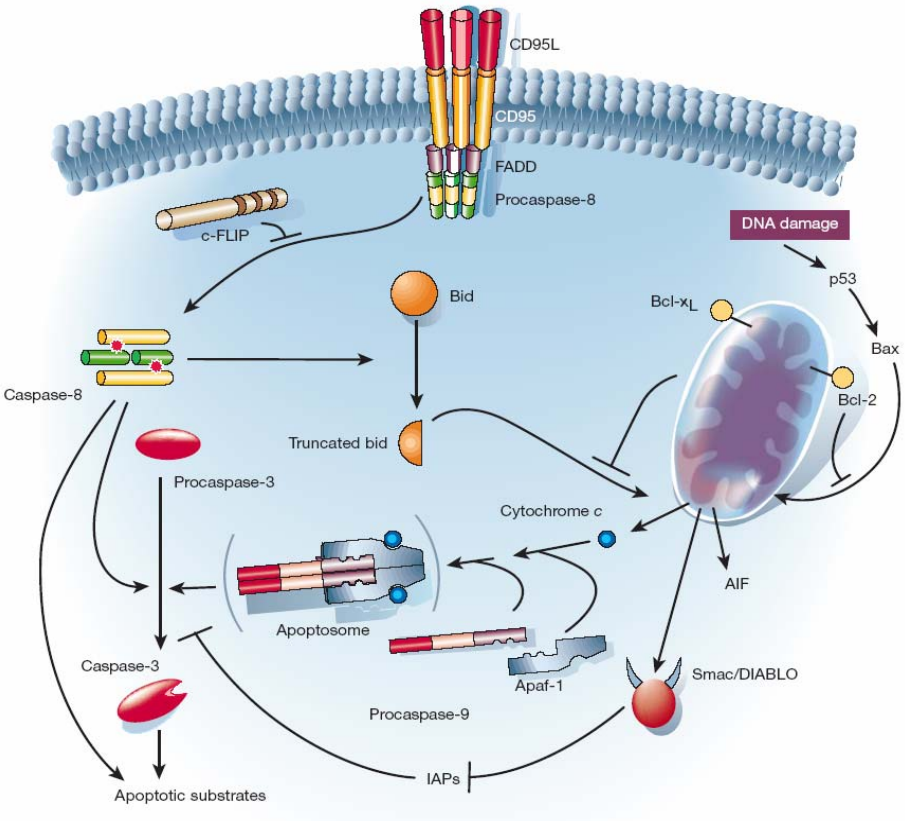

Figure 1.7 *The death receptor pathway (Hengartner, 2000).*

1.3.4 Examples of transcription factors activated by ionizing radiation

Responses of cells to ionizing radiation involve changes in the pattern and rates of gene expression. More than 30 years ago, (Kim *et al*, 1970) showed alterations on the cellular RNA and protein level after X-irradiation occurring in distinct temporal phases. The earliest nuclear targets, which by definition are rapidly induced in the absence of *de novo* protein synthesis, are referred to as the immediate-early genes (reviewed in (Weichselbaum *et al*, 1994)). Many immediate-early genes encode transcriptions factors that serve as nuclear couplers of cytoplasmic events such as the MAPKs pathways activation. They constitute the first steps in a transcriptional genes expression modification cascade, which can result either in cell-cycle arrest and repair or in cell death, depending on the level of damage. In addition, these changes also trigger a cascade of cellular modifications over a long period of time that may lead to the delayed effects of IR. Thus, products of these early response genes may represent a critical point in the cellular responses to IR, since they transduce early signals to the longer term changes in gene expression that play a role in the adaptation of cells and tissues to radiation-induced stresses (Weichselbaum *et al*, 1994).

The best-characterized members of transcriptional regulator families activated by IR in the early responses comprise AP-1, NF-κB and EGR-1 (reviewed in (Chastel *et al*, 2004; Criswell *et al*, 2003)). In the following paragraphs, the important characteristics of these modulators of the transcriptome in response to IR are briefly presented. The p53 protein described in section 1.3.2.3 also belongs to the important transcription factors that modulate the transcriptome by IR.

1.3.4.1 Activating protein-1 (AP-1)

AP-1 transcription factors consist of homodimers and heterodimers of Fos (c-Fos, v-Fos, FosB, Fra1, Fra2), Jun (c-Jun, v-Jun, JunB, JunD) and the related activating transcription factor ATF (ATF2, ATF3, B-ATF) subfamiles. These AP-1 subfamilies belong to the basic region-leucine zipper (bZIP) group of DNA binding proteins. They dimerize through a leucine zipper domain before they can bind to their DNA target sites. The Fos/Jun dimers bind with the highest affinity to a heptanucleotide palindrome consensus sequence TGA G/C TCA, referred to as the 12-O-tetradecanoylphorbol-b-acetate response element TRE (Lee *et al*, 1987). The Jun/ATF dimers only efficiently bind to the octanucleotide sequence TGA GC TCA. Following extracellular stimuli, the AP-1 transcription factor is activated. The exact

subunit composition is influenced by the nature of the extracellular stimulus and the MAPK signaling pathway that is activated (ERK, JNK, p38) (see Figure 1.8). Regulation of AP-1 activity occurs by activating transcription of *Jun* and *Fos* genes as well as through phosphorylation of existing Jun and Fos proteins at specific serine and threonine sites.

Induction of both *fos* and *jun* mRNA levels by radiation has been widely studied in a variety of cellular systems (Weichselbaum *et al*, 1994). Transcriptional activation of c-*jun* by IR in human HL-60 promyelocytic leukaemia cells was described by Sherman *et al* (Sherman *et al*, 1990). In an extension of the studies of Sherman *et al*, Datta *et al* and Hallahan *et al*, studied X-ray induction of c-Jun, c-Fos and a third early growth response (EGR-1) gene (see page 25, (Datta *et al*, 1992a; Hallahan *et al*, 1991)). They showed that while all three genes are similarly induced by serum, the response of c-*fos* to X-rays was distinct from that of the other two genes. This suggested that the response of the immediate early genes to IR is variable and that it is cell type-dependent. Transcription regulation of c-*fos* and c-*jun* following stimulation is mediated through distinct regulatory domains in their promoters (Karin, 1995).

The regulatory elements of the c-*fos* promoter, the serum-response element SRE and the cAMP response element (CRE) could be shown to be necessary for its correct transcriptional response by extracellular stimuli. The SRE was shown to be necessary and sufficient to render a heterologous promoter responsive to serum (Treisman, 1985). It is a 22 bp segment that contains the inner core sequence CCATATTAGG. This element has been described to be also responsible for radio-inducibillity of c-Fos (Datta *et al*, 1992b). The SRE is recognized by the serum response factor, whose binding results in recruitement of the ternary complex factor (TCF). Following mitogenic stimulation, Elk-1, one of the several candidate TCFs, is rapidly phosphorylated, most likely by the ERK group of MAPKs. In turn, ERK activation leads to c-*fos* induction, whose product combines with the pre-existing Jun protein to form the AP-1 complex. The cyclic AMP response element (CRE) consensus of the c-*fos* promoter controls the basal level of transcription, as well as the response of the promoter to cAMP and calcium. The cognate transcription factor CRE binding protein (CREB) contains a leucine zipper motif and binds as a dimer to the CRE sequence TGACGTCA of the c-*fos* promoter. The recent work of Amorino *et al* showed the potential role of CREB in radiation response (Amorino *et al*, 2002). They showed that following 2 Gy, CREB was phosphorylated on Ser133, correlating with MAPK/ERK activation. They suggested that CREB could play a role in the regulation of its target genes by IR (Figure 1.8).

By comparison with c-*fos*, the c-*jun* promoter is somewhat simpler, and most of its inducers such as c-Jun/ATF2 operate through a major cis-element, the c-*jun* TRE. This TRE differs from the consensus heptanucleotide TRE sequence by a 1-bp insertion, which is more efficiently recognized by c-Jun/ATF2 heterodimers than by the conventional AP-1 complexes. Unlike c-Jun, ATF2 is a constitutively expressed protein. The c-Jun protein, despite its inducible expression, is present in most cell types prior to their stimulation. Following exposure to stimuli such as IR that activate members of the JNK group of MAPKs, both c-Jun and ATF2 are rapidly phosphorylated. Constitutive occupancy of the c-*jun* TRE indicates that this phosphorylation occurs while the proteins are bound to the c-*jun* promoter. Phosphorylation of c-Jun and ATF2 by JNK or p38 MAPK stimulates their ability to activate transcription, thereby leading to c-*jun* induction. Requirement of AP-1 (c-Jun/ATF2) in the c-*jun* promoter region for induction of *jun* mRNA by IR was shown by using a chloramphenicol acetyl transferase (CAT) reporter assay (Hallahan *et al*, 1996). The requirement of AP-1 for induction of the *jun* gene was further confirmed in hypoxic HeLa cells (Minet *et al*, 2001).

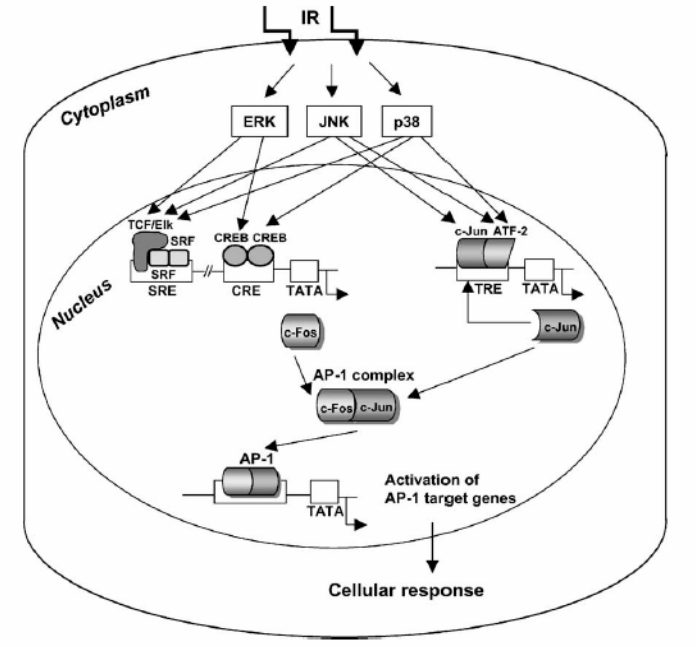

Figure 1.8 *Induction of AP-1 activity via three distinct MAPKs. Phosphorylation of TCF/Elk-1 bound to the c-fos promoter by the ERKs stimulates its transcriptional activity, thus leading to c-fos induction. JNK-mediated phosphorylation of ATF2 and c-Jun bound to the c-jun promoter stimulates their transcriptional activities leading to c-jun induction. The newly synthesized c-Fos and c-Jun proteins combine to form stable AP-1 heterodimers. A further increase in AP-1 activity is brought about by the JNKs and ERK, which phosphorylate c-Jun and c-Fos, respectively, on sites that augment their transcriptional activities. SRF, serum response factor; TRE, 12-O-tetradecanoylphorbol-b-acetate response element (Chastel et al, 2004).*

Following exposure to ionizing radiation, AP-1 activity was found to be rapidly induced. Activation of AP-1 by IR was shown *in vivo* in pig skin and *in vitro* in human fibroblasts and keratinocytes (Martin *et al*, 1997). Three and six hours after IR, the Fos and Jun proteins and their binding activity to an AP-1 consensus sequence were strongly induced by high doses of γ-rays.

Binding sites for AP-1 have been found in several promoters of X-ray inducible mammalian target genes. Among them, the promoter of TGF-β1 (Martin *et al*, 1997), vascular endothelial growth factor (VEGF) (Park *et al*, 2001) and IL-6 (Beetz *et al*, 2000) have been shown to be activated by AP-1 after IR. Interestingly, none of these genes have been found to be responsive to AP-1 activation alone. In the case of TGF-β, it was shown that AP-1 activation alone was, in fact, not sufficient for the induction of the gene transcript (Gault *et al*, 2002). Likewise, AP-1 acts synergistically with NF-κB (Beetz *et al*, 2000) to induce IL-6 transcription. Further studies of the mechanisms of AP-1 activation remain to be elucidated in detail. Additionally, it should also be noted that AP-1 activation was not found in all cells after IR exposure (Sahijdak *et al*, 1994), indicating cell specificity in this IR-responsive transcription factor and probably in JNK activation.

1.3.4.2 Nuclear factor kappa B (NF-κB)

The nuclear factor kappa B (NF-κB) is a transcription factor that is a dimeric complex of the Rel family protein members (p50, p52, C-Rel, RelB and RelA/p65). The most abundant and most studied form of NF-κB is the heterodimer p50/p65 which activates transcription of numerous genes by binding the consensus decameric DNA binding sites GGGRNYYYCC. NF-κB is found essentially in all cell types and is involved in activation of large number of genes in response to infections, inflammations and various exogenous and endogenous stimuli.

Ionizing radiation is one of the agents capable of activating NF-κB. IR induces NF-κB activation beginning 2-4 h after exposure with its activity returning to untreated levels by 8h (Brach *et al*, 1991; Mohan and Meltz, 1994; Prasad *et al*, 1994; Russell and Tofilon, 2002). Two distinct pathways may be involved in NF-κB activation (Figure 1.9). On one hand, activation of NF-κB is induced by oxidative stress agents such as H_2O_2 (Schreck *et al*, 1992). Similarly, its activation by IR appears to proceed through an oxidative stress-response cascade in which generated ROS act as second messengers (Mohan and Meltz, 1994). On the other

hand, NF-κB activation by IR involves the ATM and/or the DNA-dependent protein kinase (DNA-PK) complex implicated in the DNA DSB recognition pathway. Jung *et al* reported that the regulation of NF-κB is impaired in cells from Ataxia-Telangiectasia (AT) patients (Jung *et al*, 1995). They showed also that immunoprecipitated ATM phosphorylates IκBα *in vitro* (Jung *et al*, 1997). The same group reported that ATM was required for IκBα degradation, nuclear translocation of NF-κB and transcriptional activation by NF-κB in the same cell system by exposure to 20 Gy (Lee *et al*, 1998). Similarly, another nuclear ATM-related kinase, the DNA-PK, is implicated in the activation of NF-κB after 10 Gy exposures of HeLa cervical carcinoma and M059K glioma cell lines (Basu *et al*, 1998).

According to the classical paradigm, NF-κB activation and regulation by various stimuli are tightly controlled by the inhibitory protein IκBα. Li and Karin showed that IR activates IKK and that IR-induced IκBα degradation is phosphorylation-dependent (Li and Karin, 1998). In unstimulated cells, IκBα binds to NF-κB thereby retaining the NF-κB complex in the cytosol. Exposure of cells to stimuli induces phosphorylation of IκBα on Ser32 and Ser36 by IκB kinases (IKKα,β and γ). The phosphorylated form of IκBα is ubiquitinated and degraded by the 26S proteasome (Karin and Ben-Neriah, 2000). As a consequence, the free form of NF-κB is translocated into the nucleus where it can bind to the specific target genes. The survival effect of NF-κB is mediated by numerous genes coding for anti-apoptotic genes which block the apoptotic pathways. They include the inhibitors of apoptosis family member genes (cIAP1 and cIAP2), TNF receptor associated factor family member genes (TRAF1 and TRAF2), Bcl-xl, A1 protein among others. The pro-apoptotic Bax, induced by p53, contains also a NF-κB binding site in its promoter. In this case, NF-κB plays an inhibitory role by interfering with the transactivation of p53 in cancer cell lines (Bentires, 2001).

Elevated constitutive expression of NF-κB in cancer cells is associated with radioresistance. Recently, several teams studied the relationship between radiosensitivity and NF-κB activity (Jung and Dritschilo, 2001) in cells where NF-κB activation was blocked before the application of IR stimuli. The most commonly used technique was the transfection of cells with a vector containing a gene encoding a super-repressor of IκBα. Inhibition of IκBα phosphorylation on Ser32 and Ser36 was shown to sensitize human glioma cells to DNA damaging agents and inhibition of NF-κB activity increased the radiosensitivity of several human ovarian cell lines. Also, blocking radiation-induced NF-κB activation increased the apoptotic response and decreased the growth and clonogenic survival of irradiated colorectal

cells (Wang *et al*, 2002). Ectopic expression of mutated IκB in human malignant glioma MO54 and T98 cells led to their sensitization to IR (Ding *et al*, 2003; Honda *et al*, 2002). The authors proposed a pre-treatement which would inhibit NF-κB activity before radiotherapy application.

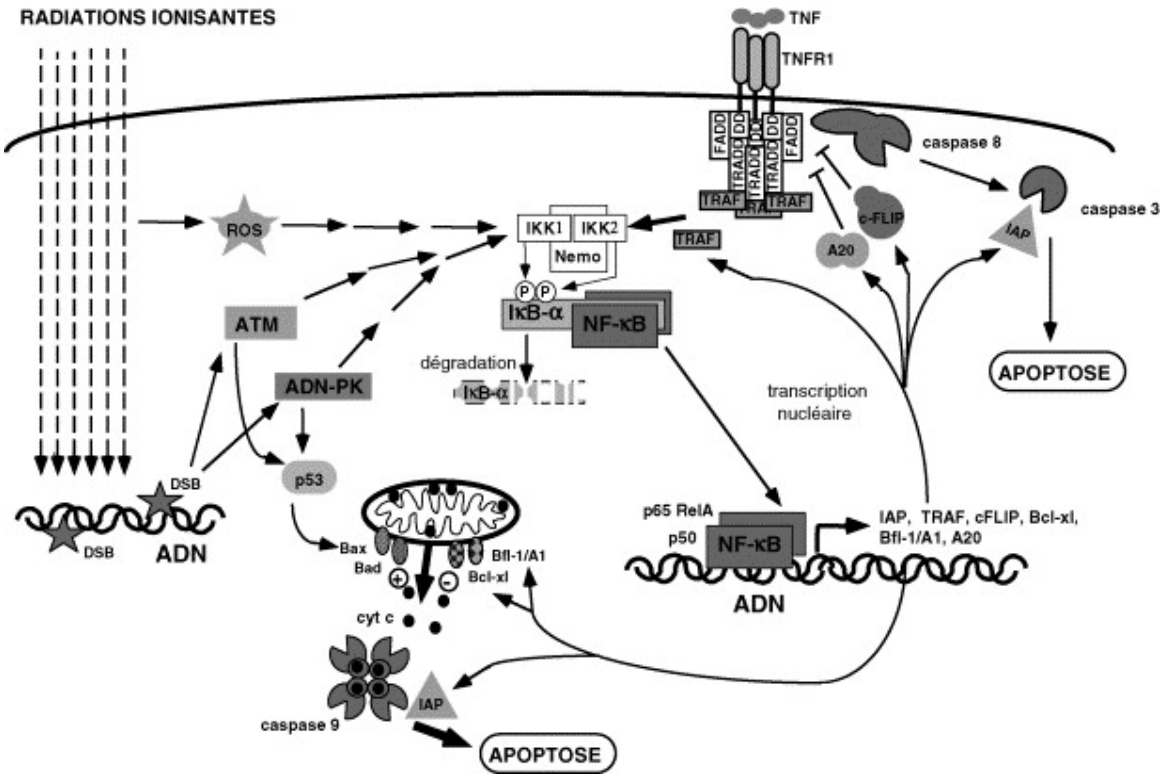

Figure 1.9 *NF-κB regulations induced by ionizing radiation (Magne et al, 2004).*

1.3.4.3 Early growth response factor gene-1 (EGR-1)

The early growth response 1 (EGR-1) gene was shown to be induced by ionizing radiation (Hallahan *et al*, 1991). Expression of the EGR-1 gene and protein are transiently induced by a variety of extracellular stimuli including X-rays. The increased expression of the EGR-1 gene occurs within 15 minutes and is terminated 3 hours following X-ray exposure.

The EGR-1 gene also known as *ZIF/268*, *TIS-8*, *NFGI-A*, and *KROX-24* encodes a 533-amino acid nuclear phosphoprotein that belongs to the three-zinc finger transcription factor family.

EGR-1 binds with high affinity to the GC-rich recognition sequences CGCCCCCGC in the regulatory regions of many downstream genes such as cytokines and growth factors including Tumor Necrosis Factor α (TNF-α) (Raju *et al*, 1999), Platelet Derived Growth Factor α (PDGF-α) and basic Fibroblast Growth Factor (bFGF) (Witte *et al*, 1989).

Functional dissection of the EGR-1 promoter revealed that the 700-bp full-length promoter includes several types of binding sites (Figure 1.10). Schwachtgen *et al* demonstrated that the promoter contains at least five copies of a characteristic transcription factor binding site designated the serum response element (SRE) (Schwachtgen *et al*, 2000). By deletion analysis, Datta *et al* showed that the three distal SRE or $CC(A/T)_6GG$ motifs, also known as CArG elements are the radiation responsive elements (Datta *et al*, 1992b). Moreover, exposure of HL-525 human leukemia cells to ROS induced EGR-1 transcription also through the CArG element (Datta *et al*, 1993).

The EGR-1 promoter is activated through the ternary complex factor Elk-1 and the serum response factor p68. Elk-1 is phosphorylated by the three MAPK (ERK, JNK, p38), which activates Elk-1 DNA binding activity, ternary complex formation and SRE-mediated transcription. In addition to SRE elements, the EGR-1 promoter contains several types of other binding sites. It comprises a JNK-dependent activated protein-1/thiophorbol ester responsive elements (AP-1/TRE), two binding sequences for EGR-1 itself (EgrBS) CGCCCCCGC (Cao *et al*, 1993) and two cAMP responsive elements (CRE). Whether the CRE sites contribute to radioinducibility of the EGR-1 promoter in normal cells was not clearly demonstrated. However, there is evidence for EGR-1 promoter activation *via* phosphorylation of the CRE binding protein (CREB) in a MAP kinase-dependent manner (Meyer *et al*, 2002).

The EGR-1 promoter has been recently utilized in IR-induced gene therapy of cancer (Senzer *et al*, 2004; Weichselbaum *et al*, 2002) and discussed in the Chapter 4, Section 4.4.

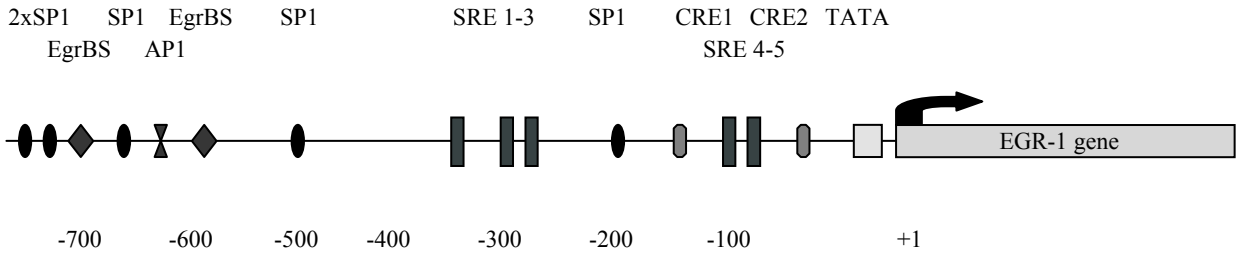

Figure 1.10 *The human EGR-1 promoter and its regulatory elements.*
The 700-bp full length EGR-1 promoter comprises a region (nucleotides –425 to –56) including a TATA box, two serum response elements (SRE 4-5) flanked by two cAMP responsive elements (CREs), one SP1 binding site, three SRE1-3, and described as sufficient for radioactivation. Other binding sites are located upstream of SRE 1-3, namely three Sp1 binding sites, two recognition sequences for the EGR-1 gene product itself (EgrBS) and an AP1 binding site (adapted from Meyer et al (Meyer et al, 2002)).

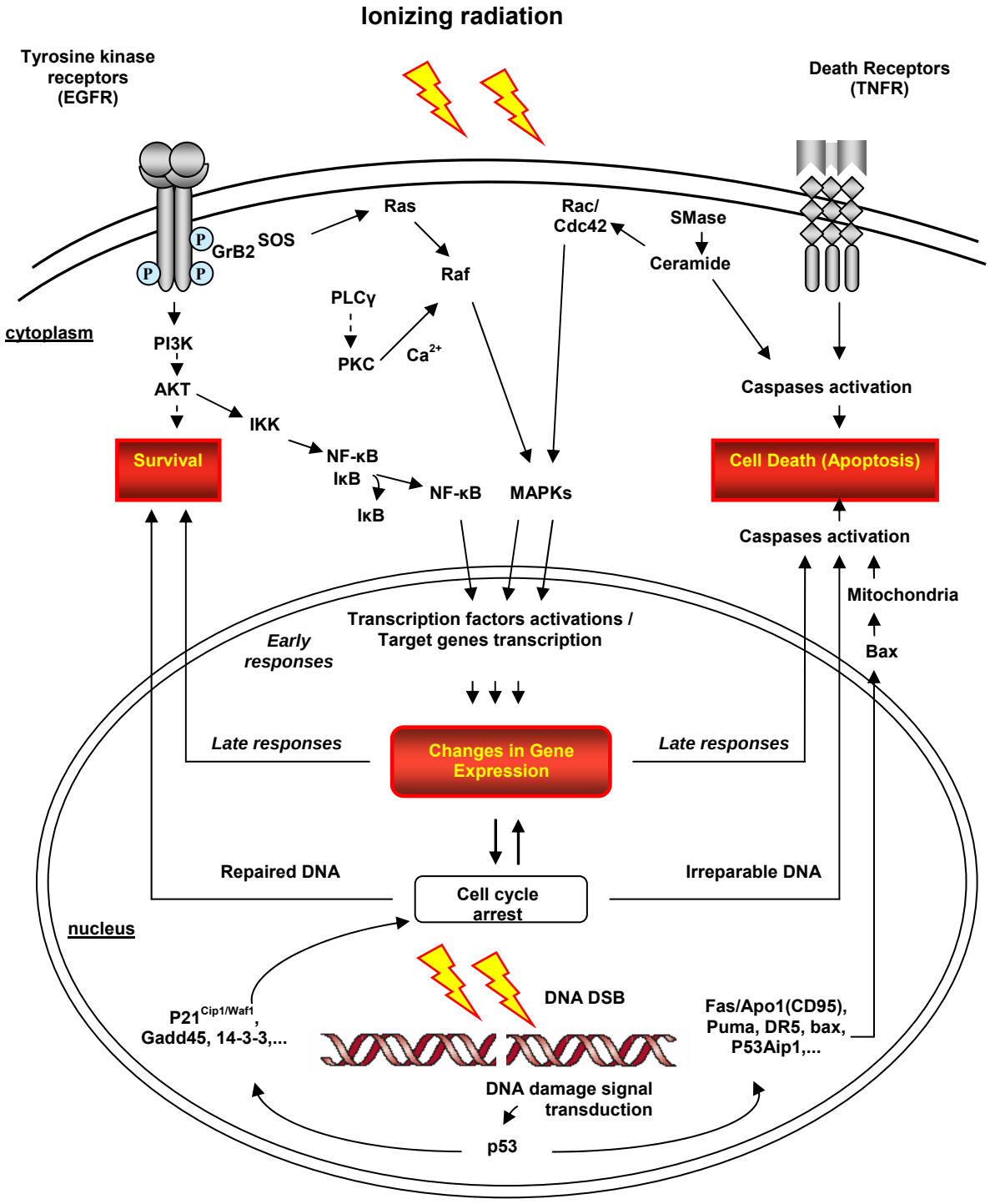

Figure 1.11 *Signaling pathways activated in response to ionizing radiation. Multiple signaling cascades are activated by IR leading either to survival or cell death (apoptosis). Signals triggered by IR occur at the plasma membrane leading to the activation of specific MAPKs. These protein kinases couple the cytoplasmic signal with the nuclear signal by inducing immediate early genes, which in turn regulate the transcription of several target genes. The global changes in gene expression and the induction of the late gene involve the ultimate cellular response. The IR exerts also its direct effect on DNA by producing double strand breaks (DSB). Specific molecules sensor the DNA damage activate specific p53-dependent pathways involved in the cell cycle arrest and DNA repair. If the lesions are too extensive the cell starts the apoptotic program by activation of other specific p53-dependent cascades.*

1.4 Ionizing radiation-combined cancer therapies: inhibition of angiogenesis and ionizing radiation

1.4.1 Angiogenesis and angiogenesis inhibition

Angiogenesis

The concept of tumor-dependent angiogenesis has been around for several decades. Thirty years ago, Folkman was the first who proposed that growth, survival and dissemination of tumors are dependent on the formation on new blood vessels from the pre-existing ones (angiogenesis) (Folkman, 1971). Nowadays, it is well-established that progression of tumors must acquire new blood vessels. Holmgren showed that, to increase their size beyond 1-2 mm^3, dormant small avascular masses of tumor cells must receive an adequate blood supply of oxygen and nutrients by adjacent blood vessel vasculature ((Holmgren *et al*, 1995) and Figure 1.12).

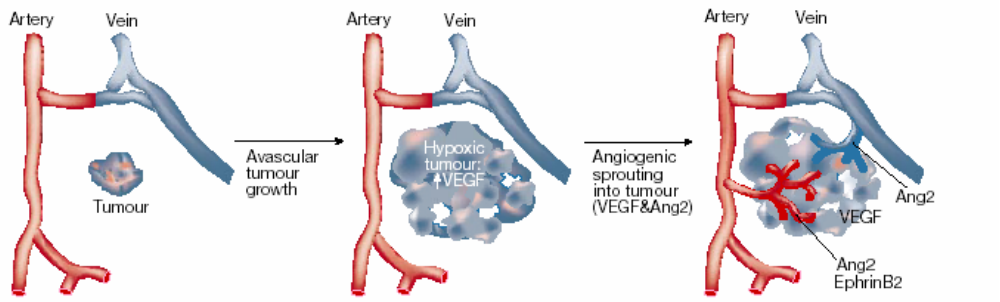

Figure 1.12 *Model of avascular tumor initiation (Yancopoulos et al, 2000).*

A variety of physiological processes requires formation of blood vessels (Carmeliet and Jain, 2000; Hanahan and Folkman, 1996; Risau, 1997). Angiogenesis is essential for normal embryogenesis, female reproductive cycles and wound healing. While endothelial cells (ECs) that line the inner surface of blood vessels are predominantly quiescent in normal adult tissues (with only 0.01% of endothelial cells in cell division cycle), they respond to different stimuli with rapid activation of the angiogenesis process. In this process, the basement membrane surrounding endothelial cells is locally degraded, leading to stimulation of the quiescent endothelial cells. Rapid proliferation, migration and differentiation of endothelial cells in response to the angiogenic stimulus leads to the formation of new capillary tubes. Under normal conditions, the angiogenic process is maintained by a balance between positive and

negative regulators. Positive regulators (pro-angiogenic molecules) comprise e.g. α and β fibroblast growth factor (α/β FGF), vascular endothelial growth factor (VEGF), placenta derived growth factor (PlGF), transforming growth factor β (TGF β), hepatocyte growth factor (HGF) angiogenin, and interleukin 8. Negative regulators (anti-angiogenic molecules) include among many others endostatin, angiostatin, thrombospondin-1, interferon-α, metalloproteinase inhibitors and platelet factor 4 (Folkman, 2001). Loss of this equilibrium contributes to the development and progression of a variety of 'angiogenic' pathologies including diabetic retinopathy, psoriasis, rheumatoid arthritis, cardiovascular diseases and tumor growth.

The change of the local equilibrium between positive and negative regulators is referred to as the 'angiogenic switch' and allows the tumor to expand rapidly. Several signals can cause tumor angiogenesis, such as internal environmental tumor metabolic stresses (low pressure in O_2, low pH), external stresses (ionizing radiation), immunitary or inflammatory responses and also genetic alterations (which can lead to activation of oncogenes or inactivation of tumor suppressor genes) (Carmeliet and Jain, 2000). Lack of oxygen (hypoxia) is probably the most potent factor stimulating angiogenesis under normal and pathologic conditions (Graubert *et al*, 2001). A link between O_2 level and angiogenesis has been demonstrated. It has been shown that upregulation of VEGF is induced by hypoxia in tumors (Shweiki *et al*, 1992) (Figure 13). The mechanism of hypoxic signaling involves the hypoxia inducing factor (HIF-1α) which binds to the hypoxia response element (HRE) located in promoter regions of numerous genes encoding e.g. VEGF, VEGF receptors (VEGFR) 1 & 2, NO synthase, angiopoietin-2 (Ang2) and PDGF (Gerber *et al*, 1997). VEGF is produced and secreted by many tumors (Gorski *et al*, 1999). It is the most potent and specific growth factor for quiescent endothelial cell activation. Its binding to endothelial receptors initiates the process of new blood vessels formation through sprouting angiogenesis.

The newly formed vasculature of solid tumors differs from the regular, ordered vasculature of normal tissues. The blood vessels in tumors are often highly structurally and functionally abnormal. As a consequence, blood flow is disturbed, chaotic and variable leading to the formation of heterogeneously distributed hypoxic areas in the tumor (Helmlinger *et al*, 1997). These latter areas often represent an obstacle for successful radiotherapy treatment as missing oxygen hampers DNA damage.

Formation of new blood vessels is also associated with immune and inflammatory responses in the pathological conditions (Carmeliet and Jain, 2000; Risau, 1997). Vasodilatation and

vascular permeability occurring during the inflammation process could be the main causes of the 'angiogenic switch' in certain pathologies. In addition, monocytes, macrophages, platelets and various leukocytes are recruited at the inflammatory site where they produce and liberate a large number of angiogenic factors such as VEGF, PlGF, angiopoietin-1 (Ang1), bFGF, TGF-β1 and PDGF (Carmeliet and Jain, 2000). Some of them chemoattract fibroblasts, endothelial cells or smooth muscle cells that in turn liberate additional angiogenic factors (Kunimoto, 1999).

Angiogenesis inhibition

As most solid tumors are angiogenesis-dependent, a therapy based on the suppression of the tumor bed vasculature represents an attractive strategy for treatment of a wide range of tumors (Keshet and Ben-Sasson, 1999). Two major types of strategies have been proposed to target the tumor vasculature: anti-angiogenic therapy, which aims at preventing the formation of new blood vessels and anti-vascular therapy, which aims at destroying the already-existing tumor vasculature (Kerbel, 2001). There are currently more than 50 anti-angiogenic agents undergoing evaluation in human clinical trials (http://www.angio.org) and a multitude of promising new candidates are under investigations, *in vitro* and in animal models.

A wide variety of the anti-angiogenic therapies has been devised to inhibit various steps of the angiogenic cascade including inhibitors of endothelial cell proliferation (e.g. fumagillin derivative TNP-470, angiostatin and endostatin), inhibitors of extracellular matrix (e.g. monoclonal antibody for the integrin $\alpha_v\beta_3$), inbibitors of cell-cell adhesion molecules (e.g. VE-cadherin-blocking antibodies), or drugs that block activators of angiogenesis and their cognate receptors have been devised (e.g VEGF and VEGFR by antibodies, VEGFR tyrosine kinase inhibitors such as SU5416, ZD4190 and PTK7871/ZK 222584). A complete list and descriptions are reported by Hagedorn and Bikfalvi (Hagedorn and Bikfalvi, 2000).

In contrast to the anti-angiogenic strategies, the approach of antivascular strategies is aiming at the destruction of tumor blood vessels by using tumor-specific agents (Taraboletti and Margosio, 2001). The mechanism of action of these agents is to selectively target the tumor vasculature that is different from the normal vasculature. Peptide antibodies, chemotherapeutic drugs (Arap *et al*, 1998), toxins (Arora *et al*, 1999) and cytokines (Halin *et al*, 2002) have been developed. Phase I trials of vascular disrupting agents such as ZD6126, a microtubular cytoskeleton targeting agent in endothelial cells, have shown significant

reduction of tumor volume (Siemann *et al*, 2004). A potential effect of ZD6126 might enhance the effect of combined radiotherapy (Wachsberger *et al*, 2005).

Targeting tumor vasculature with angiogenesis inhibitors, chemotherapeutic drugs or gene therapy delivery systems represents a very promising anti-tumor approach to inhibit tumor growth and even eradicate tumors. In contrast to standard anticancer treatments, tumor vasculature-directed therapies have several important advantages: (i) vascular endothelial cells are in direct contact with the blood stream, which facilitates the administration of the drugs (ii) the therapy is tumor-type independent (iii) the targeting is tumor-specific and has little toxicity on normal tissue (iv) contrary to tumor-cells, endothelial cells are genetically stable, thus avoiding the problem of drug resistance.

1.4.2 Angiogenesis inhibition and ionizing radiation

Recent preclinical studies suggest that combination of angiogenic blockade with IR enhances the efficiency of radiotherapy. For instance, blockade of VEGF was shown to increase the antitumor effects of IR (Gorski *et al*, 1999) and interaction between radiation inducible TNF-α and X-rays has been shown within tumor vessels (Mauceri *et al*, 1996). Negative regulators of angiogenesis such as angiostatin showed improved tumor eradication in combination with ionizing radiation (Gorski *et al*, 1998; Mauceri *et al*, 1998). Similar success was achieved by a gene therapy delivery method of endostatin in combination with ionizing radiation treatment (Shi *et al*, 2003). Hari *et al* showed that angiostatin and IR interact by inducing death of dividing endothelial cells (Hari *et al*, 2000). At this time, angiostatin is completing phase I clinical trial as an anti-angiogenic drug and radiosensitizer.

The list of the current anti-angiogenic/vascular targeting agents and in combination with radiotherapy was recently reviewed (Wachsberger *et al*, 2003). Combination of anti-angiogenic/vascular targeting agents and radiation therapy represent a highly promising strategy of cancer treatment, since additive and synergistic responses were observed. Although the mechanisms of enhancement are not well understood, it might be that interactions of drugs and ionizing radiation occur most predominantly at the level of the vascular endothelium (Hallahan *et al*, 1999). Anti-angiogenic/anti-vascular therapies might increase endothelial cell apoptosis (Lee *et al*, 2000). As a consequence, endothelial cells are more sensitive to IR, thus leading to increased endothelial cells apoptosis (Folkman and Camphausen, 2001; Gupta *et al*, 2002; Kozin *et al*, 2001) and to an increase of apoptosis of

tumor cells supported by the endothelial cells (O'Reilly *et al*, 1996). Further investigations will help in determining the involved mechanisms and to explore which compounds and combinations of compounds will work best with radiation on tumor vasculature.

2 AIM OF THE STUDY

At the start of my PhD thesis, gene therapy targeted by ionizing radiation has emerged as a promising approach to improve cancer treatment. This therapy is based on the use of promoters responsive to IR, which drive the expression of toxic molecules to the tumor. The goal of this work was to identify promoters responding to IR in endothelial cells. Such IR-activated promoters would be used to deliver anticancer factors specifically in the tumor vasculature. Indeed, the tumor vasculature has acquired the status of major target for cancer therapy, since angiogenesis was identified as a key process in tumor development. Targeting of drugs to the vascular endothelial cells has been shown to enhance the efficacy of radiotherapy.

In an attempt to develop a novel IR-inducible gene therapy system targeted to tumor vasculature, I set myself the following goals:

1) To study the gene expression patterns of endothelial cells exposed to low, high and fractionated doses of ionizing radiation.

2) To evaluate and identify potential radiation-inducible promoters from the gene profiling studies.

3) To study the response of artificial promoters to ionizing radiation.

4) To express a toxin gene under the control of the ionizing radiation-inducible promoter in endothelial cells.

3 TRANSCRIPTIONAL RESPONSES OF ENDOTHELIAL CELLS TO IONIZING RADIATION

3.1 Introduction

Exposure of mammalian cells to ionizing radiation can lead to the activation of several signal transduction pathways responsible for the maintenance of genomic integrity. These events may result in cell cycle delay, DNA repair, cell death and transcriptional responses.

Transcriptional changes are extremely complex due to their dependency on interacting signal transduction pathways, cell type specific factors and the genetic background. Modern integrative approaches enable high-throughput studies of the multiple changes resulting from the interplay of various pathways. One of the recently-developed techniques, cDNA microarray, permits the analysis and comparison of the relative expression levels of thousands of mRNA transcripts simultaneously in a single hybridization experiment.

The cDNA microarray technology was used to study changes in gene expression after ionizing radiation by several groups (reviewed in (Snyder and Morgan, 2004)). However, most of the studies focused on the effect of IR on various tumor cell types whereas none of them studied the effect of IR on tumor vasculature.

In this work, we used the cDNA microarray technology to identify gene expression in endothelial cells following ionizing radiation (Section 3.3.2). The human umbilical vein endothelial cells immortalized by fusion with a human lung carcinoma cell line (EA.hy 926) were selected as an endothelial cell model system. Gene expression profiling was examined in EA.hy 926 cells after treatment with low doses of IR (3 Gy), in order to simulate a single round of radiotherapy. Extensive analyses using high doses (20 Gy) were performed to examine the effects of total radiation delivery to the tumor. To follow the temporal pattern of gene expression modulation, three different time points (1 h, 6 h and 12 h) were examined.

Comparative cDNA microarray experiments using different IR doses, different cell culture growth conditions and different endothelial cells were performed to better understand the effects of irradiation on the cellular transcriptome.

In addition to gene expression modulations by IR treatment, the effects of IR exposure were on cell cycle progression, checkpoint signal transduction pathways, proliferation and apoptosis in EA.hy 926 were also measured (Section 3.3.1). Evaluation of these biological effects will help in understanding the relationship between the induction of these responses to IR and the IR-induced alterations in gene expression.

3.2 Materials and Methods

Cell culture The human EA.hy 926 cell line was originally obtained by fusion of human umbilical vein endothelial cells (HUVEC) with a human lung carcinoma line (Edgell *et al*, 1983). These cells were cultured at 37°C in a 5% CO_2 humidified atmosphere and maintained in DMEM (Omnilab) supplemented with 10% FBS (Seromed) and 1% penicillin and streptomycin (Omnilab).

The formation of capillaries (tube like-structures) was induced by plating the EA.hy 926 cells on gelatinized dishes and culturing as described above. As cells reached confluence, the medium was replaced with DMEM containing 10% FBS, 1% PS and 1.5 mg/ml collagen. Collagen had been extracted from sterilized rat tails by using diluted acetic acid (1:500). 5 days following the addition of collagen, the newly formed capillaries were irradiated with a dose of 3 Gy. EAHy926 in tubes were removed by partial trypsination, allowing the tubes to detach from the remaining monolayer.

The primary human microvascular endothelial cells HMEC were purchased from Cascade Biologics Company. These cells were cultured in Medium 131 supplemented with Microvascular Growth Supplement, Penicillin, Streptomycin and Amphotericin B (Cascade Biologics, Inc.). The cells were cultured at 37°C in a 5% CO_2 humidified atmosphere and used at passage 3.

Irradiation treatments Irradiation was carried out at room temperature in single doses from 1 Gy to 20 Gy using an X-ray machine (Philips PW 2184/00-Monitor SN4) in a chamber with 300 kV intensity.

Cell cycle analysis Cycling EA.hy 926 cells were harvested prior to irradiation (0 h) and at 6, 12, 24 and 48 h after 3 Gy and 20 Gy for cell cycle analysis. After trypsinisation, $1.2x10^6$ cells were harvested and spun down and washed with 1-2 ml of cold PBS. After centrifugation, the pellet was dissolved in few drops of PBS and 1ml of 70% ethanol was added dropwise. After 30 min on ice, the cells were spun down and washed with 1-2 ml of PBS. The pellet was resuspended in 250 µl of PBS, 100 µg/ml of Rnase A (Sigma) was added and the mixture was incubated for 30 min 37°C. 20 µg/ml of propidium iodide (Sigma) was added and incubated on ice in the dark for 30 min or until flow cytometry analysis. DNA

content was analyzed by flow cytometry with a FACS Epics Altra (Beckman-Coulter). The software program "Expo 32" vs1.28 was used to determine the cell cycle phase distribution.

Preparation of Protein Extracts Confluent EA.hy 926 cells were harvested prior to irradiation (0 h) and at 1, 6 and 12 h after IR exposure, for protein isolation. They were trypsinised, washed in cold PBS and pelleted. Cell lysis was performed on ice for 20 min in 50 mM Tris-Cl pH 8, 350 mM NaCl, 1% NP40 (Calbiochem), 1 mM EDTA, Complete EDTA-free proteinase inhibitors 1X (Roche), 1 mM PMSF, 2 μg/mL aprotinin, 0.7 μg/mL pepstatin. Insoluble material was pelleted by centrifugation at 14,000 rpm for 3 min at 2°C. Protein concentration in the supernatant fraction was determined using a protein assay (Bio-Rad) which is based on the Bradford method. As a standard, bovine serum albumin (BSA) was used.

Western blotting 50 μg of total proteins from each sample were loaded on a 12.5% gel SDS-PAGE and transferred to a Hybond-P membrane (Amersham pharmacia biotech).
The blots were first blocked for 1 h at 37°C with TBST (0.1% Tween 20 in Tris-buffered saline) containing 5% non-fat dry milk, and then incubated with the respective primary antibodies (Phospho ATM Ser1981, Cell Signaling 4526; Chk2 Anti-CDS1, Upstate biotechnology 07-057; Phospho Chk2 Thr68, Cell Signaling 2661; p53, Transduction Laboratories P21020; p21, Upstate 05-345; TFIIHp89, Santa Cruz sc-293) for 1 h at room temperature. After washing with TBST, the blots were incubated with secondary antibodies, horseradish peroxidase-conjugated sheep anti-mouse or anti-rabbit Ig (NA931V and NA934V Amersham Pharmacia, respectively) for 1 h at room temperature. The protein-antibody complexes were detected with the enhanced chemiluminescence system (Amersham Pharmacia). All experiments were performed at least twice.

Cell proliferation assay 100 000 EA.hy 926 cells per 60 mm plate were cultured for 5 days following ionizing radiation and then washed twice in PBS. The remaining adherent cells were stained with 1ml of the staining solution (0.1% crystal violet / 1 mM $MgCl_2$ / 10 mM potassium phosphate pH 7.4 / 250 mM saccharose) for 30 min. After solubilisation of the crystal violet stain with 10 % acetic acid, the dye uptake was calculated by measuring the

absorbance at 595 nm. Cell proliferation following ionizing radiation was calculated relative to the untreated cells. The results represent the mean of two independent experiments.

Apoptosis Assay Apoptosis following IR was detected using Cell death detection ELISA kit (Roche). This assay is based on a quantitative sandwich-enzyme-immunoassay principle, using mouse monoclonal antibodies directed against DNA and histones, respectively. This allows the specific detection and quantification of mono- and oligonucleosomes which are released into the cytoplasm of cells, which die from apoptosis. Floating and adherent EA.hy 926 cells were collected at 1, 6, 12, 24 and 48 h, harvested by centrifugation and washed with cold PBS. After cell lysis in incubation buffer (ELISA kit) during 30 min, the lysate was centrifuged at 15000 rpm for 10 min. Supernatants (= cytoplasmic fractions) were used, in triplicates, for the immunoassay. Absorbance was measured at 405 nm using an ELISA reader.

Preparation of RNA Total RNA was extracted using an affinity resin column (RNeasy Mini Kit, Qiagen) followed by a DNAse treatment (Qiagen).
Total RNA was isolated from $5x10^6$ cultured EA.hy 926 cells, unirradiated (0 h) or 1 h, 6 h and 12 h after irradiation treatment with 3 Gy or 20 Gy. Cells were harvested at the respective time points and stored in RNA later (Ambion) until total RNA extraction. Extraction was performed in triplicates for confluent EA.hy 926.
Total RNA was extracted from EA.hy 926 cells, unirradiated (0 h) or 6 h after irradiation with 3 Gy, 3+3+3 Gy (12 h intervals) or 9 Gy, from capillary-like EA.hy 926 cells unirradiated (0 h) or 6 h post 3 Gy and from confluent HMEC cells, unirradiated (0 h) or 1 h, 6 h and 12 h after 3 Gy.

Microarray experiments Twenty micrograms of total RNA were used to synthesize double-stranded cDNA using a cDNA synthesis kit (Invitrogen). The resulting template was used to synthesize biotin-labeled antisense cRNAg in a T7 RNA polymerase-catalysed reaction (MEGA Script™ T7 *in vitro* transcription kit, Ambion, Austin, TX) with biotin-containing ribonucleotides (LOXO). Labeled cRNAs were then purified (RNeasy Mini Kit, Qiagen) and chemically fragmented. 15 µg of cRNA were hybridized with human U95Av2 GeneChip arrays (Affymetrix Inc.) carrying *in situ* synthesized oligonucleotides representing 12625

functionally characterized sequences. The GeneChips were scanned using the Agilent GeneArray Scanner.

Microarray data Analysis Raw microarray data were extracted from Microarray Suite software (Affymetrix). The data were analyzed using two different softwares.

GeneSpring software (Silicon Genetics) was used to analyze the gene expression profiles of irradiated EA.hy 926, irradiated capillaries and irradiated HMEC cells.
Selection of the expressed genes on the cDNA microarray GeneChip (referred as to the unsupervised hierarchical clustering analysis) was obtained using the pre-selected criteria: (i) Normalization "Per Chip and per Gene"; (ii) at least half of the total number of experiments with the flags "Present". Statistical analysis on the selected expressed genes was referred to as the supervised hierarchical clustering analysis. The statistically significant gene sets were obtained using the parameter distinguishing the treated from the non-treated samples and using a statistical parametric test (p-value of 0.05) without multiple corrections. The gene expression clustering trees were visualized using Cluster and Tree-View tools with a Pearson correlation.
A further statistical analysis was performed. A signal ratio value based on the signal value of the treated (or non-treated) samples *versus* untreated (or non-treated) samples was applied. In addition, a fold change with a cut-off of 1.5 was applied leading to a stringent statistically significant gene list.

Data Mining Tool software (Affymetrix) was used to analyze the gene expression modulations in irradiated EA.hy 926 1 h, 6 h and 12 h post 3 Gy and 20 Gy.
For each time point, three independent experiments were carried out and the corresponding controls. The data were evaluated with absolute analysis, which measures, for each array, the abundance of transcripts (signal) and the specificity of hybridization (P=present, M=marginally present, A=absent). The fold change was generated by the Affymetrix software based on the comparison of the average transcript signal values of IR-treated cells *versus* the average transcript signal value of three non-treated cells (Signal Log Ratio).
The following formula shows the fold change calculated by the software:

$$\text{Fold Change} = \begin{cases} 2^{\text{Signal Log Ratio}} & \text{Signal Log Ratio} > 0 \\ (-1) * 2^{-(\text{Signal Log Ratio})} & \text{Signal Log Ratio} < 0 \end{cases}$$

In order to eliminate genes with low abundance and to identify significant changes, we used the following selection procedure. We analyzed the data according (i) to the level of modulation (>1.5-fold change for activation and <1.5-fold change for repression), (ii) to the signal value; average transcript level in treated cells for up-regulated genes (or average transcript level in untreated cells for down-regulated ones) >100 (iii) to the presence of at least two 'P=present' values in the three experiments for up-regulated genes (or in the three untreated experiments for down-regulated), (iv) to the significance of a statistical T-Test (p-value cut-off of 0.05, unpaired T-Test).

Quantitative RT-PCR EA.hy 926 cells were harvested prior to irradiation (0 h) and at 1, 6 and 12 h after 3 Gy or 20 Gy exposures for total RNA isolation (RNA samples used for the cDNA microarray experiments). The three replicas from each time point of each irradiation dose were pooled together. One-step RT-Real time PCR was performed with the Roche LightCycler System using the Light Cycle-RNA Master SYBR Green I (Roche) kit according to the manufacturer's instructions. 0.3 μM of each oligonucleotide primer (Microsynth) and 300 ng of total RNA were used in 20 μl reaction volume.

Six genes were tested to confirm the altered expression from the cDNA microarray data. The primers are listed in the Table 3.1 and the quantitative RT-PCR conditions are shown in Table 3.2.

Table 3.1 *Primers used for quantitative RT-PCR.*

Gene	Forward primer (5'-3')	Reverse primer (5'-3')	PCR product size (bp)
BTG2	AGGAGGCACTCACAGAGCACTAC	CTGCCGAGGTAGACGCAGAACAT	221
NK4	TGCCAACTCTGCCTCTCTTCAC	ACTGTCTCCAGGTAGCCCTCTTTG	143
4-1BB	AGCCACTCTGTTGCTGGTCCTC	ACTGCCTGCATATGTCACAGGTCC	175
RANTES	TGCGCTCCTGCATCTGCCTCC	TCTCTGGGTTGGCACACACTTGG	180
Fas/Apo1	TGAACCAGACTGCGTGCCCTGC	TCTGCACTTGGTATTCTGGGTCCG	151
p50 NF-κB	ACCTCGTGCTCATGCCCACAGTC	AGCGGAGCCGCTGCCTCTG	178
GAPDH	ACGGTGCCATGGAATTTGCCATGG	GGTTTAGGCAACTGAGGCTGGAAG	168

Table 3.2 *Quantitative RT-PCR conditions.*

	Temp (°C)	Time (sec)	Cycles
Reverse transcription	61	1200	1
Denaturation	95	120	1
Amplification			35
Denaturation	95	5	
Annealing	55	5	
Extension	72	10	
Melting curve			1
Phase 1	95	5	
Phase 2	65	15	
Cooling	40	30	1

The cycle corresponding to the beginning of the log phase amplification was denominated 'threshold amplification cycle' (TAC). One cycle difference in TAC corresponds theoretically to a two-fold change in RNA concentration. Fold changes were obtained by normalizing to GAPDH used as an internal reference. All experiments were performed in duplicate and the specificity of each amplification product was verified on a 2 % agarose gel electrophoresis.

3.3 Results

3.3.1 Biological responses of endothelial cells to ionizing radiation

3.3.1.1 Cell cycle arrest

It is known that exposure of cells to ionizing radiation delays the normal progression through the cell cycle (see Chapter 1, Section 1.3.2). Here we examined the cell cycle distribution of EA.hy 926 using flow cytometry. The result in Figure 3.1 shows that exposure of cells to low doses of 3 Gy has little effect with a transient slight arrest of the cell cycle in G2/M at 6 h and 12 h post-IR. In contrast, cells exposed to higher doses of 20 Gy underwent cell cycle arrest over a long time period. Following 20 Gy, cells showed an evident arrest in G2/M phase at 12h, 24 h and 48 h. A transient delay in the progression through S phase at 6 h was also observed at 20 Gy. The disappearance of cells in S-phase at 48 h post 20 Gy suggests that the cells were arrested in G1/S phase.

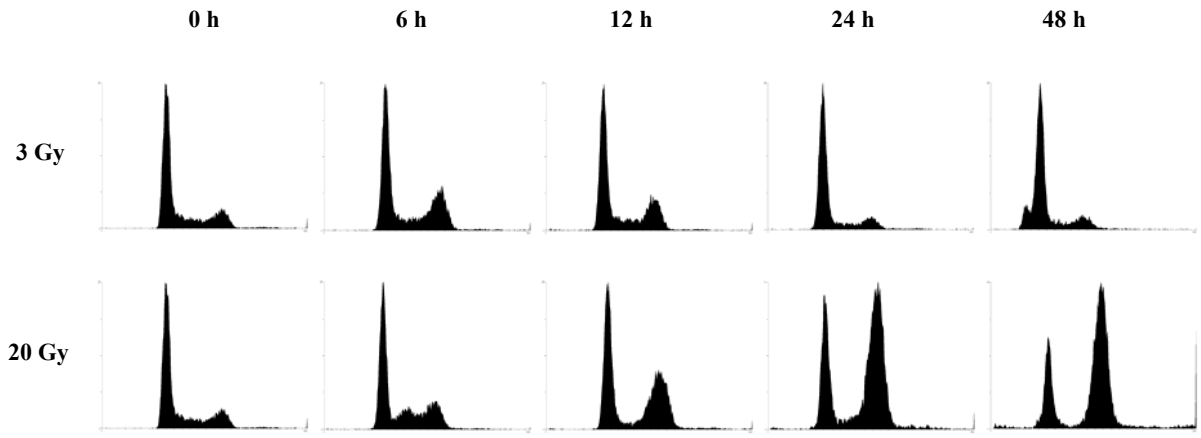

Figure 3.1 *Flow-cytometric analysis of cell cycle progression of EA.hy 926 after ionizing radiation treatment (3 Gy and 20 Gy). Following 3 Gy, cells show a slight transient arrest in G2/M whereas Following 20 Gy cells underwent a pronounced G2/M arrest, a transient delay in S phase and a G1/S arrest. Y axis represents the number of cells; X axis represents the DNA content.*

3.3.1.2 Signal transduction

As shown in the previous paragraph, radiation induced cell cycle delays in endothelial cells. To inhibit cell cycle progression, checkpoint pathways are activated by DNA damage inducers such as IR (see Chapter 1, Section 1.3.2). These radiation-induced cell cycle checkpoints are widely thought to reduce or eliminate inherited genetic abnormalities by providing cells with more time to repair DNA damage prior to replication (G1/S transition) or mitosis (G2/M transition). ATM and Chk2 are two important checkpoint proteins involved in the DNA damage signal transduction pathway. In Figure 3.2, activation of these checkpoints by IR is shown in endothelial cells by Western blotting. Activation of ATM by phosphorylation on serine 1981 was observed at the lowest (1 Gy) and the highest (20 Gy) tested dose. A dose-dependent response was observed at 1 h post-IR, whereas at 12 h post-IR, saturation of ATM phosphorylation occured for 6, 9 and 20 Gy. In the signal transduction cascade, ATM phosphorylates Chk2 on threonine 68 (Thr68). In Figure 3.2, Chk2 phosphorylation on Thr68 was detected in a range of doses from 3 Gy to 20 Gy. Higher levels of Chk2 Thr68 were detected at 1 h and 6 h as compared to the 12 h time point. In addition, for each time point, Chk2 Thr68 phosphorylation levels decreased when the IR doses increased. The highest levels among the tested IR doses are shown at 1 h, 6 h and 12 h following 3 Gy. Correlation of total Chk2 decrease with Chk2 phosphorylation event was visible at 1 h post-IR.

In the IR-induced signal transduction cascade, p53 is activated and stabilized by post-translational modifications such as phosphorylations by upstream kinases such as ATM and Chk2. In this study, p53 phosphorylations were not tested but the quantity of p53 was assessed. In Figure 3.2, p53 was detectable at high doses after 6 and 12 h post-IR. Its target gene $p21^{Cip1/WAF1}$ was also induced at high doses (9 Gy and 20 Gy) but also in a more modest manner at lower doses. Indeed, p53 acts as a transcription factor by inducing the transcription of $p21^{Cip1/WAF1}$. The detectable increase of $p21^{Cip1/WAF1}$ at 12 h after 1, 3, 6, 9 and 20 Gy and at 6 h after 9 and 20 Gy suggests its transactivation by p53. The $p21^{Cip1/WAF1}$ is an inhibitor of cyclin-dependent kinases that control entry into S phase.

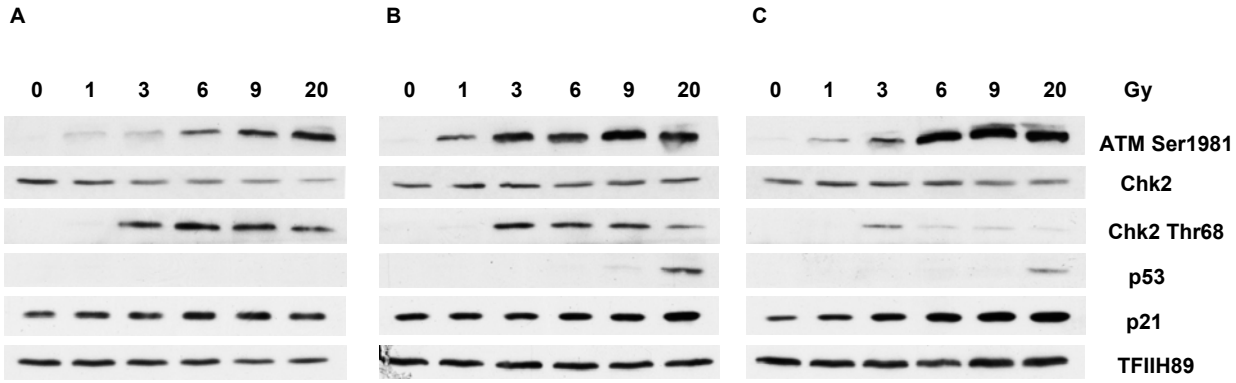

Figure 3.2 *Western blotting analyses in confluent EA.hy 926 exposed or not to IR and harvested 1 h (panel A), 6 h (panel B) and 12 h (panel C) post IR treatment. Results show phosphorylations of ATM protein on serine 1981 and Chk2 protein on threonine 68 by IR (panel A, B and C), total Chk2 modulation (panel A, B and C), p53 increase with 9 Gy (panel B) and with 20 Gy (panels B and C), upregulation of p21 Cip1/WAF1 level (panels B and C). TFIIH p89: loading control.*

3.3.1.3 Antiproliferation activity

Ionizing radiation treatment inhibits cellular proliferation. To detect the antiproliferative effect of ionizing radiation on endothelial cells, we treated EA.hy 926 with increasing doses of X-rays. 5 days after IR treatment, cell proliferation was assessed with crystal violet staining. EA.hy 926 proliferation activity decreased in an IR dose-dependent manner. Following 3, 6, 9 and 20 Gy, significantly reduced proliferation activity was observed, whereas no significant decrease was measured at 1 Gy. At the highest measured dose of 20 Gy, proliferation activity was decreased to 30 % compared to non-irradiated cells (Figure 3.3).

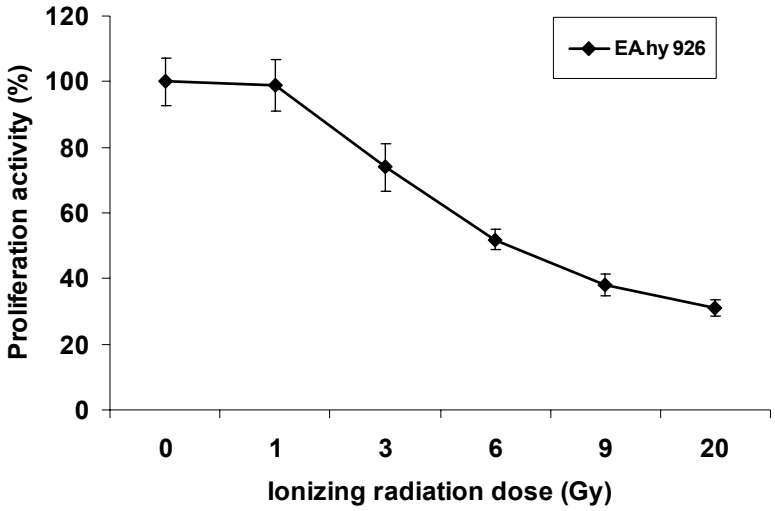

Figure 3.3 *Effect of ionizing radiation on proliferation activity in EA.hy 926 cells. 5 days after ionizing radiation treatment, cell proliferation was determined by staining with crystal violet. The cell proliferation of non-irradiated cells was used as 100%. Y-axis values are presented as means (± SD) for two independent experiments.*

3.3.1.4 Apoptosis activity

To assess apoptosis induction in EA.hy 926 cells, we performed a photometric enzyme immunoassay based on cytoplasmic and histone-associated DNA fragment (mono- and oligonucleosomes) detection after induced cell death (Cell Death detection ELISA, Roche). We performed a time course, with increasing doses of X-rays on EA.hy 926. After 1 h, 6 h, 12 h and 24 h, we could not detect significant apoptosis (background), whereas at the time point of 48 h significant apoptosis was detected (Figure 3.4). The experiment was repeated in triplicate at 48 h post-IR and the results are shown in Figure 3.5. Significant increase in apoptosis was observed after 48 h with 3 Gy, 6 Gy, 9 Gy and 20 Gy. Maximum apoptosis was detected with 6 Gy and 9 Gy, whereas at higher doses such as 20 Gy, less apoptosis was detected. The level of apoptosis at 20 Gy was comparable to the level of 3 Gy.

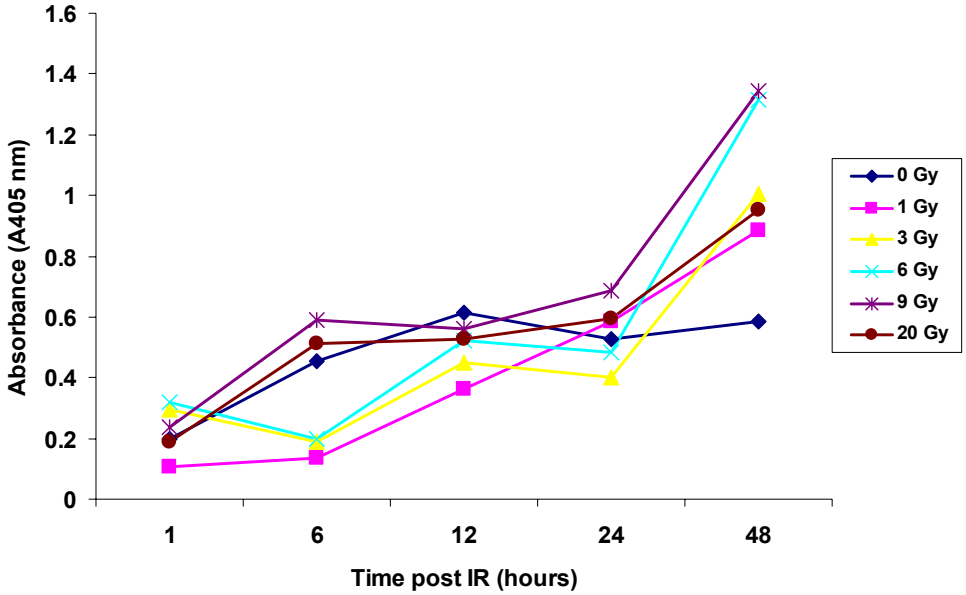

Figure 3.4 *Effect of ionizing radiation on the apoptotic machinery in EA.hy 926 cells at various time points after IR. Apoptosis was measured in cytoplasmic cell extracts 1, 6, 12, 24 and 48 h after IR treatment using a photometric enzyme immunoassay. Absorbance values at 405 nm are shown here 30 min after addition of the colorimetric substrate (2,2'-azino-di-[3-ethylbenzthiazoline sulfonate]).*

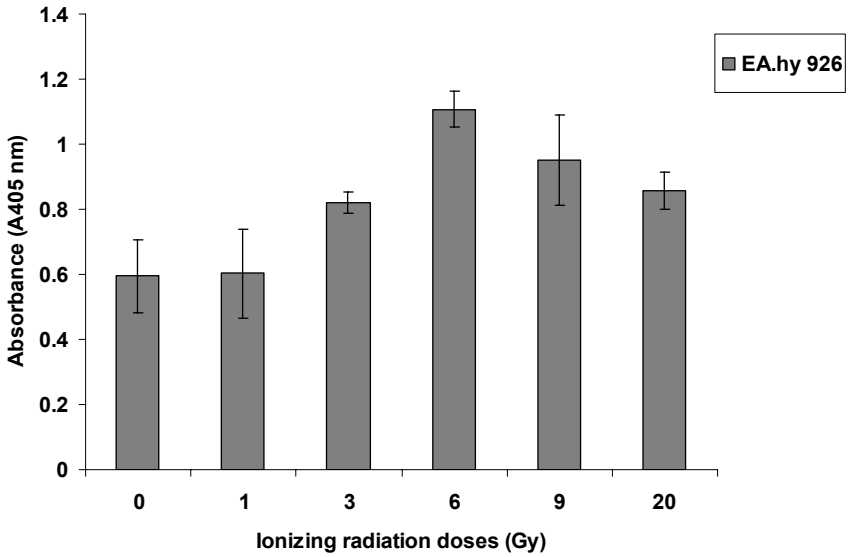

Figure 3.5 *Effect of ionizing radiation on the apoptotic machinery in EA.hy 926 cells 48 h post-IR. Apoptosis was measured in cytoplasmic cell extracts using a photometric enzyme immunoassay. Absorbance values at 405 nm are shown here 30 min after addition of the colorimetric substrate ((2,2'-azino-di-[3-ethylbenzthiazoline sulfonate]). Measurements were performed in triplicates.*

3.3.2 Gene expression profiling of endothelial cells exposed to ionizing radiation

3.3.2.1 Gene expression profiling of irradiated EA.hy 926

Overview of the gene expression patterns following IR exposure

RNA was isolated from EA.hy 926 at 1, 6 and 12 h post 3 Gy and post 20 Gy. These early time points were expected to reflect the rapid and acute alterations induced by IR in the transcriptome.

Figure 3.6 and Figure 3.7 show an overview of the gene expression patterns in EA.hy 926 with respect to doses and time after IR. We used the clustering gene tree organization from Genespring software with selection filters as described in *Materials and Methods*. Hierarchical unsupervised clustering at 3 Gy (Figure 3.6, left panel) and 20 Gy (Figure 3.7, left panel) show the genes that were expressed among the 12625 genes on the cDNA microarray. In these analyses, the samples clustered according to their similarities in gene expression levels. After statistical analysis, 349 significantly modulated genes at 3 Gy (Figure 3.6, right panel) and 424 significantly modulated genes at 20 Gy (Figure 3.7, right panel) were selected. These latter numbers correspond to the number of genes that are modulated taking into account the comparison parameter of three non-IR treated samples to nine IR treated samples without time discrimination. The supervised clustering analyses reveal that activation or repression were a function of IR dose. Clusters of significantly activated or repressed genes were distinguishable for 20 Gy, whereas at 3 Gy, the weak amplitude of modulation did not allow to discriminate obvious clusters. At 20 Gy, the pattern of modulated genes changed considerably at 6 h and 12 h post-IR whereas at the early time point (1 h), only a few modulated genes could be identified (Figure 3.7, right panel). A transient expression of activated or repressed genes peaked 6 h following 20 Gy and returned to basal levels by 12 h post-irradiation. Other clusters of genes were repressed/activated at 6 h and remained repressed/activated at 12 h. In contrast, at 3 Gy, no obvious pattern of repression/activation could be distinguished.

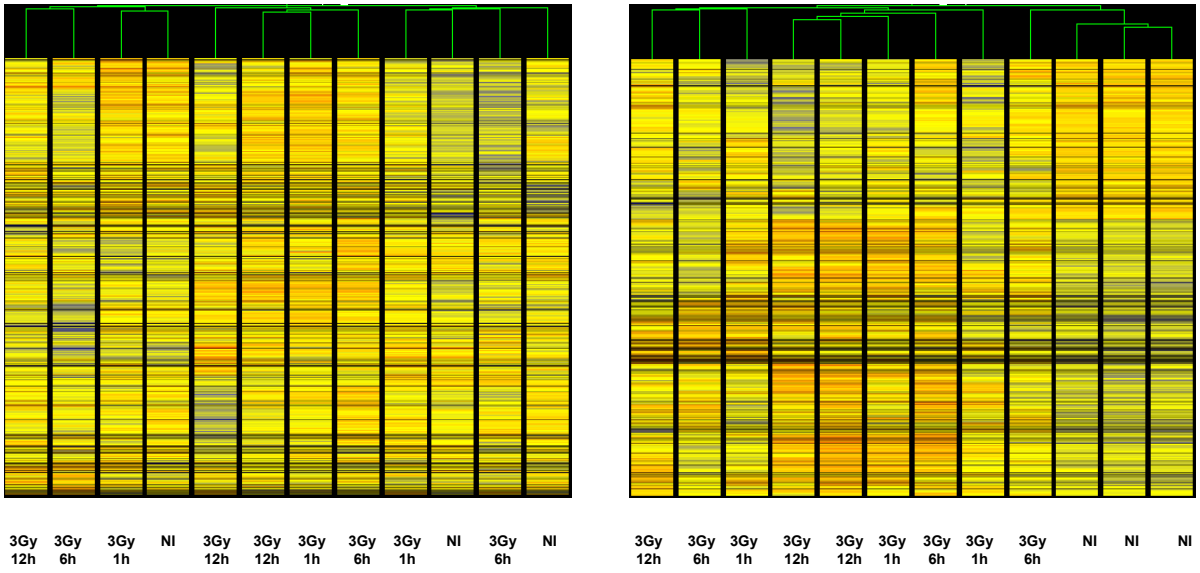

Figure 3.6 *Hierarchal unsupervised (on the left) and supervised (on the right) clustering analysis of 9 irradiated samples (1, 6 and 12 h post 3 Gy) and 3 non-irradiated samples (0 h) in EA.hy 926. The clustering of the samples (Y-axis) is based on the 5909 expressed (on the left) and on the 349 statistically significant expressed genes (on the right) represented on the X-axis. The grouping of the genes is based on the similarity between them. Genes are color-coded to indicate their expression levels relative to the median level for the gene across the entire sample (blue: lower expression; red: higher expression; yellow: no change). NI: non-irradiated. A total number of 12625 genes on the chips were tested. Applied filters for gene selection in Genespring software are described in Materials and Methods.*

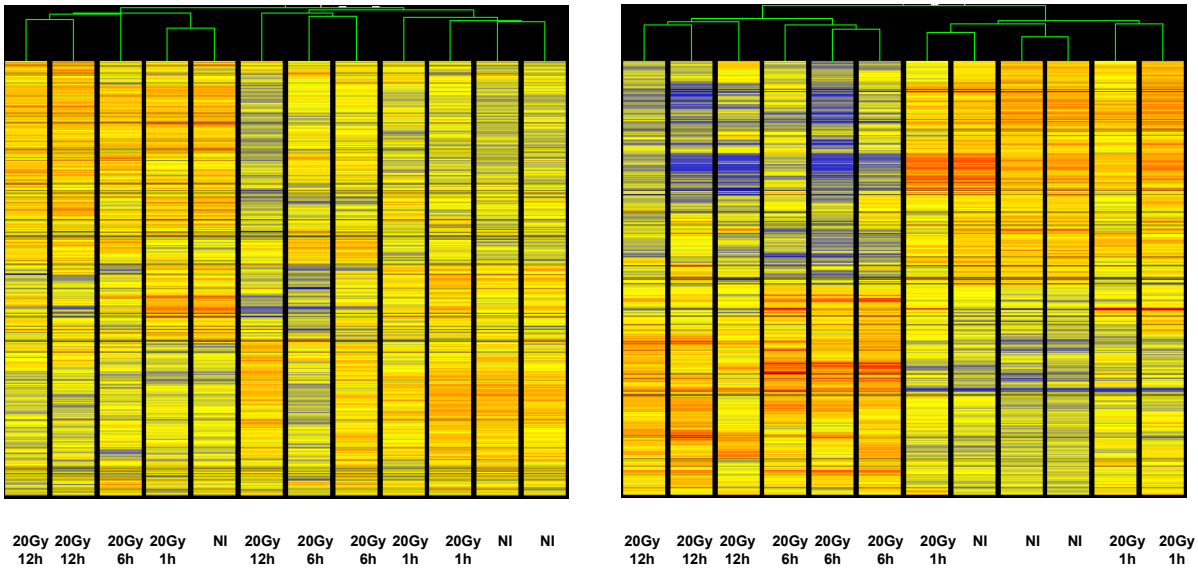

Figure 3.7 *Same as Figure 3.6, but after 20 Gy exposures. The clustering of the samples (Y-axis) is based on the 5988 expressed genes (on the left) and on the 424 statistically significant expressed genes (on the right) represented on the X-axis.*

View of IR-responsive genes: selected examples

Some examples of the significant genes are shown in Figure 3.8 and Figure 3.9.

In Figure 3.8, zoom-in on the hierarchical supervised clustering tree permits to visualize modulated genes at 3 Gy. Genes were color-coded to indicate their expression levels relative to the median level for the gene across the entire sample (blue: lower expression; red: higher expression; yellow: no change). BTG2 gene expression was increase at 3 Gy. The brightness of the colors reflects a high number of the transcript copies hybridized to the chip. In contrast, TNFRSF6 expression level is lower as compared to the more dull color-coded view. However, a statistical significant induction of TNFRSF6 is shown following 3 Gy.

Figure 3.9, zooms-in or the hierarchal supervised clustering tree and permits to visualize modulated genes at 20 Gy. Genes including BTG2, CDKN1A, PPM1D/Wip1, XPC, TNFRSF6, NK4, CDC25C among many others were shown to be modulated at 20 Gy.

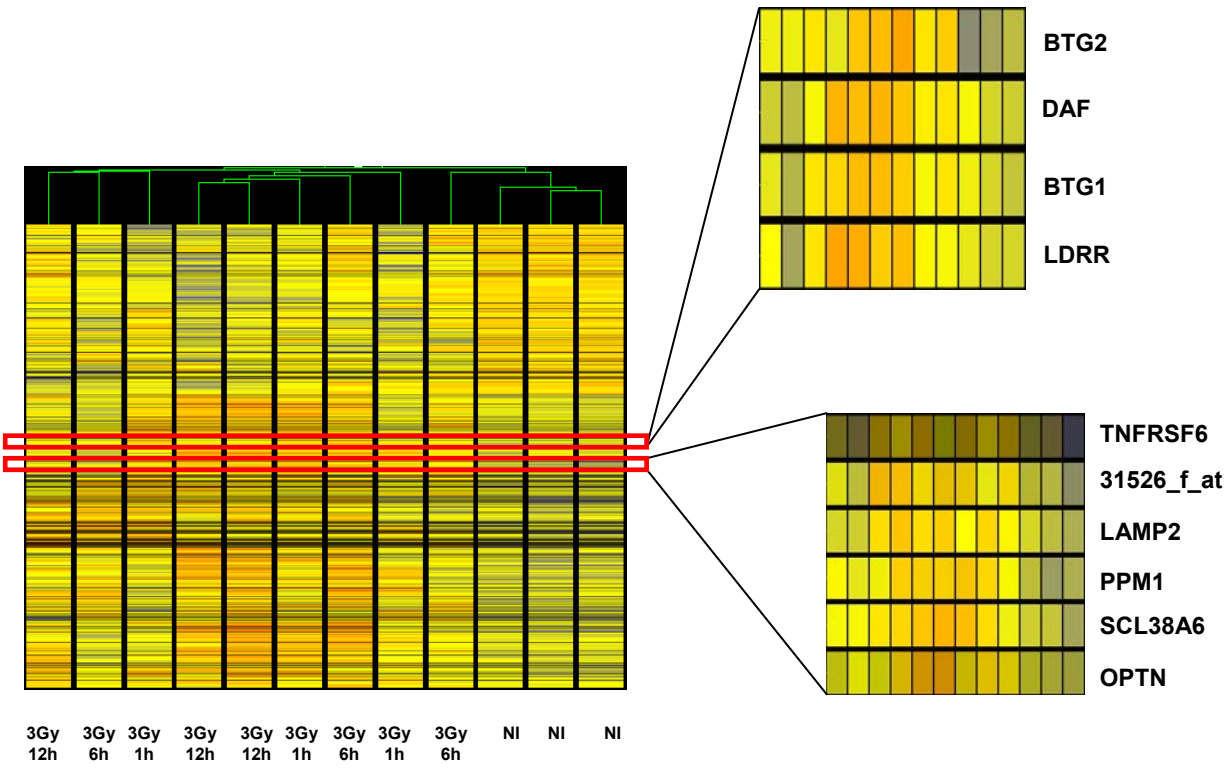

Figure 3.8 *Hierarchal supervised clustering tree of 9 irradiated samples (1, 6 and 12 h post 3 Gy) and 3 non-irradiated samples (0 h) in EA.hy 926 (refer to Figure 3.6 right). Selected examples are enlarged. The annotations correspond to the gene symbol name. The Affymetrix ID number is shown when no gene name is given in the GenBank database.*

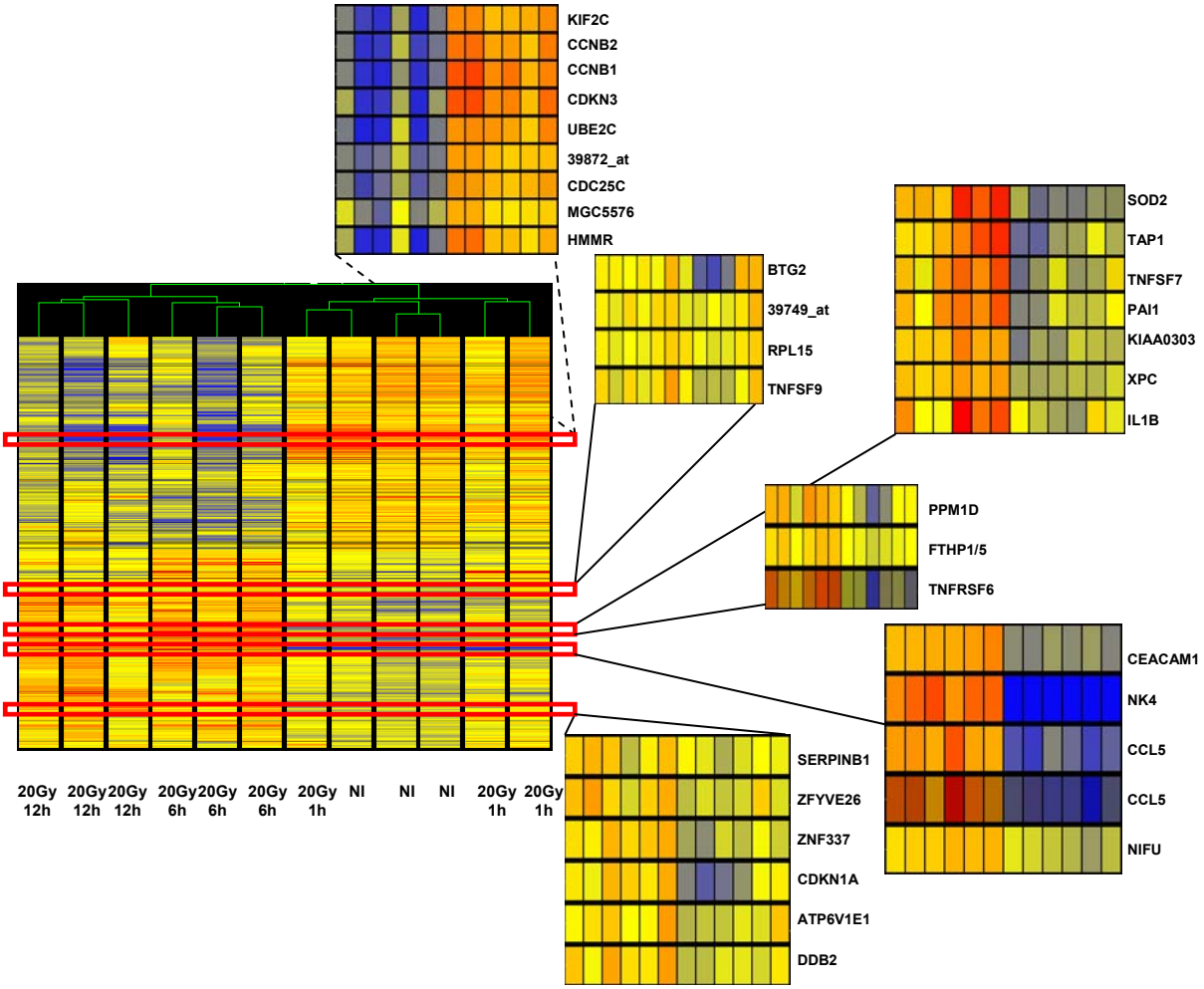

Figure 3.9 *Hierarchal supervised clustering tree of 9 irradiated samples (1, 6 and 12 h post 20 Gy) and 3 non-irradiated samples (0 h) in EA.hy 926 (refer to Figure 3.7 right). Selected examples are enlarged. The annotations correspond to the gene symbol name. The Affymetrix ID number is shown when no gene name is given in the GenBank database.*

A further selection was performed on the 349 genes and 424 genes modulated after 3 Gy and 20 Gy, respectively. A cut-off fold change of 1.5 was applied for each time point and for both doses of IR. The number of differentially regulated genes is given in Table 3.3. The output list of IR-responsive genes using Genespring software is not shown. Only the up-regulated and down-regulated genes in common with the significant genes generated by using Data Mining tool software (Affymetrix) are marked in Table 3.5 and Table 3.6.

Table 3.3 *Number of genes more than 1.5-fold up- and down-regulated in EA.hy 926 at 1 h, 6 h and 12 h post 3 Gy or 20 Gy. A total number of 12625 genes onto the chips were tested. Applied filters in the Genespring software are described in Materials and Methods.*

	3 Gy			20 Gy		
Time post-IR	1 h	6 h	12 h	1 h	6 h	12 h
Up-regulated genes	46	40	93	23	115	111
Down-regulated genes	5	13	14	8	156	135

The IR-responsive genes

IR-responsive genes following 3 Gy and 20 Gy exposures

The analysis of IR-responsive genes in EA.hy 926 at 1 h, 6 h and 12 h post 3 Gy and 20 Gy was performed using the Data Mining tool software (Affymetrix) with the applied selection criteria described in *Materials and Methods.*

24, 30 and 72 significantly up-regulated genes and 10, 18 and 18 significantly down-regulated genes were identified at 1, 6 and 12 h after 3 Gy, respectively (Table 3.4). 9, 147 and 92 significantly up-regulated genes and 8, 143 and 88 significantly down-regulated genes were identified at 1, 6 and 12 h after 20 Gy, respectively (Table 3.4). As already shown in the previous analysis (Figure 3.6, Figure 3.7 and Table 3.3), the change in expression level and number of genes was higher at the high dose. In Table 3.4, the maximal gene modulation is shown to occur at 6 h post-20 Gy and represents 1.2% of modulation. Following 3 Gy, no gene was up-regulated more than a factor 3 and one was down-regulated 3.21 fold (D-dopachrome tautomerase).

Table 3.4 *Number of more than 1.5-fold modulated genes in EA.hy 926 at 1 h, 6 h and 12 h post 3 Gy or 20 Gy (Relative numbers were given in %). FC stands for fold change. A total number of 12625 genes on the chips were tested (100%). Applied filters in the Data Mining Tool (Affymetrix) are described in Materials and Methods.*

	3 Gy						**20 Gy**					
Time post-IR	**1 h**		**6 h**		**12 h**		**1 h**		**6 h**		**12 h**	
Activated genes	**24**	0.2%	**30**	0.23%	**72**	0.57%	**9**	0.07%	**147**	1.2%	**92**	0.73%
1.5<FC< 3	**24**	0.2%	**30**	0.23%	**72**	0.57%	**7**	0.06%	**108**	0.9%	**84**	0.67%
FC>3	**0**	0%	**0**	0%	**0**	0%	**2**	0.02%	**39**	0.3%	**8**	0.06%
Repressed genes	**10**	0.08%	**18**	0.15%	**18**	0.15%	**8**	0.06%	**143**	1.1%	**88**	0.7%
1.5<FC<3	**10**	0.08%	**18**	0.15%	**17**	0.14%	**8**	0.06%	**111**	0.9%	**62**	0.5%
FC>3	**0**	0%	**0**	0%	**1**	0.01%	**0**	0%	**32**	0.3%	**26**	0.21%

The function of IR-responsive genes following 3 Gy and 20 Gy exposures

Classification of IR-responsive genes was performed according to their putative function (LocusLink and SwissProt databases). These groups include a wide variety of categories:

Angiogenesis	Cell proliferation	Homeostasis	Signaling
Apoptosis	Chromatin binding	Immune response	Stress response
Anti-apoptosis	Chromosome organization	Meiosis/Mitosis	Transcription
Biosynthesis	Cytoskeleton	Metabolism	Translation
Cell adhesion	Development	Proteasome degradation	Transport
Cell cycle	DNA catabolism	Protein folding	Miscellaneous
Cell growth	DNA repair	RNA catabolism	
Cell motility	DNA replication	RNA processing	

The distribution of the IR responder genes according to their function is given in Table 3.5 and Table 3.6. These gene lists correspond to the genes selected by Affymetrix statistical analysis listed in Table 3.4.

IR-responsive genes following 3 Gy exposure

Table 3.5 shows the genes modulated by 3 Gy. Among the up-regulated transcripts were the products of several pro-apoptotic genes (TNFRSF6/Fas/Apo1, TNFRSF10B/KILLER/DR5), cell cycle regulators (GADD45), growth inhibitors (BTG2, TIEG), signaling genes (PI3K SMGI, MAPK12) and stress response genes (PPM1D/Wip1).
Among the down-regulated genes were cell cycle regulators (E2F1, B-MYB, PLK4, GADD34).

IR-responsive genes following 20 Gy exposure

Table 3.6 shows the genes modulated by 20 Gy. Among the up-regulated transcripts were genes encoding pro-apoptotic proteins (TNFRSF6/Fas/Apo1, TNFRSF10B/KILLER/DR5), cell cycle regulators (CDKN1A), growth inhibitors (BTG2, BTG1), transcription (ATF3, NF-κB enhancers), stress response (PPM1D/Wip1), DNA repair (XPC), angiogenesis (VEGF) and immune response (NK4) factors. NK4 was the most up-regulated gene with fold changes of 85.41 and 92.06 at 6 h and 12 h, respectively.

The down-regulated transcripts included many genes involved in the cell cycle regulation such as cyclins, E2F1, B-MYB, CDC25C, CDC2 and CHK2. In addition, DNA repair (BRCA1, FANCG, XRCC3, DNAPK, RPA1), apoptosis (CASP9), anti-apoptosis (API5), angiogenesis (FLT1/VEGFR1) genes were down-regulated at 20 Gy.

Common IR-responsive genes between 3 Gy and 20 Gy

The common IR-responsive genes to 3 Gy and 20 Gy are shown in bold in Table 3.5 and Table 3.6. There are 13 genes up-regulated in common at 3 Gy and 20 Gy. They include TNFRF6/Fas/Apo-1, NFKBIA, TNFRSF10B/KILLER/DR5, BTG2, PDE4B, CBLB, PPM1D/Wip1, BCL6, ZFYVE26, SLC6A4, STC1, TPST2 and STX6.

Among the 6 common genes down-regulated at 3 Gy and 20 Gy, we identified B-MYB, E2F1, COX6A2, DHRS2, HMBS, C6orf18 and PPP5C.

Table 3.5 *Genes significantly up- or down-regulated (more than 1.5-fold) in EA.hy 926 following 3 Gy exposure. Applied filters in the Data Mining Tool (Affymetrix) are described in Materials and Methods.*

Category [a] GenBank access. no.	Gene symbol	Title	Fold Change[b]		
			1h	6h	12h
Up-regulated genes					
Apoptosis					
M58603	NFKB1	nuclear factor kappa B light polypeptide gene enhancer in B-cells 1 (p105)			1.52
M69043	**NFKBIA**	**nuclear factor kappa B light polypeptide gene enhancer in B-cells inhibitor, alpha**			2.18
AI950382	PTDSR [e]	phosphatidylserine receptor			1.61
AF016266	**TNFRSF10B** [e]	**tumor necrosis factor receptor superfamily, member 10b**			1.55
X63717/Z70519	**TNFRSF6/FAS/APO1** [e]	**tumor necrosis factor receptor superfamily, member 6**	1.7		1.67
Cell adhesion					
X79981	CDH5 [e]	cadherin 5, type 2, VE-cadherin (vascular epithelium)			1.6
X17033	ITGA2	integrin, alpha 2 (CD49B, alpha 2 subunit of VLA-2 receptor)			1.84
M55210	LAMC1	laminin, gamma 1 (formerly LAMB2)			1.52
Cell cycle					
U17105	CCNF	Cyclin F		1.66	
U83410	CUL2 [e]	cullin 2	1.81		
M60974	GADD45	growth arrest and DNA-damage-inducible, alpha	1.58		
Cell growth					
U72649	**BTG2** [d, e]	**B cell translocation gene 2**	1.84	1.94	1.61
AF050110	TIEG	TGFB inducible early growth response			1.63
X63547	USP6 [e]	ubiquitin specific protease 6 (Tre-2 oncogene)	1.6		1.51
DNA repair					
AL096744	REV3L	REV3-like, catalytic subunit of DNA polymerase zeta (yeast)			1.55
Homeostasis					
AJ006267	ClpX [e]	ClpX caseinolytic protease X homolog (E. coli)	1.85		2.11
Metabolism					
AF030555	ACSL4 [e]	acyl-CoA synthetase long-chain family member 4			1.71
U69611	ADAM17	Tumor necrosis factor, alpha, converting enzyme	1.74		
AB014511	ATP9A	ATPase, Class II, type 9A			1.56
AF038662	B4GALT4 [e]	UDP-Gal:betaGlcNAc beta 1,4- galactosyltransferase, polypeptide 4			1.67
D16611	CPOX	coproporphyrinogen oxidase			1.59
AB020645	GLS	glutaminase			1.51
U73338	MTR [e]	5-methyltetrahydrofolate-homocysteine methyltransferase	1.52		
AB002359	PFAS	phosphoribosylformylglycinamidine synthase	1.54		
L13972	SIAT4A	sialyltransferase 4A			1.54
Y14155	TMEM23 [e]	Transmembrane protein 23	2.28		
Meiosis/Mitosis					
AB002357	KIF3B [e]	kinesin family member 3B		1.52	1.51
Protein folding					
D85429	HSP 40 [e]	DnaJ (Hsp40) homolog, subfamily B, member 1		1.55	
M59830	HSP-70A1A	heat shock 70kDa protein 1A			1.85
M11717	HSPA1A/ HSPA1B [e]	heat shock 70kDa protein 1A / heat shock 70kDa protein 1B		1.85	1.83
L11066	HSPA9B	heat shock 70kDa protein 9B (mortalin-2)	1.56		
Signaling					
M18185	GIP	gastric inhibitory polypeptide	2.14		
W26023	C1orf39 [e]	chromosome 1 open reading frame 39			1.64
U26710	**CBLB**	**Cas-Br-M (murine) ecotropic retroviral transforming sequence b**			1.57
AB007860	DDEF2	development and differentiation enhancing factor 2			1.85
L36645	EPHA4	EPH receptor A4		1.95	
M57730	ephrin-A1	ephrin-A1			1.86
M21535	ERG	v-ets erythroblastosis virus E26 oncogene like (avian)			1.62

AB026118	MALT1	mucosa associated lymphoid tissue lymphoma translocation gene 1		2.25	
U07358	MAP3K12	mitogen-activated protein kinase kinase kinase 12		1.61	
AL050366	OGT	O-linked N-acetylglucosamine transferase		1.84	
U63717	OSTF1 [e]	osteoclast stimulating factor 1	1.71		
L20971	**PDE4B** [e]	**phosphodiesterase 4B**			1.72
AI610467	PI3K SMG1	PI-3-kinase-related kinase SMG-1			2.04
Y15801	PRKY	protein kinase, Y-linked	1.7		
D87467	RAPGEF5 [e]	Rap guanine nucleotide exchange factor (GEF) 5		1.84	2.18
U08316	RPS6KA3	ribosomal protein S6 kinase, 90kDa, polypeptide 3			1.64
U10117	SCYE1	small inducible cytokine subfamily E, member 1 (endothelial monocyte-activating)			1.58
M97935	STAT1	signal transducer and activator of transcription 1			1.58
U25997	**STC1**	**stanniocalcin 1**			1.7
Stress response					
U78305	**PPM1D/Wip1** [e]	**Protein phosphatase 1D magnesium-dependent, delta isoform**		1.57	1.59
Transcription					
U00115	**BCL6**	**B-cell CLL/lymphoma 6 (zinc finger protein 51)**		1.64	
AL080209	CREB3L2 [e]	cAMP responsive element binding protein 3-like 2			1.73
S68134	CREM [e]	cAMP responsive element modulator			1.51
AI635895	DSIPI [e]	delta sleep inducing peptide, immunoreactor		1.77	
AJ132917	MECP2	methyl CpG binding protein 2 (Rett syndrome)			1.64
L13773	MLLT2	myeloid/lymphoid or mixed-lineage leukemia (trithorax homolog, Drosophila); translocated to, 2			1.85
L07648	MXI1	MAX interactor 1			1.59
D45132	PRDM2 [e]	PR domain containing 2, with ZNF domain			1.62
X89750	TGIF [e]	TGFB-induced factor (TALE family homeobox)		1.67	1.94
AL080216	TRIM33	Tripartite motif-containing 33		1.54	
AB011165	THRAP1	thyroid hormone receptor associated protein 1	1.69	2.24	
U69274	ZBTB11	zinc finger and BTB domain containing 11			1.64
AF071771	ZNF143	zinc finger protein 143	1.79		
D83032	ZNF638 [e]	zinc finger protein 638		1.6	
Transport					
AB002387	MYO6	myosin VI		1.67	
AF070578	SLC38A6 [e]	solute carrier family 38, member 6		1.54	1.52
AF038202	**STX6**	**syntaxin 6**			1.56
Miscellaneous					
U50534	13CDNA73	hypothetical protein CG003	1.84		1.69
AB009672	ADAM23	a disintegrin and metalloproteinase domain 23			1.62
AB014597	ANKRD17	ankyrin repeat domain 17		1.65	1.89
D87717	ARHGAP11A	Rho GTPase activating protein 11A	1.58		
AF052105	C12orf22 [e]	chromosome 12 open reading frame 22		2.03	1.97
AF055016	C13orf1 [e]	chromosome 13 open reading frame 1			1.56
AI761567	CCPG1 [e]	cell cycle progression 1			1.51
AB002306	CHD9 [e]	chromodomain helicase DNA binding protein 9			1.77
AB023157	CPEB3	cytoplasmic polyadenylation element binding protein 3			1.51
AF070590	DHX57	DEAH (Asp-Glu-Ala-Asp/His) box polypeptide 57			2.36
AB028449	DICER1	Dicer1, Dcr-1 homolog (Drosophila)			1.61
AB014578	DNAJC13 [e]	DnaJ (Hsp40) homolog, subfamily C, member 13			2.1
U53445	DOC1	downregulated in ovarian cancer 1			1.79
AB011147	GREB1 [e]	GREB1 protein		2.06	2.15
D29677	HELZ	helicase with zinc finger domain			1.6
M11058	HMGCR [e]	3-hydroxy-3-methylglutaryl-Coenzyme A reductase		1.78	
AB018319	KIAA0776			1.81	
AB020638	KIAA0831 [e]				1.53
AB023182	KIAA0965	KIAA0965 protein		1.91	
AL033538	KIAA1043	KIAA1043 protein			1.54
AB018338	KLHL18	kelch-like 18 (Drosophila)		1.52	
AB007890	LKAP	limkain b1			1.65
AB011169	MARCH-VI	membrane-associated RING-CH protein VI	1.81		2.01
D79997	MELK [e]	maternal embryonic leucine zipper kinase	1.61		
U79272	MGC21416	hypothetical protein MGC21416			1.56
U79272	MGC21416 [e]	hypothetical protein MGC2141		1.6	
AL021546	P53CSV	p53-inducible cell-survival factor	2.08		
AI146846	PARD3	par-3 partitioning defective 3 homolog (C. elegans)	1.56		
AL120687	PLEKHB2	Pleckstrin homology domain containing, family B (evectins) member 2			1.6
W28743	pp9099 [e]	PH domain-containing protein		2.08	
X58288	PTPRM [e]	protein tyrosine phosphatase, receptor type, M			1.84
L05568	**SLC6A4**	**solute carrier family 6 (neurotransmitter transporter, serotonin), member 4**			1.74

U80017	SMN1/ SMN2	survival of motor neuron 2, centromeric / survival of motor neuron 1, telomeric		1.53	
Z99129	TDE2	tumor differentially expressed 2			1.51
AF082557	TNKS		1.76		
AF049891	**TPST2** [e]	**tyrosylprotein sulfotransferase 2**			1.6
Z78315	WDR45	WD repeat domain 45			1.51
AB029019	XTP2	HBxAg transactivated protein 2			1.77
AB002319	**ZFYVE26** [e]	**zinc finger, FYVE domain containing 26**		1.73	1.66
HG1751-HT1768					
TIGR	*Unknown*		2.04		

Down-regulated genes

Cell adhesion					
X53587	ITGB4	integrin, beta 4	-1.55		
Z22555	SCARB1	scavenger receptor class B, member 1	-1.59		
Cell cycle					
X13293	**B-MYB** [e]	**v-myb myeloblastosis viral oncogene homolog (avian)-like 2**			-1.61
M96577	**E2F1**	E2F transcription factor 1			-1.53
PPP1R15A	GADD34	protein phosphatase 1, regulatory (inhibitor) subunit 15A			-1.71
Y13115	PLK4 [e]	polo-like kinase 4 (Drosophila)		-1.84	
Chromosome organization					
X03473	H1F0 [e]	H1 histone family, member 0		-1.76	
Development					
Z20656	MYH6	myosin, heavy polypeptide 6, cardiac muscle, alpha (cardiomyopathy, hypertrophic 1)	-1.67		
Immune response					
X04430	IL6	interleukin 6 (interferon, beta 2)		-1.7	
Metabolism					
U31875	**DHRS2**	**dehydrogenase/reductase (SDR family) member 2**		-2.23	
U31875	DHRS2	dehydrogenase/reductase (SDR family) member 2			-2.2
AF007155	LOC254531 [e]	PLSC domain containing protein		-1.95	
Signaling					
AJ243937	GPSM3	G-protein signalling modulator 3 (AGS3-like, C. elegans)			-1.61
M37190	RIN2 [e]	Ras and Rab interactor 2		-2.43	
Transcription					
X12492	NFIC [e]	nuclear factor I/C (CCAAT-binding transcription factor)			-1.54
D26121	SF1	splicing factor 1		-2.6	
X82018	ZNF482 [e]	zinc finger protein 482	-1.58	-2.54	
Transport					
AB006190	AQP7	aquaporin 7	-1.51		
F27891	**COX6A2**	**cytochrome c oxidase subunit VIa polypeptide 2**	-1.64		
Miscellaneous					
AB029343	**C6orf18** [e]	**chromosome 6 open reading frame 18**			-1.65
M75106	CPB2 [e]	carboxypeptidase B2 (plasma, carboxypeptidase U)	-1.6		
U49785	DDT	D-dopachrome tautomerase			-3.21
D87120	FAM3C	family with sequence similarity 3, member C			-1.96
AJ223349	HIRIP3 [e]	HIRA interacting protein 3			-1.97
M95623	**HMBS**	**hydroxymethylbilane synthase**		-1.51	
AB012853	ING1L	inhibitor of growth family, member 1-like			-1.71
AF072468	JRK	jerky homolog (mouse)	-1.57		
W28518	LOC133619	Hypothetical protein MGC12103			-1.85
M27937	MEA [e]	male-enhanced antigen			-1.61
D78611	MEST	mesoderm specific transcript homolog (mouse)			-1.51
U06452	MLANA	melan-A		-1.66	
U88153	PELP1	proline-, glutamic acid-, leucine-rich protein 1	-1.51		
U38964	PMS2L1	postmeiotic segregation increased 2-like 1		-1.81	
AA524802	PPP1R3E [e]	Protein phosphatase 1, regulatory (inhibitor) subunit 3E	-2.67		
X89416	**PPP5C** [e]	**protein phosphatase 5, catalytic subunit**			-1.55
AB018566	PROSC	proline synthetase co-transcribed homolog (bacterial)		-1.64	
M87339	RFC4	replication factor C (activator 1) 4, 37kDa		-1.61	
AI627877	RNF126				-1.65
U79266	SHD1	likely ortholog of mouse Sac3 homology domain 1 (S. cerevisiae)			-1.64
U75679	SLBP	stem-loop (histone) binding protein		-1.53	

AL050148	SNX1	Sorting nexin 1	-1.84	
AB002330	SR140	U2-associated SR140 protein	-1.56	
M99436	TLE2	transducin-like enhancer of split 2 (E(sp1) homolog, Drosophila)	-1.6	
D87002	*Unknown*		-2.49	
D87002	*Unknown*			-1.86

[a] Derived from LocusLink and SwissProt databases or recent publications
[b] See fold change formula described in *Materials and Methods*
[c] Similar genes with different Affymetrix targets
[d] Genes those IR-responsive modulation was confirmed by quantitative RT-PCR
[e] Genes up-regulated (or down-regulated) at 1 h, 6 h or 12 h after 3 Gy (using Genespring analysis, Fold change cutoff of 1.5 fold) IN COMMON with the same time points of the up-regulated (or down-regulated) genes of the present list.
Genes in bold show significant common up-regulation or common down-regulation at 3 Gy and 20 Gy (see Table 3.6)

Table 3.6 *Genes significantly up- or down-regulated (more than 1.5-fold) in EA.hy 926 following 20 Gy exposure. Applied filters in the Data Mining Tool (Affymetrix) are described in Materials and Methods.*

Category [a] GenBank access. no.	Gene symbol	Title	Fold Change[b]		
			1h	6h	12h
Up-regulated genes					
Angiogenesis					
M27968	FGF2 [e]	fibroblast growth factor 2 (basic)		1.97	
M92357	TNFAIP2	tumor necrosis factor, alpha-induced protein 2		2.49	
U43142	VEGFC / Flt4-L [c]			5.1	
X94216	VEGFC / Flt4-L [c, e]	vascular endothelial growth factor C		5.39	1.9
Anti-apoptosis					
M58603	NFKB1 [c]	nuclear factor of kappa light polypeptide gene enhancer in B-cells 1 (p105)		1.88	
M58603	NFKB1 [c]			1.88	
AF099935	TNFAIP8	tumor necrosis factor, alpha-induced protein 8		2.6	
Apoptosis					
U27467	BCL2A1	BCL2-related protein A1		4.9	
AF079221	BNIP3L [e]	BCL2/adenovirus E1B 19kDa interacting protein 3-like		1.7	1.96
U67319	CASP 7	caspase 7, apoptosis-related cysteine protease		2.23	
M87507	CASP1	caspase 1, apoptosis-related cysteine protease (interleukin 1, beta, convertase)		1.76	1.91
AF010313	EI24	etoposide induced 2.4 mRNA		1.67	
AI670788	MOAP1	modulator of apoptosis 1		1.76	
M69043	**NFKBIA** [e]	**nuclear factor kappa B light polypeptide gene enhancer in B-cells inhibitor, alpha**		1.7	
AF061034	OPTN [c]	optineurin		2.72	
AF070533	OPTN [c, e]	optineurin		3.5	
AF070533	OPTN [c, e]	optineurin		3.56	
AF016266	**TNFRSF10B / KILLER/DR5** [e]	**tumor necrosis factor receptor superfamily, member 10b**		1.95	
X63717	TNFRSF6 / FAS/APO1 [e]	tumor necrosis factor receptor superfamily, member 6		4.19	2.77
X63717/Z70519	**TNFRSF6 / FAS/APO1** [d, e]	**tumor necrosis factor receptor superfamily, member 6**		5.44	
X83490	TNFRSF6 / FAS/APO1 [e]	tumor necrosis factor receptor superfamily, member 6		5.6	3.2
Z70519	TNFRSF6 / FAS/APO1 [e]	tumor necrosis factor receptor superfamily, member 6		3.04	1.79
U03397	TNFRSF9 / 41BB [d]	tumor necrosis factor receptor superfamily, member 9		10.66	
L08096	TNFSF7 [e]	tumor necrosis factor (ligand) superfamily, member 7		3.8	
U03398	TNFSF9 / 41BB-ligand [e]	tumor necrosis factor (ligand) superfamily, member 9	1.54		
U19261	TRAF1	TNF receptor-associated factor 1		15.13	
Biosynthesis					
U19523	GCH1	GTP cyclohydrolase 1 (dopa-responsive dystonia)		4.08	
Cell adhesion					
X16354	CEACAM1 [e]	carcinoembryonic antigen-related cell adhesion molecule 1 (biliary glycoprotein)		3.41	2.77
M24283	ICAM1	intercellular adhesion molecule 1 (CD54), human rhinovirus receptor		6.92	
U91512	NINJ1	ninjurin 1		1.93	
AB002341	NRCAM	neuronal cell adhesion molecule		1.66	1.76
Cell cycle					
U03106	CDKN1A / p21/Waf1[e]	cyclin-dependent kinase inhibitor 1A (p21, Cip1)		2.8	
AL050166(16)	CYLD	Cylindromatosis (turban tumor syndrome)		4.61	
U82130	TSG101	tumor susceptibility gene 101		1.75	
Cell growth					
X61123	BTG1	B-cell translocation gene 1, anti-proliferative		1.87	
U72649	**BTG2** [d, e]	**B cell translocation gene 2**	3.26	3.07	2.73

Cell proliferation					
M12783	PDGFB	platelet-derived growth factor beta polypeptide (simian sarcoma viral (v-sis) oncogene homolog)		1.67	
D38305	TOB1	transducer of ERBB2, 1		1.72	
Chromosome organization					
AI885852	HIST2H2AA [e]	histone 2, H2aa		3.92	4.34
Cytoskeleton					
X13839	ACTA2 [e]	actin, alpha 2, smooth muscle, aorta		4.73	9.69
DNA repair					
X83441	LIG4 [e]	ligase IV, DNA, ATP-dependent			1.77
D21089	XPC [e]	xeroderma pigmentosum, complementation group C		2.44	1.92
Immune response					
M26683	CCL2	chemokine (C-C motif) ligand 2		2.45	
M13560	CD74	CD74 antigen (invariant polypeptide of major histocompatibility complex, class II antigen-associated)		1.64	
L47738	CYFIP2 [e]	cytoplasmic FMR1 interacting protein 2		1.75	
AA203213	G1P2 [e]	interferon, alpha-inducible protein (clone IFI-15K)		1.74	
M55542	GBP1	guanylate binding protein 1, interferon-inducible, 67kDa		2.87	
J03909	IFI30	interferon, gamma-inducible protein 30		2.68	2.68
J03909	IFI30	interferon, gamma-inducible protein 30			1.7
U72882	IFI35 [e]	interferon-induced protein 35			1.92
M24594	IFIT1	interferon-induced protein with tetratricopeptide repeats 1		3.28	3.17
M24594	IFIT1	interferon-induced protein with tetratricopeptide repeats 1		3.12	2.92
AF026939	IFIT3	interferon-induced protein with tetratricopeptide repeats 3		2.76	
U34605	IFIT5	interferon-induced protein with tetratricopeptide repeats 5		1.69	1.54
AF043129	IL7R	interleukin 7 receptor		2.36	
Y14768	LTB [e]	lymphotoxin beta (TNF superfamily, member 3)		5.35	1.97
AA631972	NK4 [d, e]	natural killer cell transcript 4		85.41	92.06
U02556	TCTE1L	t-complex-associated-testis-expressed 1-like		1.74	
Metabolism					
U46689	ALDH3A2 [e]	aldehyde dehydrogenase 3 family, member A2			1.98
U29926	AMPD3	adenosine monophosphate deaminase (isoform E)		2	
AL050025	CA12	carbonic anhydrase XII	1.56		
L07956	GBE1	glucan (1,4-alpha-), branching enzyme 1 (glycogen branching enzyme, Andersen disease, glycogen storage disease type IV)		1.64	
AB016789	GFPT2 [e]	glutamine-fructose-6-phosphate transaminase 2		1.85	1.6
U57721	KYNU [e]	kynureninase (L-kynurenine hydrolase)		3.21	1.7
U67963	MGLL [e]	monoglyceride lipase		1.67	
X83368	PIK3CG	phosphoinositide-3-kinase, catalytic, gamma polypeptide			1.94
X07834	SOD2 [e]	superoxide dismutase 2, mitochondrial		8.08	2.78
Proteasome degradation					
U07234	HLA-A [e]	major histocompatibility complex, class I, A			1.77
Protein folding					
AB023421	APG-1	heat shock protein (hsp110 family)		2.28	
L08069	DNAJA1	DnaJ (Hsp40) homolog, subfamily A, member 1		1.6	
Signaling					
S82240	ARHE	ras homolog gene family, member E		2.01	
AJ006288	BCL10 [e]	B-cell CLL/lymphoma 10		2.37	
U26710	**CBLB**	**Cas-Br-M (murine) ecotropic retroviral transforming sequence b**		1.6	
M21121	CCL5/RANTES [d, e]	chemokine (C-C motif) ligand 5			7.49
M21121	CCL5/RANTES [d, e]	chemokine (C-C motif) ligand 5			4.65
U67615	CHS1	Chediak-Higashi syndrome 1		2.11	
X54489	CXCL1	chemokine (C-X-C motif) ligand 1 (melanoma growth stimulating activity, alpha)	24.63		
L20817	DDR1 [e]	discoidin domain receptor family, member 1			2.3
AF070621	DIXDC1	DIX domain containing 1			1.52
U61843	DLG5	discs, large homolog 5 (Drosophila)			1.74
U85267	DSCR1	Down syndrome critical region gene 1		1.83	
AF038844	DUSP14 [e]	dual specificity phosphatase 14		2.37	2.3
M60459	EPOR	erythropoietin receptor			1.73
U03858	FLT3LG	fms-related tyrosine kinase 3 ligand			1.84

U10550	GEM	GTP binding protein overexpressed in skeletal muscle			2.76
M63904	GNA15	guanine nucleotide binding protein (G protein), alpha 15 (Gq class)		2.02	
X80818	GRM4	glutamate receptor, metabotropic 4	1.54		
Z82244	HMOX1	heme oxygenase (decycling) 1			2.51
Z34897	HRH1	histamine receptor H1		2.43	
AF031167	IL15	interleukin 15		3.16	
AJ001684	KLRC1/KLRC2	killer cell lectin-like receptor subfamily C, members 1 & 2			1.57
U83993	P2RX4 [e]	purinergic receptor P2X, ligand-gated ion channel, 4		1.69	1.82
U77735	PIM2 [e]	pim-2 oncogene		1.66	1.97
X02419	PLAU [e]	plasminogen activator, urokinase		2.23	1.63
AF017786	PPAP2B	phosphatidic acid phosphatase type 2B		1.78	
D10495	PRKCD	protein kinase C, delta		1.95	
D42087	RAB21	RAB21, member RAS oncogene family		1.79	
AI762248	RABL3	RAB, member of RAS oncogene family-like 3			1.52
W68830	RAC2 [e]	ras-related C3 botulinum toxin substrate 2 (rho family, small GTP binding protein Rac2)			1.71
M29893	RALA [e]	v-ral simian leukemia viral oncogene homolog A (ras related)		2.18	
S82240	RND3	Rho family GTPase 3			1.59
U25997	**STC1** [e]	**stanniocalcin 1**		2	2.53
X70340	TGFA	transforming growth factor, alpha			2.3
U21092	TRAF3	TNF receptor-associated factor 3		2.12	
X80200	TRAF4 [e]	TNF receptor-associated factor 4		2	
AF104304	ZFYVE9	zinc finger, FYVE domain containing 9	1.61		
Stress response					
U65416	MICB	MHC class I polypeptide-related sequence B		1.64	
U78305	**PPM1D/Wip1** [e]	**protein phosphatase 1D magnesium-dependent, delta isoform**	1.78	2.97	2.38
Transcription					
U88047	ARID3A [e]	AT rich interactive domain 3A (BRIGHT- like)			1.73
S66427	ARID4A	AT rich interactive domain 4A (RBP1-like)			1.72
L19871	ATF3 [e]	activating transcription factor 3	2.31		
AB021663	ATF5	activating transcription factor 5		1.95	
U00115	**BCL6** [e]	**B-cell CLL/lymphoma 6 (zinc finger protein 51)**		2.83	2.16
AB004066	BHLHB2 [e]	basic helix-loop-helix domain containing, class B, 2			1.77
U03644	CIR	CBF1 interacting corepressor		1.8	
M24069	CSDA	cold shock domain protein A		1.73	1.64
U88629	ELL2	elongation factor, RNA polymerase II, 2		2.68	
AJ001589	FOXO3A [e]	forkhead box O3A		1.82	
AB018287	HDAC9 [e]	histone deacetylase 9		8.96	
AL023584	HIVEP2	human immunodeficiency virus type I enhancer binding protein 2		3.26	
U53831	IRF7 [e]	interferon regulatory factor 7		1.73	
M87503	ISGF3G [e]	interferon-stimulated transcription factor 3, gamma 48kDa			1.8
M97676	MSX1	msh homeo box homolog 1 (Drosophila)		1.97	
M97676	MSX1 [e]	msh homeo box homolog 1 (Drosophila)		2.58	
M97676	MSX1 [e]	msh homeo box homolog 1 (Drosophila)		2.04	
D89377	MSX2 [e]	msh homeo box homolog 2 (Drosophila)		1.87	
U20816	NFKB2	nuclear factor of kappa light polypeptide gene enhancer in B-cells 2 (p49/p100)		9.38	
X61498	NFKB2	nuclear factor of kappa light polypeptide gene enhancer in B-cells 2 (p49/p100)		4.5	
S76638	NFKB2 [d]	nuclear factor of kappa light polypeptide gene enhancer in B-cells 2 (p49/p100)		6.14	
S76638	NFKB2 [d,]	nuclear factor of kappa light polypeptide gene enhancer in B-cells 2 (p49/p100)		4.4	
AB021868	PIAS3	protein inhibitor of activated STAT, 3			1.77
AI744294	POLR2K	polymerase (RNA) II (DNA directed) polypeptide K, 7.0kDa		1.63	
L19067	RELA	v-rel reticuloendotheliosis viral oncogene homolog A, nuclear factor of kappa light polypeptide gene enhancer in B-cells 3, p65 (avian)		1.73	
M83221	RELB	v-rel reticuloendotheliosis viral oncogene homolog B, nuclear factor of kappa light polypeptide gene enhancer in B-cells 3 (avian)		12.03	2.73

Y00630	SERPINB2 [e]	serine (or cysteine) proteinase inhibitor, clade B (ovalbumin), member 2	3.14	
U68019	SMAD3	SMAD, mothers against DPP homolog 3 (Drosophila)	2.25	
AI557062	SNAPC5 [e]	small nuclear RNA activating complex, polypeptide 5, 19kDa		1.58
X84002	TAF12	TAF12 RNA polymerase II, TATA box binding protein (TBP)-associated factor, 20kDa		1.64
U18543	TRIM32 [e]	tripartite motif-containing 32	1.67	1.61
U09848	ZKSCAN1	zinc finger with KRAB and SCAN domains 1		1.57
Z11773	ZNF187	zinc finger protein 187		2.04
AF041259	ZNF217 [e]	zinc finger protein 217	1.99	1.71
AL049942	ZNF337 [e]	zinc finger protein 337	1.89	
Translation				
D30655	EIF4A2	eukaryotic translation initiation factor 4A, isoform 2		1.57
Transport				
L05568	**SLC6A4**	**solute carrier family 6 (neurotransmitter transporter, serotonin), member 4**		2.4
AL035306	STX12 [e]	syntaxin 12	1.86	
AF038202	**STX6**	**syntaxin 6**	1.69	
X57522	TAP1 / RING4 [e]	transporter 1, ATP-binding cassette, sub-family B (MDR/TAP)	6.64	2.36
Miscellaneous				
AL050374	ABTB2 [e]	ankyrin repeat and BTB (POZ) domain containing 2	3.26	1.68
X99459	AP3S2 [e]	adaptor-related protein complex 3, sigma 2 subunit		1.84
U85995	B1	parathyroid hormone-responsive B1 gene	2.14	2.31
U87408	B1 [e]	parathyroid hormone-responsive B1 gene		2.17
AL050089	BAZ1A	bromodomain adjacent to zinc finger domain, 1A	1.72	
AL080118	C14orf109 [e]	chromosome 14 open reading frame 109		1.56
AL080097	C3orf4	chromosome 3 open reading frame 4	1.69	
AF035313	C5orf15	chromosome 5 open reading frame 15	1.95	
U15782	CSTF3	cleavage stimulation factor, 3' pre-RNA, subunit 3, 77kDa		1.54
U79259	DJ159A19.3	hypothetical protein DJ159A19.3		1.82
AB006713	DPYSL4	dihydropyrimidinase-like 4		2.35
AF023917	DUSP11	dual specificity phosphatase 11 (RNA/RNP complex 1-interacting)	1.8	
AI655015	DUSP7	Dual specificity phosphatase 7		1.67
Y12735	DYRK3 [e]	dual-specificity tyrosine-(Y)-phosphorylation regulated kinase 3	3.2	2.52
M55267	EVI2A	ecotropic viral integration site 2A		1.89
AB007962	FLJ23790	hypothetical protein FLJ23790	1.75	
W28281	GABARAPL1 [e]	GABA(A) receptor-associated protein like 1	1.62	
AB011147	GREB1 [e]	GREB1 protein		4.48
L19779	HIST2H2AA	histone 2, H2aa	1.67	
D28915	IFI44	interferon-induced protein 44		1.84
U47101	ISCU [e]	iron-sulfur cluster assembly enzyme	1.84	
AB002301	KIAA0303 [e]	KIAA0303 protein	2.86	
AL031447	KIAA0469 [e]	KIAA0469 gene product	2.62	2.15
W72733	KIAA1536	KIAA1536 protein		1.87
D21851	LARS2	leucyl-tRNA synthetase 2, mitochondrial		1.53
D86961	LHFPL2	lipoma HMGIC fusion partner-like 2	1.91	
D80010	LPIN1	lipin 1	1.61	
AB002301	MAST4 [e]	microtubule associated serine/threonine kinase family member 4		1.88
AB023155	NAV3	neuron navigator 3	2.99	
U47101	NIFUN [e]	NifU-like N-terminal domain containing		1.56
L20971	**PDE4B**	**phosphodiesterase 4B, cAMP-specific (phosphodiesterase E4 dunce homolog, Drosophila)**	1.96	
AB002313	PLXNB2	plexin B2	1.83	
U03105	PNRC1	proline-rich nuclear receptor coactivator 1	1.77	
U97519	PODXL	podocalyxin-like		1.55
N36638	PPP1R3C	protein phosphatase 1, regulatory (inhibitor) subunit 3C		2.39
M65254	PPP2R1B	protein phosphatase 2 (formerly 2A), regulatory subunit A (PR 65), beta isoform	1.73	
AF051160	PTP4A1	protein tyrosine phosphatase type IVA, member 1	1.64	
M25393	PTPN2	protein tyrosine phosphatase, non-receptor type 2	1.71	
AB029014	RAB6IP1 [e]	RAB6 interacting protein 1	1.64	

AL080235	RIS1	Ras-induced senescence 1			2.08
AI539439	S100A2 [e]	S100 calcium binding protein A2		1.61	
L26081	SEMA3A [e]	sema domain, immunoglobulin domain (Ig), short basic domain, secreted, (semaphorin) 3A		1.67	
M93056	SERPINB1 [e]	serine (or cysteine) proteinase inhibitor, clade B (ovalbumin), member 1			1.71
J03764	SERPINE1 [e]	serine (or cysteine) proteinase inhibitor, clade E (nexin, plasminogen activator inhibitor type 1), member 1		3.63	
M14083	SERPINE1 [e]	serine (or cysteine) proteinase inhibitor, clade E (nexin, plasminogen activator inhibitor type 1), member 1		2.81	
D15050	SNF1LK	SNF1-like kinase		1.68	
U40571	SNTA1	syntrophin, alpha 1 (dystrophin-associated protein A1, 59kDa, acidic component)	1.87		
M62800	SSA1 [e]	Sjogren syndrome antigen A1 (52kDa, ribonucleoprotein autoantigen SS-A/Ro)		2.5	
X85116	STOM [e]	stomatin		1.71	
AB018322	TMCC1	transmembrane and coiled-coil domains 1			1.53
AF049891	**TPST2**	**tyrosylprotein sulfotransferase 2**			2.14
X82200	TRIM22 [e]	tripartite motif-containing 22		2.77	2.68
AC002400	UBPH	similar to ubiquitin binding protein			1.63
H93123	VAMP3 [e]	vesicle-associated membrane protein 3 (cellubrevin)		1.63	
AB020700	WDR47	WD repeat domain 47		1.61	
AB002319	**ZFYVE26** [e]	**zinc finger, FYVE domain containing 26**			1.79
HG172-HT3924 TIGR	*Unknown* [e]			3.3	
HG1103-HT1103 TIGR	*Unknown*			1.9	
HG4322-HT4592 TIGR	*Unknown*			1.67	
AL040137	*Unknown*	MRNA; cDNA DKFZp667B1718 (from clone DKFZp667B1718)			1.83

Down-regulated genes

Angiogenesis					
U01134	FLT1 [e]	fms-related tyrosine kinase 1 (vascular endothelial growth factor/vascular permeability factor receptor)			-1.63
S77812	FLT1 / VEGFR1 [e]	fms-related tyrosine kinase 1 (vascular endothelial growth factor/vascular permeability factor receptor)		-1.91	-2.1
Anti-apoptosis					
Y15906	API5	apoptosis inhibitor 5	-2.39		
D86970	TIAF1/MYO18A [e]	TGFB1-induced anti-apoptotic factor 1 myosin XVIIIA		-1.66	
Apoptosis					
U60521	CASP9 [e]	caspase 9, apoptosis-related cysteine protease		-1.96	
Biosynthesis					
AF029893	B3GNT6	UDP-GlcNAc:betaGal beta-1,3-N-acetylglucosaminyltransferase 6		-1.65	
X79865	MRPL12 [e]	mitochondrial ribosomal protein L12		-1.98	
D88674	OAZIN	ornithine decarboxylase antizyme inhibitor			-1.56
Cell adhesion					
M25280	SELL	selectin L (lymphocyte adhesion molecule 1)			-1.65
Cell cycle					
U75285	BIRC5 [e]	baculoviral IAP repeat-containing 5 (survivin)		-2.17	-2.91
X13293	**B-MYB** [e]	**v-myb myeloblastosis viral oncogene homolog (avian)-like 2**		-2.55	-4.08
X51688	CCNA2 [e]	cyclin A2		-4.69	-5.98
M25753	CCNB1 [e]	cyclin B1			-5.32
AL080146	CCNB2 [e]	cyclin B2		-4.25	-6.42
M92287	CCND3	cyclin D3		-1.99	
M92287	CCND3	cyclin D3		-1.51	
M73812	CCNE1	cyclin E1		-1.92	-2.31
U17105	CCNF [e]	cyclin F		-3.07	-2.59
X05360	CDC2 [e]	cell division cycle 2, G1 to S and G2 to M		-3.5	-4.05
M34065	CDC25C [e]	cell division cycle 25C		-2.81	-3.45
L04658	CDK5	cyclin-dependent kinase 5		-1.98	
U40343	CDKN2D	cyclin-dependent kinase inhibitor 2D (p19, inhibits CDK4)		-1.76	

L25876	CDKN3 [e]	cyclin-dependent kinase inhibitor 3 (CDK2-associated dual specificity phosphatase)		-5.54	-7.03
AF070552	CDT1 [e]	DNA replication factor		-2.38	-2.31
U30872	CENPF [e]	centromere protein F, 350/400ka (mitosin)		-3.9	
AF086904	CHK2	CHK2 checkpoint homolog (S. pombe)		-3.58	
D63880	CNAP1 [e]	chromosome condensation-related SMC-associated protein 1			-3.55
M96577	**E2F1** [e]	E2F transcription factor 1		-2.2	-2.57
D79987	ESPL1 [e]	extra spindle poles like 1 (S. cerevisiae)		-2.48	-3.07
AL022325	GTSE1 [e]	G-2 and S-phase expressed 1		-3.72	-4.86
AL031588	GTSE1 [e]	G-2 and S-phase expressed 1		-2.55	-3.13
AB017430	KIF22 [e]	kinesin family member 22		-3.72	-5.77
AL021366	KIFC1	Kinesin family member C1		-3.24	-4.02
D14678	KIFC1	Kinesin family member C1		-2.13	-3.26
D14678	KIFC1 [e]	Kinesin family member C1			-4.3
X74794	MCM4 [e]	MCM4 minichromosome maintenance deficient 4 (S. cerevisiae)			-3.51
X74795	MCM5 [e]	MCM5 minichromosome maintenance deficient 5, cell division cycle 46 (S. cerevisiae)			-2.12
Z29066	NEK2 [e]	NIMA (never in mitosis gene a)-related kinase 2		-2.65	-5.51
AF014118	PKMYT1	protein kinase, membrane associated tyrosine/threonine 1			-1.55
Cell motility					
AF032862	HMMR [e]	hyaluronan-mediated motility receptor (RHAMM)			-5.41
Cell proliferation					
U52100	EMP2 [e]	epithelial membrane protein 2		-2.15	-4.51
U63743	KIF2C [e]	kinesin family member 2C		-3.9	-5.1
X65550	MKI67 [e]	antigen identified by monoclonal antibody Ki-67		-4.14	-4.27
X65550	MKI67 [e]	antigen identified by monoclonal antibody Ki-67		-4.13	-5.5
Chromatin binding					
U20979	CHAF1A [e]	chromatin assembly factor 1, subunit A (p150)		-2.18	-2.18
Chromosome organization					
Z97630	H1F0 [e]	H1 histone family, member 0		-1.89	
Cytoskeleton					
X95677	ABI2 [e]	abl interactor 2			-1.51
W87858	KIF2 [e]	Kinesin heavy chain member 2	-1.92		
W87858	KIF2 [e]	Kinesin heavy chain member 2		-1.65	
AF001691	PPL	periplakin		-3.28	-1.53
DNA catabolism					
X90392	DNASE1L1 [e]	deoxyribonuclease I-like 1		-1.53	
DNA repair					
U64805	BRCA1 [e]	breast cancer 1, early onset		-3.03	-2.14
AJ007669	FANCG [e]	Fanconi anemia, complementation group G		-2.12	-1.99
D16581	NUDT1 [e]	nudix (nucleoside diphosphate linked moiety X)-type motif 1			-1.92
AF057160	PARP4	poly (ADP-ribose) polymerase family, member 4		-1.61	
U94703	POLG2	polymerase (DNA directed), gamma 2, accessory subunit	-1.93		
U47077	PRKDC / DNAPK	protein kinase, DNA-activated, catalytic polypeptide			-1.79
X97795	RAD54L	RAD54-like (S. cerevisiae)			-1.91
L07540	RFC5	replication factor C (activator 1) 5, 36.5kDa			-1.86
M63488	RPA1 [e]	replication protein A1, 70kDa			-1.69
AF035586	XRCC3	X-ray repair complementing defective repair in Chinese hamster cells 3		-2.04	
DNA replication					
AF092563	SMC2L1	SMC2 structural maintenance of chromosomes 2-like 1 (yeast)		-2.64	
M87338	RFC2 [e]	replication factor C (activator 1) 2, 40kDa			-1.72
Immune response					
AF018253	TNFRSF11A	tumor necrosis factor receptor superfamily, member 11a, activator of NFKB		-1.74	-1.86
Metabolism					
DHRS3		dehydrogenase/reductase (SDR family) member 3			-2.62
AF037335	CA12 [e]	carbonic anhydrase XII		-4.39	-2.03
M83670	CA4	carbonic anhydrase IV	-1.55		-1.53

D78586	CAD [e]	carbamoyl-phosphate synthetase 2, aspartate transcarbamylase, and dihydroorotase		-1.76	-1.79
L39211	CPT1A [e]	carnitine palmitoyltransferase 1A (liver)		-1.51	
M14565	CYP11A1 [e]	cytochrome P450, family 11, subfamily A, polypeptide 1		-1.92	
U31875	**DHRS2**	**dehydrogenase/reductase (SDR family) member 2**		-2.58	
L16991	DTYMK	deoxythymidylate kinase (thymidylate kinase)			-1.75
X56832	ENO3 [e]	enolase 3 (beta, muscle)			-1.77
AF001903	HADHSC	L-3-hydroxyacyl-Coenzyme A dehydrogenase, short chain			-1.77
S81916	PGK1	phosphoglycerate kinase 1			-1.56
X59618	RRM2 [e]	ribonucleotide reductase M2 polypeptide			-3.47
X59618	RRM2 [e]	ribonucleotide reductase M2 polypeptide		-3.12	
U13395	WWOX	WW domain containing oxidoreductase			-1.86
Protein folding					
U42031	FKBP5 [e]	FK506 binding protein 5		-1.66	-1.52
RNA catabolism					
Z97029	RNASEH2A	ribonuclease H2, large subunit			-1.75
RNA processing					
U07563	EXOSC2 [e]	exosome component 2		-1.53	-1.89
AL031681	SFRS6	splicing factor, arginine/serine-rich 6			-1.71
Signaling					
L22214	ADORA1	adenosine A1 receptor		-2.41	
U13616	ANK3	ankyrin 3, node of Ranvier (ankyrin G)		-1.82	
AF106941	ARRB2 [e]	arrestin, beta 2		-1.58	
AB002328	CABIN1 [e]	calcineurin binding protein 1		-2.12	
M54914	FSHB	follicle stimulating hormone, beta polypeptide	-1.85	-2.85	
L37882	FZD2	frizzled homolog 2 (Drosophila)		-3.14	
S81944	GABRA6	gamma-aminobutyric acid (GABA) A receptor, alpha 6		-3.55	
D90150	GNAZ	guanine nucleotide binding protein (G protein), alpha z polypeptide		-2.48	
AF017656	GNB5 [e]	guanine nucleotide binding protein (G protein), beta 5		-1.54	
U54999	GPSM2	G-protein signalling modulator 2 (AGS3-like, C. elegans)		-3.12	
AI955897	INPP4A	Inositol polyphosphate-4-phosphatase, type I, 107kDa		-2.25	
U39064	MAP2K6	mitogen-activated protein kinase kinase 6		-3.7	-2.97
M64925	MPP1 [e]	membrane protein, palmitoylated 1, 55kDa		-1.68	-1.99
AB023192	NISCH [e]	nischarin		-1.59	
M28526	PECAM1	platelet/endothelial cell adhesion molecule (CD31 antigen)		-1.74	-1.56
Y11312	PIK3C2B [e]	phosphoinositide-3-kinase, class 2, beta polypeptide		-2.07	
AB020630	PPP1R16B [e]	protein phosphatase 1, regulatory (inhibitor) subunit 16B		-4.54	
M34181	PRKACB	protein kinase, cAMP-dependent, catalytic, beta		-2.06	
AF095448	RAI3 [e]	retinoic acid induced 3		-2.07	
M22995	RAP1A	RAP1A, member of RAS oncogene family		-1.53	
U27768	RGS4 [e]	regulator of G-protein signalling 4		-3.33	
AI267373	RGS4 [e]	regulator of G-protein signalling 4		-2.85	
M37192	RIN1	Ras and Rab interactor 1		-2.06	
L36463	RIN1	Ras and Rab interactor 1		-1.69	
X99656	SH3GL1 [e]	SH3-domain GRB2-like 1		-2.04	
D17517	TYRO3 [e]	TYRO3 protein tyrosine kinase		-1.67	
Stress response					
AF002715	MAP3K4	mitogen-activated protein kinase kinase kinase 4		-1.88	
Transcription					
U20240	CEBPG [e]	CCAAT/enhancer binding protein (C/EBP), gamma			-1.55
M68891	GATA2	GATA binding protein 2		-2.4	
M68891	GATA2	GATA binding protein 2		-2.21	
AF052389	LDB2 [e]	LIM domain binding 2		-3.38	
AI312646	NFIB	Nuclear factor I/B		-2.08	
AI222594	NFIB [e]	Nuclear factor I/B		-1.73	
U22662	NR1H3 [e]	nuclear receptor subfamily 1, group H, member 3		-4.83	
U22662	NR1H3 [e]	nuclear receptor subfamily 1, group H, member 3		-2.74	
X16155	NR2F1 [e]	nuclear receptor subfamily 2, group F, member 1		-2.27	-1.77
Z21966	POU6F1	POU domain, class 6, transcription factor 1	-1.75		
D45132	PRDM2	PR domain containing 2, with ZNF domain	-1.65		
AL031666	PRKCBP1	protein kinase C binding protein 1		-2.52	
AL049432	RAI17	retinoic acid induced 17		-1.53	
U66616	SMARCC2 [e]	SWI/SNF related, matrix associated, actin dependent regulator of chromatin, subfamily c, member 2		-1.93	

AF083105	SOX13 [e]	SRY (sex determining region Y)-box 13		-1.83	
U36500	SP140	SP140 nuclear body protein		-1.52	
AL080218	STAT5B	signal transducer and activator of transcription 5B		-1.59	
U48730	STAT5B	signal transducer and activator of transcription 5B			-1.69
M99435	TLE1	transducin-like enhancer of split 1 (E(sp1) homolog, Drosophila)		-1.63	
AI375913	TOP2A [e]	topoisomerase (DNA) II alpha 170kDa		-5.02	-5.66
AJ007042	WHSC1 [e]	Wolf-Hirschhorn syndrome candidate 1			-1.64
AL096880	ZNF278 [e]	zinc finger protein 278		-1.72	
AL022393	ZNF307	zinc finger protein 307	-1.61		
Transport					
AF022853	ABCC1	ATP-binding cassette, sub-family C (CFTR/MRP), member 1		-1.58	
J04027	ATP2B1	ATPase, Ca++ transporting, plasma membrane 1		-2.65	
F27891	**COX6A2**	**cytochrome c oxidase subunit VIa polypeptide 2**		-1.72	
D14582	EPIM	epimorphin			-1.67
AB029003	GGA2	golgi associated, gamma adaptin ear containing, ARF binding protein 2		-1.51	
X76648	GLRX	glutaredoxin (thioltransferase)		-1.53	
AF031815	KCNN3 [e]	potassium intermediate/small conductance calcium-activated channel, subfamily N, member 3		-3.46	
AF052169	KCTD12	potassium channel tetramerisation domain containing 12		-2.48	
U17566	SLC19A1	solute carrier family 19 (folate transporter), member 1		-2.17	
AL050021	SLC7A1	solute carrier family 7 (cationic amino acid transporter, y+ system), member 1			-2.12
M55047	SYT1 [e]	synaptotagmin I		-1.91	
AB019694	TXNRD2 [e]	thioredoxin reductase 2		-2.28	
Miscellaneous					
D31883	ABLIM1	actin binding LIM protein 1		-1.85	
U54645	AK2 [e]	adenylate kinase 2		-1.86	-2.11
D87717	ARHGAP11A [e]	Rho GTPase activating protein 11A			-4.21
U79256	ARHGAP19[e]	Rho GTPase activating protein 19			-1.86
X79204	ATXN1 [e]	ataxin 1		-1.59	
M60315	BMP6	bone morphogenetic protein 6		-2.27	
U90546	BTN3A2	butyrophilin, subfamily 3, member A2		-1.54	
AB029343	**C6orf18**	**chromosome 6 open reading frame 18**		-1.84	
AF043897	C9orf3	chromosome 9 open reading frame 3		-5.49	-1.61
AF054177	CHD1L	chromodomain helicase DNA binding protein 1-like		-2.64	
M33653	COL13A1	collagen, type XIII, alpha 1			-1.97
AF091080	FLJ10374	hypothetical protein FLJ10374			-1.71
AA021140	FLJ13305	Hypothetical protein FLJ13305			-2.64
AI862521	FLJ20580	hypothetical protein FLJ20580			-1.52
AL049261	FRAG1 [e]	FGF receptor activating protein 1			-1.61
W52003	HEG	HEG homolog		-1.58	
AF052288	HIP1 [e]	huntingtin interacting protein 1		-1.53	
M95623	**HMBS**	**hydroxymethylbilane synthase**		-3.5	
AB002365	KIAA0367	KIAA0367		-1.86	
AB011095	KIAA0523	KIAA0523 protein		-1.6	
AB018254	KIAA0711	KIAA0711 gene product		-3.38	
AB020637	KIAA0830 [e]	KIAA0830 protein		-1.86	-1.67
AL050125	LOC283824 [e]	hypothetical protein LOC283824		-2.48	
U89942	LOXL2 [e]	lysyl oxidase-like 2			-1.57
D87436	LPIN2	lipin 2		-1.97	
M16038	LYN [e]	v-yes-1 Yamaguchi sarcoma viral related oncogene homolog		-2.85	
M79321	LYN [e]	v-yes-1 Yamaguchi sarcoma viral related oncogene homolog		-2.4	
AF041210	MID1	midline 1 (Opitz/BBB syndrome)		-2.04	
AL022327	MLC1 [e]	megalencephalic leukoencephalopathy with subcortical cysts 1			-2.26
M16750	PIM1	pim-1 oncogene		-1.76	
X06745	POLA	polymerase (DNA directed), alpha			-2.15
AF034803	PPFIBP2	PTPRF interacting protein, binding protein 2 (liprin beta 2)		-1.9	
X89416	**PPP5C** [e]	**protein phosphatase 5, catalytic subunit**		-2.18	
AB011167	PPRC1 [e]	peroxisome proliferative activated receptor, gamma, coactivator-related 1			-1.7

X54131	PTPRB	protein tyrosine phosphatase, receptor type, B	-1.82	-1.94
D42043	RAFTLIN	raft-linking protein	-1.61	
AB002372	SNPH	syntaphilin	-2.15	
U57452	SNRK [e]	SNF-1 related kinase	-2.64	
AB007925	SRGAP2 [e]	SLIT-ROBO Rho GTPase activating protein 2	-1.75	
AF095791	TACC2	transforming, acidic coiled-coil containing protein 2	-1.64	
AF098162	TIMELESS	timeless homolog (Drosophila)	-1.7	
D87119	TRIB2 [e]	tribbles homolog 2 (Drosophila)	-7.62	-3.19
Q92519	TRIB2 [e]	tribbles homolog 2 (Drosophila)	-3.47	-2.22
W28360	UBE2J1	ubiquitin-conjugating enzyme E2, J1 (UBC6 homolog, yeast)		-1.65
X95808	ZNF261	zinc finger protein 261	-1.55	
HG3510-HT3704 TIGR	*Unknown* [e]		-1.98	
HG2379-HT3997 TIGR	*Unknown*		-1.75	
HG2059-HT2114 TIGR	*Unknown* [e]		-1.73	
AI184710			-1.54	
HG3510-HT3704 TIGR	*Unknown* [e]			-1.92

[a] Derived from LocusLink and SwissProt databases or recent publications
[b] See fold change formula described in *Materials and Methods*
[c] Similar genes with different Affymetrix targets
[d] Genes those IR-responsive modulation was confirmed by quantitative RT-PCR
[e] Genes up-regulated (or down-regulated) at 1 h, 6 h or 12 h after 20 Gy (using Genespring analysis, Fold change cutoff of 1.5 fold) IN COMMON with the same time points of the up-regulated (or down-regulated) genes of the present list.
Genes in bold show significant common up-regulation or common down-regulation at 3 Gy and 20 Gy (see Table 3.5)

Temporal responses of significantly IR-modulated genes

The response to irradiation in EA.hy 926 was transient for most of the significant genes. Only a few genes were commonly modulated at two or three time points tested. The majority were modulated at 6 h and 12 h for 20 Gy (Figure 3.10). At the three time points 1h, 6h and 12 h, there was one gene up-regulated more than 1.5 fold after 3 Gy, namely BTG2. Upon the same IR dose, PPM1/Waf1 was found to be up-regulated at 6 h and 12 h. Although its fold change was below 1.5 (1.42), PPM1/Waf1 was also significantly up-regulated at 1 h post 3 Gy. BTG2 and PPM1/Waf1 were also found to be up-regulated at 1 h, 6 h and 12 h post 20 Gy. The temporal induction patterns of these two genes are illustrated in Figure 3.11. The temporal response of these two genes was radiation dose-dependent.

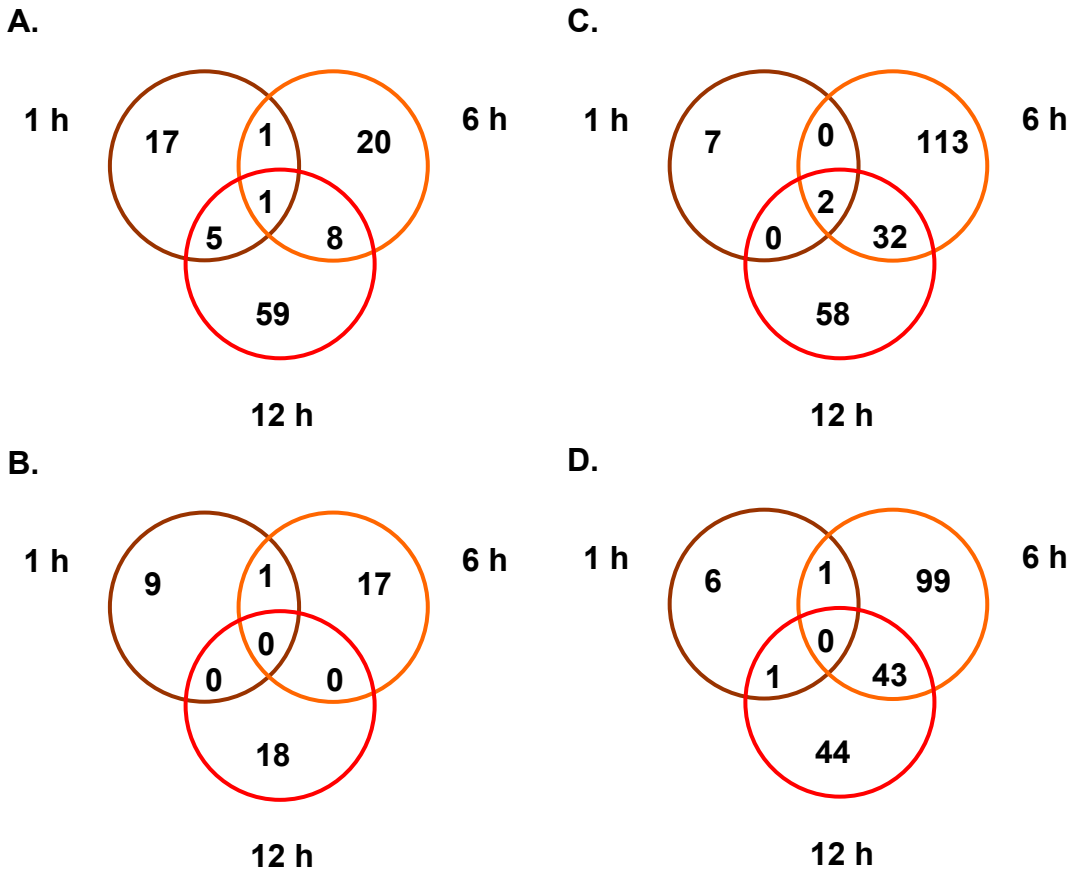

Figure 3.10 *Venn diagrams showing the number of genes modulated more than 1.5-fold in common at 1, 6 and 12 h after 3 Gy and 20 Gy,* ***A*** *significantly up-regulated genes after 3 Gy,* ***B*** *significantly down-regulated genes after 3 Gy,* ***C*** *significantly up-regulated genes after 20 Gy,* ***D*** *significantly down-regulated genes after 20 Gy.*

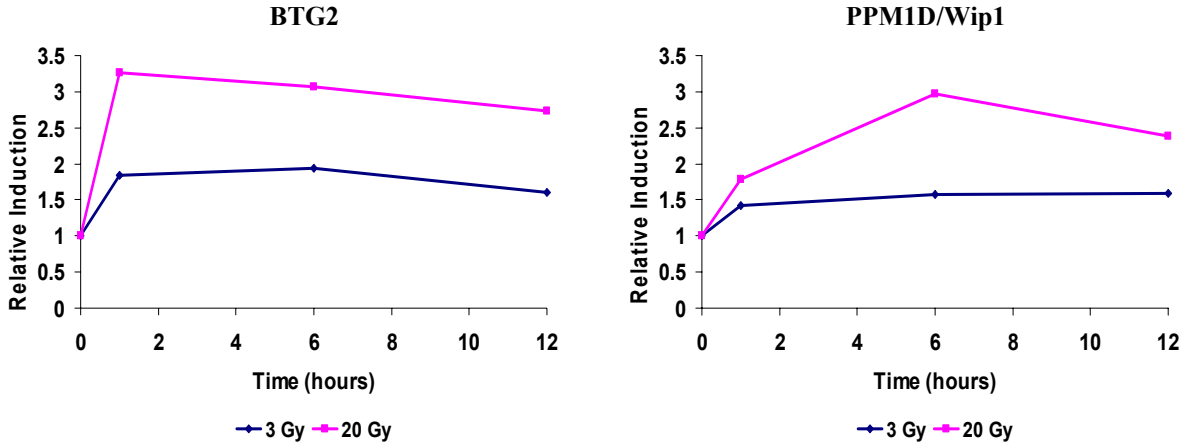

Figure 3.11 *Representation of temporal induction pattern of BTG2 (left panel) and PPM1D/Wip1 (right panel) genes after irradiation of EA.hy 926. The EA.hy 926 cells were exposed to 3 and 20 Gy and total RNA was extracted at 1, 6 and 12 h after irradiation. Among the significantly modulated genes from the cDNA microarray analysis, only BTG2 and PPM1D/Wip1 display significant induction at all three time points.*

Confirmation of IR-induction of selected genes

The reproducibility of induction some genes was validated by quantitative RT-PCR. Due to higher fold-changes at 20 Gy as compared to 3 Gy, we applied this technique for genes induced predominantly by 20 Gy (Figure 3.12). The IR-inducibility of BTG2 was confirmed by RT-PCR at high (Figure 3.12) and at low doses (see Chapter 4, Section 4.3.1.1). In all cases except for Fas/Apo1, the quantitative RT-PCR results confirmed the GeneChip data (Table 3.7). The differences in the fold changes are due to the different sensitivities and conditions of the applied methods.

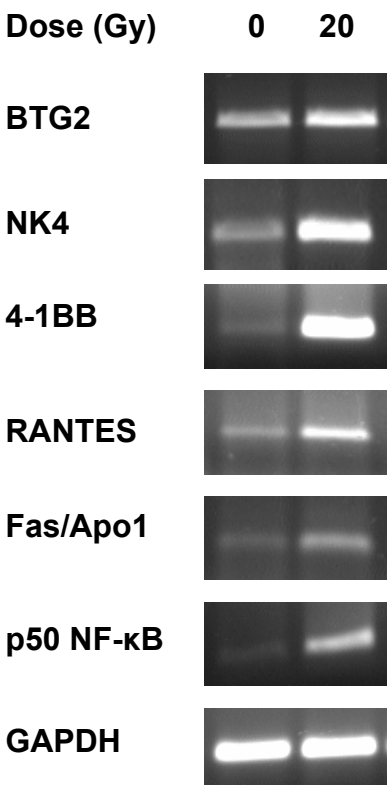

Figure 3.12 *Qualitative analysis of transcripts by RT-PCR in non-irradiated and irradiated EA.hy 926 cell line. Expression of the gene is normalized relative to GAPDH expression. The time points after 20 Gy were 1 h for BTG2, 6 h for 4-1BB, Fas/Apo1, p50 NF-κB, 12 h for NK4, RANTES. GAPDH expression is shown here 1 h post 20 Gy, but the level of RNA was similar at the other time points.*

Table 3.7 *Comparison of the fold change values of irradiation-inducible genes by quantitative RT-PCR and cDNA microarray methods. RT-PCR values for irradiated and non-irradiated samples (see Figure 3.12) were normalized to the corresponding values of the internal control GAPDH. RT-PCR fold changes were calculated as described in Materials and Methods.*

		Fold change	
Gene symbol	**GenBank Number**	**RT-PCR**	**cDNA microarray**
BTG2	U72649	2.82	3.25
NK4	AA631972	7.66	92.06
4-1BB	U03397	8.48	10.66
RANTES	M21121	1.84	4.65
Fas/Apo1	X83490	0.86	5.6
p50 NF-κB	S76638	3.52	6.14

3.3.2.2 Comparative gene expression induced by ionizing radiation

Gene expression profiling of EA.hy 926 irradiated with single doses, fractionated doses and of single dose irradiated capillaries EA.hy 926

Another study of the project involved the culturing of EA.hy 926 endothelial cells under different conditions and the application of single and fractionated irradiation doses. cDNA microarray experiments were performed as pilot experiments for a better understanding of the effects of IR on endothelial cells and their microenvironment.

EA.hy 926 cells were induced to form capillaries in the presence of collagen as shown in Figure 3.13. This assay aimed to develop an *in vitro* model to simulate the *in vivo* morphology of endothelial cells as they form blood vessels. A cDNA microarray experiment on irradiated capillaries EA.hy 926 cells was performed and compared with the results from irradiated EA.hy 926 cells grown in monolayers. Analysis of this data may provide a better understanding of the influence of EA.hy 926 morphology on gene expression in order to identify radiation-inducible endothelial cell promoters that would function *in vivo* (see Chapter 4).

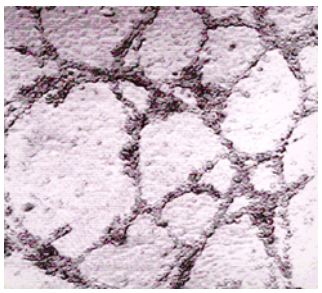

Figure 3.13 *EA.hy 926 cells grown into three dimensional capillaries tube-like structure in presence of 1.5 mg/ml collagen during 5 days.*

Administration of fractionated doses is the standard mode of radiotherapy, as it shows higher efficacy and less severe side effects in comparison with a single dose. In this respect, we treated EA.hy 926 cells with a fractionated dose of three times 3 Gy (intervals of 12 h) and a single dose of 9 Gy. Identification of genes induced by several fractionated doses may allow to better understand the underlying mechanisms of IR toxicity, and help to identify radiation-inducible endothelial cell promoters (see Chapter 4).

All these conditions were compared in the analysis shown in Figure 3.14 (left panel). The supervised clustering tree (Figure 3.14, right panel), shows that three dimensional structures formed on the cells do not influence the IR gene expression pattern and that fractionated IR doses do significantly alter the IR induction patterns. A cut-off fold change of 1.5 was applied and the list of genes is shown in the Table 3.8.

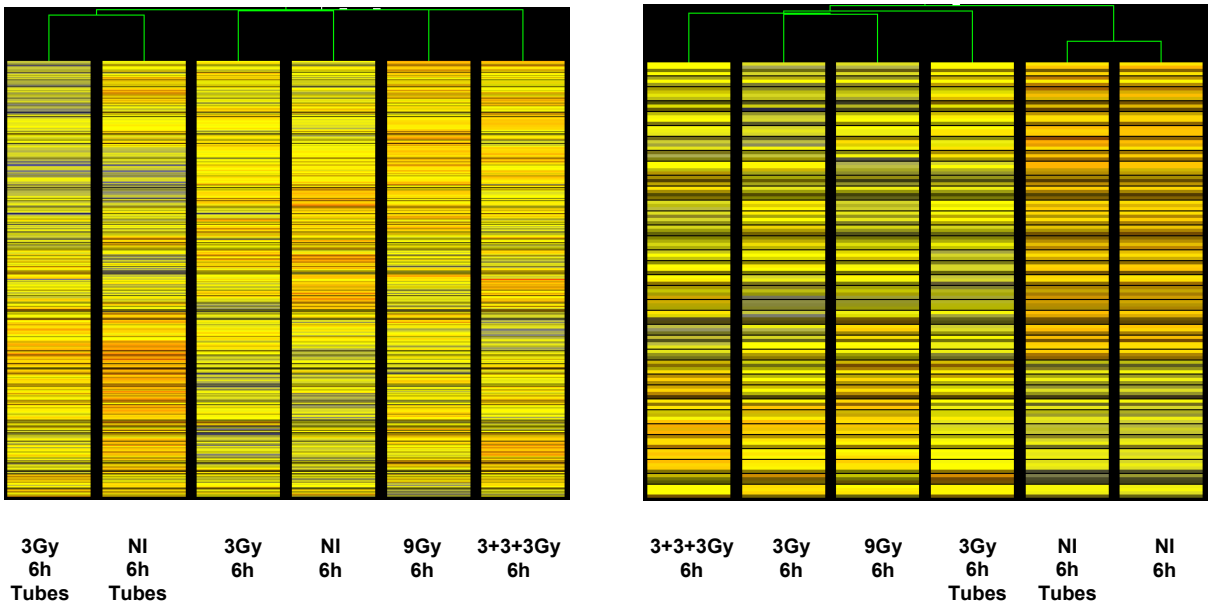

Figure 3.14 *hierarchical unsupervised (left) and supervised (right) clustering analyses of 4 irradiated (6 h post 3 Gy) and 2 non-irradiated (0 h) EA.hy 926 cells. Monolayers of EA.hy 926 cells were irradiated with 3 Gy, 3 x 3 Gy (12 h intervals) and 9 Gy or non-irradiated. Capillaries EA.hy 926 were irradiated with 3 Gy or non-irradiated. The clustering of the samples (Y-axis) is based on the 5656 expressed genes (on the left) and on the 123 statistically-significant expressed genes (right) represented on the X-axis. The grouping of the genes is based on the similarity between them. Genes are color-coded to indicate their expression levels relative to the median level for the genes across the entire sample (blue: lower expression; red: higher expression; yellow: no change). NI: non-irradiated. A total number of 12625 genes on the chips were tested. Applied filters for gene selection in the Genespring software are described in Materials and Methods.*

Table 3.8 *Genes that were up- or down-regulated in the conditions described in Figure 3.14, right with a selection of the genes that were more than 1.5-fold modulated. Applied filters in Genespring software are described in Materials and Methods.*

GenBank Accession Number	Gene symbol	Title	Fold change
Up-regulated genes >1.5 fold change			
U28687	ZNF157	zinc finger protein 157 (HZF22)	1.781
M55422	H-plk	Krueppel-related zinc finger protein	1.769
X84746	ABO	H.sapiens Histo-blood group AB0 gene, exon 1.	1.769
AF027150	SIP1	survival of motor neuron protein interacting protein 1	1.686
AA128249	FABP4	fatty acid binding protein 4, adipocyte	1.593
D50931	KIAA0141	KIAA0141 gene product	1.568
AB018340	SENP6	SUMO1/sentrin specific protease 6	1.552
Down-regulated genes <1.5 fold change *			
X59841	PBX3	pre-B-cell leukemia transcription factor 3	0.657
AB002405	EVER1	epidermodysplasia verruciformis 1	0.644
AL022729	RABL4	RAB, member of RAS oncogene family-like 4	0.637
M96824	NUCB1	nucleobindin 1	0.635
L06237	MAP1B; MAP5; FUTSCH	Human microtubule-associated protein 1B (MAP1B) gene, complete cds.	0.632
U81607	AKAP12	A kinase (PRKA) anchor protein (gravin) 12	0.632
X07948	TNP1; TP1	unnamed protein product; TP1 (AA 1-55); Human mRNA for transition protein 1 (TP1).	0.627
U72206	ARHGEF2; P40; GEFH1; LFP40; GEF-H1; KIAA0651; DKFZp547L106	similar to lfc oncogene product; Human guanine nucleotide regulatory factor (LFP40) mRNA, complete cds.	0.626
AF029669	RAD51C	RAD51 homolog C (S. cerevisiae)	0.619
U43959	ADD2	adducin 2 (beta)	0.616
U42390	TRIO	triple functional domain (PTPRF interacting)	0.612
AB007447	FLN29	FLN29 gene product	0.606
J05448	POLR2C	polymerase (RNA) II (DNA directed) polypeptide C, 33kDa	0.602
U43916	EMP1	epithelial membrane protein 1	0.601
M32313	SRD5A1	steroid-5-alpha-reductase, alpha polypeptide 1 (3-oxo-5 alpha-steroid delta 4-dehydrogenase alpha 1)	0.59
U38847	TARBP1	TAR (HIV) RNA binding protein 1	0.529
AF070626	LOC54499	putative membrane protein	0.505

* Fold change (FC) <1.5: equivalent to 0.66>FC>0 in Genespring software.

Gene expression profiling of irradiated EA.hy 926 and irradiated HMEC

To evaluate the specificity of gene modulation of endothelial cells, the primary endothelial cells HMEC were compared to the EA.hy 926 after 3 Gy. HMEC were irradiated with 3 Gy and harvested after 1 h, 6 h and 12 h or non-irradiated (0 h).

The hierarchal supervised clustering (Figure 3.15 left) shows that HMEC display a different gene expression pattern background than EA.hy 926. In the supervised analysis, the profiles by IR treatment are shown. Only a few genes were modulated in common. Among the IR-modulated genes in treated samples *versus* non-treated samples of EA.hy 926 and HMEC, BTG2 and CUL2 genes were found to be up-regulated (Table 3.9).

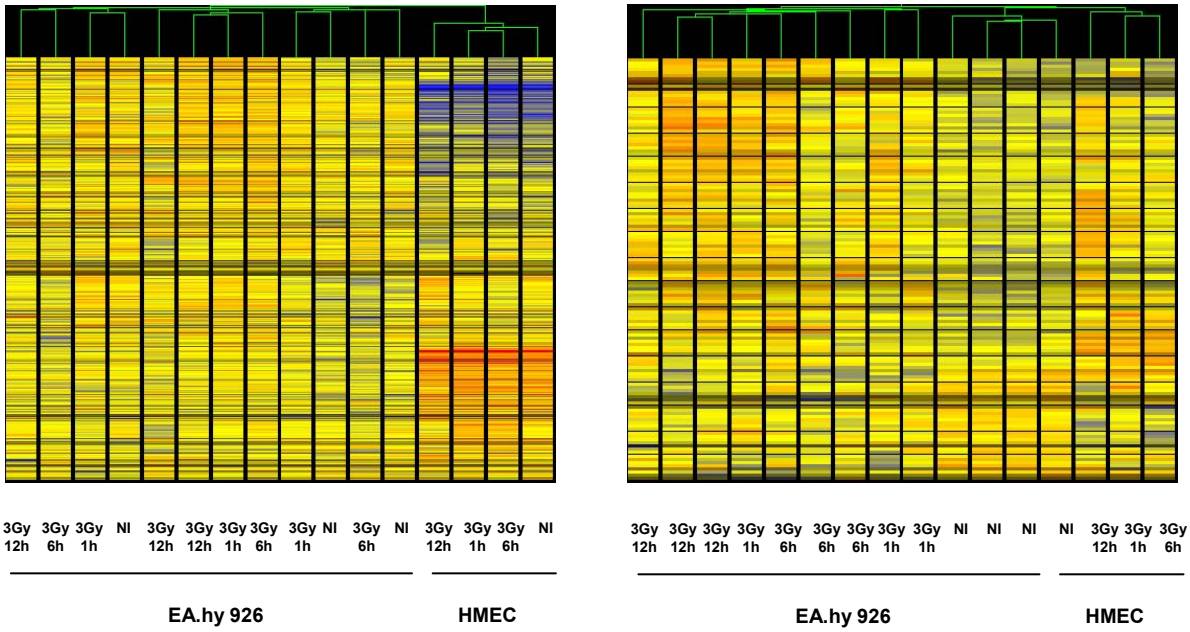

Figure 3.15 *Hierarchical unsupervised (left) and supervised (right) clustering analysis of 9 irradiated samples (1, 6 and 12 h post 20 Gy) and 3 non-irradiated samples (0 h) in EA.hy 926 and 3 irradiated samples (1, 6 and 12 h post 3 Gy) and 1 non-irradiated sample1 (0 h) in HMEC. The clustering of the samples (Y-axis) is based on the 5863 expressed genes (left) and on the 129 statistically significant expressed genes (right) represented on the X-axis. The grouping of the genes is based on the similarity between them. Genes are color-coded to indicate their expression levels relative to the median level for the genes across the entire sample (blue: lower expression; red: higher expression; yellow: no change). NI: non-irradiated. A total number of 12625 genes onto the chips were tested. Applied filters for gene selection in the Genespring software are described in Materials and Methods.*

Table 3.9 *Genes up- or down-regulated under the conditions described in Figure 3.15 (right panel) with a selection of the genes that were more than 1.5-fold modulated. Applied filters in the Genespring software are described in Materials and Methods.*

GenBank Accession Number	Gene symbol	Title	Fold change
Up-regulated genes >1.5 fold change			
AB011165	THRAP1	thyroid hormone receptor associated protein 1	2.008
U72649	BTG2	BTG family, member 2	1.843
U83410	CUL2	cullin 2	1.674
AF025654	RNGTT	RNA guanylyltransferase and 5'-phosphatase	1.668
AB023182	STK38L	serine/threonine kinase 38 like	1.65
AB014578	RME8	RME8 protein	1.567
X98296	USP9X	ubiquitin specific protease 9, X-linked (fat facets-like, Drosophila)	1.526
U46691	SUPT6H	Human putative chromatin structure regulator (SUPT6H) mRNA, complete cds.	1.509
Down-regulated genes <1.5 fold change			
M37190	RIN2	Ras and Rab interactor 2	0.653
AA524802		CDNA FLJ32819 fis, clone TESTI2002937, weakly similar to HISTONE H3.2	0.614

* Fold change (FC) <1.5: equivalent to 0.66>FC>0 in Genespring software.

3.4 Discussion

Microarray analyses were performed to identify the gene expression pattern in the endothelial cells EA.hy 926 after ionizing radiation. The transcriptional changes, resulting from low and high doses of IR were investigated at various times following treatment to elucidate the molecular events involved in the IR responses in endothelial cells.

Comparison of the clustering gene trees of cells exposed to 3 Gy and 20 Gy revealed different patterns of IR modulation depending on the IR-dose and the expression time (Figures 3.6 and 3.7 right panels). The analysis of the IR-responsive genes resulted in 24, 30 and 72 significantly up-regulated genes and 10, 18 and 18 significantly down-regulated genes at 1, 6 and 12 h after 3 Gy, respectively (Table 3.4 and Table 3.5). 9, 147 and 92 significantly up-regulated genes and 8, 143 and 88 significantly down-regulated genes were identified at 1, 6 and 12 h after 20 Gy, respectively (Table 3.4 and Table 3.6).

At low and high doses, only a weak response to IR was displayed after 1 h. The time period following treatment was probably too short as it did not cover all early responses to IR. Responses to IR at the transcriptional level become apparent at later recording times (6 h and 12 h). A considerable change in the transcriptome of EA.hy 926 after 6 h and 12 h following 20 Gy exposures with a transient modulation at 6 h. These data contrasted with the levels of RNA in cells exposed to 3 Gy. Indeed, a larger magnitude in the modulation as well as a higher number of IR-modulated genes (see above) was observed after 20 Gy in comparison to 3 Gy. This may be due to more DNA damages being caused by higher radiation doses, resulting in a more intensive response in comparison to low doses. As IR chiefly causes double strand breaks in DNA, a large proportion of IR-responsive genes after 3 Gy and 20 Gy were found to be involved in cell cycle regulation, DNA repair or apoptosis.

In these latter processes, the p53 protein plays a key role. The increase in p53 protein level causes the induction of many genes involved in cell cycle arrest, DNA repair and apoptosis (see references in Chapter 1). In this investigation, p53-dependent genes such as CDKN1A/p21/Waf1, GADD45, TNFRF6/Fas/Apo-1, TNFRSF10B/KILLER/DR5, BTG2 and PPM1D/Wip1 were altered by IR. The transcription factor p53 could be detected by Western blotting only following high doses such as 9 Gy and 20 Gy (Figure 3.2). Increases in CDKN1A/p21/Waf1 protein also occurred at high doses, probably due to p53 transactivation of the CDKN1A/p21/Waf1 target gene. Slight increases of CDKN1A/p21/Waf1 protein were also seen at lower doses such as at 12 h post 3 Gy (Figure 3.2). At the transcription level,

CDKN1A/p21/Waf1 induction occurred at 20 Gy but not at 3 Gy. This data suggests that CDKN1A/p21/Waf1 requires a relatively high amount of p53 to be significantly increased and detected.

CDKN1A/p21/Waf1 plays an important role in cell cycle regulation by causing a G1/S arrest in response to genotoxic stress such as IR, thus allowing repair to occur. Induction of CDKN1A/p21/Waf1 was reported in numerous microarray experiments utilizing IR (Amundson *et al*, 1999a; Amundson *et al*, 1999b; Amundson *et al*, 2000; Balcer-Kubiczek *et al*, 1999; Heinloth *et al*, 2003a; Heinloth *et al*, 2003b; Jen and Cheung, 2003; Li *et al*, 2001; Marko *et al*, 2003; Robles *et al*, 2001; Stassen *et al*, 2003; Tusher *et al*, 2001). This study illustrated induction of CDKN1A/p21/Waf1 mRNA at 6 h post 20 Gy. This observation supports, in collaboration with the reports in the literature, the consistency of CDKN1A/p21/Waf1 induction after the IR genotoxic stress in different cell types. GADD45 is another cell cycle regulation and DNA repair gene that was shown to be induced by IR in many other studies. IR-induction of the cell cycle regulator GADD45 was found despite differences in cell type, genetic background, IR-doses and test time following irradiation. Its induction by IR has been observed in several microarray experiments (Amundson *et al*, 1999b; Amundson *et al*, 2000; Jen and Cheung, 2003; Marko *et al*, 2003; Tusher *et al*, 2001). Also here, GADD45 responded rapidly and at low doses (at 1 h after 3 Gy).

A cessation and delay of the cell cycle in EA.hy 926 cells occurred at low and high doses (Figure 3.1). A G2/M arrest was rapid and short at 3 Gy, whereas a later and more pronounced cell cycle arrest in G2/M phase, a transient S phase delay at 6 h and a G1/S arrest were observed at 20 Gy. The transcriptional responses revealed that at 6 h post 20 Gy, cell cycle regulators such as E2F1, B-MYB, cyclin A2, B2, D3, E1, F or CDC25C were down-regulated. These genes are known to be involved in the different phases of the cell cycle progression. Their down-regulation suggests that they may contribute to cell cycle arrests in EA.hy 926 cells.

At high doses, the DNA repair systems may become down-regulated as the time progresses to 6 h and while the apoptotic cell death machinery gets activated. Indeed, genes such as FANCG, BRCA1, DNAPK, XRCC3 were found to be down-regulated. In contrast, the repair gene XPC was up-regulated at 6 h and 12 h post 20 Gy. XPC is known to increase the nucleotide excision repair (NER) after ultraviolet radiation. IR was recently proved to be another source of lesions plausibly recognized by the NER system by involving XPC and p53 (Amundson *et al*, 2002). The induction of XPC after IR, demonstrated in this study and

previous investigations (Amundson *et al*, 2000; Tusher *et al*, 2001). However, the role of XPC in the repair of lesions generated by IR has still to be proven.

When the damage caused by IR is too intensive and cannot be repaired, cells undergo apoptosis. Cell death in EA.hy 926 cells was measured at 48 h post-IR (Figure 3.4 and Figure 3.5). However, apoptosis is activated much earlier. Indeed, induction of the death receptors, TNFRF6/Fas/Apo-1 and TNFRSF10B/KILLER/DR5, occurred immediately at 1 h and 6 h following 3 Gy and 20 Gy exposures, respectively. TNFRF6/Fas/Apo-1 and the TNFRSF10B/KILLER/DR5 were previously shown to be induced by IR (Embree-Ku *et al*, 2002; Gong and Almasan, 2000; Reap *et al*, 1997). This study's results further support the idea that these death receptor pathways may play an important role in IR-related apoptosis.

While many genes were only altered at a specific IR-dose or at a certain time, the B cell translocation gene 2 (BTG2) and the wild-type-p53-induced phosphatase PPM1D/Wip1 were modulated at both IR doses and at all three time points (Figure 3.11). In several studies, BTG2 was reported to be induced in response to genotoxic stresses including IR (Amundson *et al*, 2003; Cortes *et al*, 2000; Rouault *et al*, 1996). Here, induction of BTG2 was shown in EA.hy 926 as well as in HMEC (Table 3.9), suggesting BTG2 plays an important role in endothelial cells after IR. BTG2 has been proposed to exercise anti-proliferative abilities (Guehenneux *et al*, 1997; Matsuda *et al*, 1996; Rouault *et al*, 1992), but its role in IR stress responses remains to be elucidated. The PPM1D/Wip1 is a serine/threonine phosphatase that was revealed to be transcriptionally up-regulated by p53 following IR (Choi *et al*, 2000; Choi *et al*, 2002). Recent evidence has revealed that PPM1D/Wip1 activation occurs via p38 MAP kinase (Bulavin *et al*, 2002; Bulavin *et al*, 2004). However, the understanding of the role of PPM1D/Wip1 and its relation with the p38 MAPK and p53 in the IR responses requires further investigations.

Some of the most strongly up-regulated genes were tested for the reproducibility of induction. The six IR-inducible genes selected for analysis by real time RT-PCR were: BTG2, NK4, 4-1BB, RANTES, Fas/Apo1 and the p50 subunit of NF-κB. Quantitative inductions of these genes were not completely correlated between cDNA microarray and quantitative RT-PCR due to the different sensitivities of these methods (Table 3.7). Indeed, the RT-PCR technique provides more precise quantification in comparison to the cDNA microarray. This could be due to the fact that RT-PCR is based on the amplification of one single transcript, whereas cDNA microarray provides expression profiles over a larger numbers of genes. In this latter case, variation in sensitivity might be due to overexpression of target oligonucleotide probes

on the chip. In all cases except Fas/Apo1, irradiation inducibilities were confirmed (Table 3.7 and Figure 3.12). The natural killer transcript 4 (NK4) was found to be the most up-regulated gene in the cDNA microarray. It was induced at an amplitude of 85.4 and 92.1 at 6 h and 12 h after 20 Gy, respectively. Regarding these time points it would be of interest to determine whether NK4 is induced directly by IR or by products of IR-inducible genes. Evidence of NK4 increasing after ionizing radiation has not been previously reported. Thus, specific endothelial event after IR may be suggested.

In this study, certain components of the network of genes involved in the responses to IR have been described. These findings contribute to a better understanding of the consequences of radiation with the ultimate aim of assisting in the development of new IR-based strategies for cancer treatment.

4 PROMOTER STUDY IN RESPONSE TO IONIZING RADIATION

4.1 Introduction

Eukaryotic gene expression is a highly coordinated process involving regulation at many different levels. Although several types of *cis*-acting DNA sequence elements contribute to this regulation, the simplest elements involved may be promoters as these are chiefly located upstream of the transcription start site. In this study, the response of promoters to ionizing radiation (IR) was investigated. Radiation-inducible promoters are candidates to play a future role in the application of cancer gene therapy. Genes that were up-regulated in irradiated endothelial cells (see Chapter 3) were selected according to criteria such as high fold-induction, transient induction or non-induction in non-irradiated cells. Induction of genes such as BTG2, 4-1BB and NK4 following IR was confirmed by RT-PCR. Transfection and luciferase reporter gene assays were utilized to record the activities of the endogenous promoters of BTG2 and 4-1BB upon IR. Preliminary investigations were conducted in an attempt to characterize and map the promoter of NK4.

Initiation and regulation of transcription processes require, alongside RNA polymerase, transcription factors and co-factors. Exploiting IR-inducible transcription factors may yield a promising strategy for improving cancer gene therapy. In this study, NF-κB transcription factor, known to be induced after IR, was studied for its transactivation characteristics. For this purpose, an artificial vector composed of specific binding sites for NF-κB was utilized to evaluate the transactivation effect of NF-κB. The activity of NF-κB binding to the specific target sequence was followed by transfection and luciferase reporter gene assays.

Endothelial cells represent a very promising target for gene therapy (see Chapter 1, Section 1.4.2). However, transfection efficiencies of human endothelial cells by use of standard protocols have been reported by this study and current literature, to be generally low (Tanner *et al*, 1997). In this investigation, other cell lines with high transfection efficiency and proven IR-inducibility for the gene of the corresponding studied promoter were used for proof of principle. The readouts of the luciferase assays were taken into account when potential promoter or transcription factors regulatory elements were selected for further investigations concerning the cancer radio-inducible gene therapy concept.

4.2 Materials and Methods

Cell culture All cells were cultured at 37°C in an incubator with a humidified atmosphere of 5% CO_2 and 95% room air. The human EA.hy 926 cell line was originally obtained by fusion of human umbilical vein endothelial cells (HUVEC) with a human lung carcinoma line (Edgell *et al*, 1983). The human embryonic kidney 293 (HEK 293) cells expressing the adenovirus large T antigen (293-T) were kindly provided by K. Ballmer-Hofer (Paul Scherrer Institute, Villigen Switzerland). The human HeLa malignant cell line, derived from the cervical carcinoma of Henrietta Lacks, was obtained from the American Type Culture Collection. EA.hy 926, 293-T and HeLa were maintained in DMEM (Omnilab) supplemented with 10% FBS (Seromed) and 1% PS (Omnilab). The human colorectal carcinoma cell line HCT116 originated from the American Type Culture Collection and was cultured in McCoy's 5A medium (Omnilab) with 10% FBS (Seromed) and 1% PS (Omnilab).

Irradiation treatments Irradiation was carried out at room temperature in single doses from 1 Gy to 20 Gy using an X-ray machine (Philips PW 2184/00-Monitor SN4) in a chamber with 300 kV intensity.

Quantitative RT-PCR Quantitative RT-PCR was performed as described in *Materials and Methods* in Chapter 3. Total RNA was extracted from EA.hy 926, HCT116, HeLa and 293-T cells at the indicated time and IR doses. Triplicates of each irradiation dose or time points were pooled together. BTG2, 4-1BB and NK4 genes were amplified using primers shown in Table 3.1. Primers used for NK4 variants amplifications and their respective melting temperatures (Tm = 69.3+ (0.41*(GC/base number*100) - (650/base number) -3) are shown in Table 4.1.

Table 4.1 *Primers used for NK4 RT-PCR amplifications.*

Primer name	Orientation	Primer (5'-3')	Tm (° C)	PCR product size (bp)
NK4_FW1	**Forward**	TGCCAACTCTGCCTCTCTTCAC	59.1	143
NK4_REV1	**Reverse**	ACTGTCTCCAGGTAGCCCTCTTTG	61.4	
NK4_FW2	**Forward**	AGCCAGGGACGGACCCTCATTC	62.8	394
NK4_REV1	**Reverse**	ACTGTCTCCAGGTAGCCCTCTTTG	61.4	
NK4_FW3	**Forward**	TGGCTCCTTGAACTTTTGGCCGC	61.2	335
NK4_REV1	**Reverse**	ACTGTCTCCAGGTAGCCCTCTTTG	61.4	

Genomic DNA isolation. Genomic DNA was extracted from EA.hy 926 cells using the GeneElute Mammalian Genomic DNA Kit (Sigma).

Cloning of the 4-1BB promoter in a luciferase reporter plasmid. The 4-1BB promoter with a length of 1741 bp was amplified by PCR from genomic DNA using a *KpnI-HindIII*-flanked primer set. The forward and reverse primers were flanked with *KpnI* or *HindIII* restriction enzyme sequences, respectively (see underlined sections below). Restriction site flaps at 5' of each primer were added during their synthesis (Microsynth). The forward and reverse primer sequences were as follows: 5′-ATCCAGGTACCTGCCATGTTGGACAGTCTAGTGTC-3′and 5′-GTAGTAAGCTTGATGAAATCTGGCACAGGTATGATAC-3′, respectively. The melting temperatures (Tm = 69.3+ (0.41*(GC/base number*100) - (650/base number) -3) were 59.7 °C and 58.6 °C for the forward primer and the reverse primer, respectively. The PCR conditions are described on page 86. These primers were designed from the genomic sequence extracted from Ensembl databases (www.ensembl.org) using GeneBank accession number U03397. The reverse primer was designed upstream of the 4-1BB translational start site ATG. The 4-1BB promoter region PCR product was subcloned into the Firefly luciferase reporter pGL3-basic (Promega). The cloned 4-1BB promoter sequence was verified by sequencing (Microsynth).

Cloning of the NK4 5'-upstream region in a luciferase reporter plasmid. The NK4 5'-upstream region was amplified by PCR from genomic DNA using an *XhoI-HindIII*-flanked primer set. Several subclonings into the Firefly luciferase reporter pGL3-basic (Promega) were performed. The forward and reverse primers flanked with *XhoI* or *HindIII* restriction enzyme sequences, respectively, are shown in Table 4.2. The underlined sections correspond to the restriction sequences. Restriction site flaps at 5' of each primer were added during their synthesis (Microsynth). These primers were designed from the genomic sequence extracted from Ensembl databases (www.ensembl.org) using GeneBank accession number AA631972. The cloned 5'-upstream regions of the NK4 constructs were verified by sequencing (Microsynth).

Table 4.2 *Primers used for NK4 PCR amplifications.*

Primer name	Orientation	Primer (5'-3')	Tm (° C)	PCR product size (bp)
NK4P_FW1	**Forward**	ATCCACTCGAGAGAAAGTAGATGAGGCCAGACACAG	59.9	2159
NK4P_REV1	**Reverse**	ATAGTAAGCTTAATGAGGGTCCGTCCCTGGCTG	62.8	
NK4P_FW2	**Forward**	ATCAACTCGAGAGCCAGGCTGGAGGGTCAGAAC	62.8	564
NK4P_REV1	**Reverse**	ATAGTAAGCTTAATGAGGGTCCGTCCCTGGCTG	62.8	
NK4P_FW2	**Forward**	ATCAACTCGAGAGCCAGGCTGGAGGGTCAGAAC	62.8	916
NK4P_REV2	**Reverse**	ATAGTAAGCTTTGGCGGCCAAAAGTTCAAGGAGCC	63.1	

The BAC clone containing NK4 was kindly donated by Bernot et *al* (GENOSCOPE, Evry-France). This BAC clone from the RP11 library and referred to as RP11-473M20 has been entirely sequenced by the DOE Joint Genome Institute (www.jgi.doe.gov). The sequence of this BAC clone (AC108134) has been annotated to encompass the complete NK4 gene limits, including large upstream and downstream segments.

Cloning of NF-κB binding sites and the thymidine kinase gene. The NF-κB cis-enhancer element quintet repeated $(TGGGGACTTTCCGC)_5$, a TATA box and the thymidine kinase gene (TK) were cloned into the pGL3-basic vector. The oligonucleotides containing NF-κB

binding sites, synthesized by Microsynth, are shown in Table 4.3. They were annealed in annealing buffer (1 x) diluted from a 5 x stock solution (10 mM Tris pH8, 1 mM $NaCl_2$, 25 mM NaCl) incubated for 10 min at 95° and progressively cooled to room temperature. The underlined flanking regions of the primers comprise the restricted *XhoI* or *HindIII* sites (see Table 4.3). The annealed product was cloned into the pGL3-basic vector (Promega).

Table 4.3 *Complementary oligonucleotides containing NF-κB binding sites, a TATA box sequence and restricted flanking sites for cloning.*

	Oligonucleotide orientation (5'-3')
Oligo 1	TCGAGTGGGGACTTTCCGCTGGGGACTTTCCGCTGGGGACTTTCCGCTGGGGACT TTCCGCTGGGGACTTTCCGCGGAGACTCAAGAGGGTATATAA
Oligo 2	AGCTTTATATACCCTCTTGAGTCTCCGCGGAAAGTCCCCAGCGGAAAGTCCCCAG CGGAAAGTCCCCAGCGGAAAGTCCCCAGCGGAAAGTCCCCAC

Amplification of the thymidine kinase gene (TK) was performed by PCR using the vector pSBCTKBSD as a template (kindly provided by Karreman ((Karreman, 1998) for details). The forward and reverse primers were flanked with *NcoI* or *XbaI* restriction enzyme sequences, respectively (see underlined sections below). Restriction site flaps at 5' of each primer were added during their synthesis (Microsynth). The sequences of the forward and reverse primer were 5′-GATACGCCATGGCGTCTGCGTTCGACCAGGC-3′, and 5′-CAACGCTCTAGATCAGTTAGCCTCCCCCATCTCCCGG-3′, respectively. The melting temperatures (Tm = 69.3+ (0.41*(GC/base number*100) - (650/base number) -3) were 62.5 °C and 62.6 °C for the forward primer and the reverse primer, respectively. Overnight digestion of the 1103 bp PCR product was performed with *NcoI* and *XbaI* restriction enzymes (New England Biolabs) to generate cohesive ends for cloning. The pGL3-NF-κB was digested by *NcoI* and *XbaI* restriction enzymes to remove the Firefly luciferase gene. The PCR-amplified TK gene was cloned into the pGL3-NF-κB luciferase gene-less vector. The pGL3-NF-κB and pTK-NF-κB clone sequences were verified by sequencing (Microsynth).

PCR. Cloning by PCR was performed in a 50 µL reaction mix using primers (0.5 µM), dNTPs (200 µM), H_2O, reaction buffer 10x (1x), Pfu Turbo DNA polymerase (Stratagene, 2.5U) and genomic DNA (100-200 ng) or plasmid DNA (10-100 ng). The PCR reaction conditions are shown in Table 4.4. The annealing temperature is dependent on the primers melting temperature (Tm = 69.3+(0.41*(GC/base*100)-(650/nb bases)-3). The extension time is dependent on the length of the target to amplify (~ 1min/kb).

Table 4.4 *PCR reaction conditions.*

	Temp (°C)	Time (min)	Cycles
Denaturation	95	2	1
Amplification			30
Denaturation	95	1	
Annealing	variable	1	
Extension	72	variable	
Final extension	72	10	1

Plasmids and transfections

Table 4.5 *Plasmids and their transfection conditions.*

Plasmid	Description	Transfected Cell lines Transfection types	Transfection Reagent
pGL3-BTG2/p2658	5'-flanking region of BTG2 gene cloned in a Firefly luciferase reporter. Kindly donated by Duriez *et al,* INSERM U453, Lyon France.	HCT116, transient	FuGENE6
pGL3-BTG2/p373	Partial 5'-flanking region of BTG2 gene cloned in a Firefly luciferase reporter. Kindly donated by Duriez *et al,* INSERM U453, Lyon France.	HCT116, transient	FuGENE6 Lipofectamine
pCMV-p53	P53 gene under the control of the CMV promoter. Kindly donated by Duriez *et al,* INSERM U453, Lyon France.	HCT116, transient	FuGENE6 Lipofectamine
pGL3-basic	Plamid containing the Firefly luciferase gene and lacking eukaryotic promoter and enhancer sequences in the cloning cassette. Purchased from Promega.	HCT116, transient	FuGENE6 Lipofectamine
pRL-SV40	Plamid containing the Renilla luciferase gene under the control of the SV40 promoter. Normalization plasmid for the pGL3 constructs. Purchased from Promega.	HCT116, transient	FuGENE6 Lipofectamine
pGL3-4-1BB/p1741	5'-flanking region of NK4 gene (1741 bp) cloned into pGL3-basic. Cloned during this work.	EA.hy 926 293-T, transient	FuGENE6 Lipofectamine
pGL3-NK4/p2159	5'-flanking region of NK4 gene (2159 bp) cloned into pGL3-basic Cloned during this work.	293-T HeLa, transient	FuGENE6 Lipofectamine
pGL3-NK4/p564	5'-flanking region of NK4 gene (564 bp) cloned into pGL3-basic Cloned during this work.	293-T HeLa, transient	FuGENE6 Lipofectamine
pGL3-NK4/p916	5'-flanking region of NK4 gene (916 bp) cloned into pGL3-basic Cloned during this work.	293-T HeLa, transient	FuGENE6 Lipofectamine
RP11-473M20 BAC-NK4	NK4 gene and its upstream and downstream segments cloned in pBACe3.6 vector Kindly provided by Bernot *et al,* GENOSCOPE, Evry France.	293-T, transient	Lipofectamine

pNF-κB-Luc	Plasmid containing five binding sites tandemly-repeated for NF-κB and the Firefly luciferase gene Purchased from Stratagene.	EA.hy 926 transient; stable: *in progress* 293-T, transient and stable	FuGENE6 Lipofectamine
pFC-MEKK	Plasmid that contains the CMV promoter followed by MEKK cDNA partial sequence (360-672). Positive Control for pNF-κB-Luc. Purchased from Stratagene.	EA.hy 926 293-T, transient	FuGENE6
pGL3-NF-κB	Parental plasmid for the construction of pTK -NF-κB. Contains five binding sites for NF-κB. Cloned during this work.	293-T, transient	
pTK-NF-κB	Construction by substitution of the Firefly luciferase gene from the pGL3-NF-κB plasmid by the thymidine kinase gene. Cloned during this work.	293-T, stable: *in progress*	

Transient transfections

Cells were plated at a density of 1.10^5 cells per 3.5 cm well-plate. Plasmids shown in Table 4.5 were transiently transfected using two protocols. In the protocol using FuGENE6 (Roche), cells were transfected 24 h after seeding according to the manufacturer's instructions. The Firefly luciferase reporter (1000 ng), mixed with 50 ng of the internal standard Renilla luciferase plasmid pRL-SV40 (Promega) were suspended in 50 µl serum-free DMEM containing FuGENE6. The FuGENE6 mix was incubated for 15 min at room temperature and then added with gentle swirling. The pRL-SV40 plasmid was co-transfected to normalize for the variation in transfection efficiency. In the protocol using Lipofectamine transfections reagents (Invitrogen), cells were transfected 24 h after seeding according to the manufacturer's instructions and optimized for low amounts of transfected plasmid. The Firefly luciferase reporter (40 ng), mixed with 2 ng of the internal standard pRL-SV40 (Promega) were suspended in 25 µl serum-free DMEM. 2 µl of lipofectamine (Invitrogen) mixed with 3 µl of Plus reagent (Invitrogen) were added in another 25 µl of serum-free DMEM. After 15 min, the plasmid mix and the lipofectamine mix were added together for 15 min at room temperature and then added gently to the cells in a serum-free medium. After 6 h, cells were washed twice with DMEM and provided with fresh medium containing serum and antibiotics.

Stable transfections

Stably transformed 293-T cell lines were established using hygromycin selection. pNF-κB-Luc was co-transfected with pTK-Hyg coding for the Hygromycin resistance gene (Clontech) in a ratio of 1/10. One day after transfection, cells were re-plated at various cell densities. Selection was initiated with 300 μg /ml hygromycin B (Omnilab). After three to four weeks in the incubator, clones were isolated and additionally propagated with 300 μg /ml hygromycin B. The screening of the positive stable clones that integrated the pNF-κB-Luc into the genome of the host cells was performed by PCR using specific probes for the Firefly luciferase gene.

Luciferase reporter gene assays. Cells were either treated with IR twenty four hours after transfection or remained untreated. Twenty four hours later, cells were washed with cold PBS, exposed to 200 μl of 1 × passive lysis buffer (Promega) for 15 min, and harvested. Debris was removed from cytosolic cell extracts by centrifugation. A total of 5 μl of each supernatant lysate was used in the dual luciferase reporter assay system (Promega). Luciferase activities were measured in a luminometer (Lumat). The transactivation activity of each construct was normalized to the Renilla luciferase control. All luciferase experiments were repeated at least three times.

Northern blotting. Total RNA was extracted from EA.hy 926 and 293-T at 0 h (non-irradiated) and 12 h post 20 Gy. 30 μg of total RNA were suspended in formamide loading buffer and electrophoresed on a 1% denaturing agarose gel containing formaldehyde. The positions of the 28S and 18S rRNAs were determined on a UV transilluminator and by comparison to the RNA Molecular Weight Marker II (Boehringer Mannheim). The gel was washed 4 x 10 min in DEPC water and blotted overnight in 10 x SSC pH7. The ARN were transferred by capillarity onto a Zeta-probe GT blotting nylon membranes (Biorad). The membranes were rinced briefly in 2 x SSC and dried at 80°C for 1 hour. Prehybridizations were performed for 30 min at 42°C in ULTRAhyb solution (Ambion). The natural killer transcript 4 (NK4) and the glyceraldehyde-3-phosphate dehydrogenase (GAPDH) probes were prepared by PCR and by random primer labeling (Random Primed DNA Labeling Kit, Roche) in presence of 50 μCi [α-32P]dCTP. After purification on sephadex G50 matrix and

denaturation, the probes were hybridizations in ULTRAhyb solution to the membranes during 16 hours at 42°C under rotation. The membranes were washed in 2 x SSC, 0.1% SDS (2 x 5 min) at room temperature and in 0.1 x SSC, 0.1% SDS at 42°C (2 x 15 min). The probes were detected with Typhoon 9400 software after exposition of the membrane on a phosphoscreen.

Immunofluorescence. 10^5 cells were plated and grown on cover-slip in 6 well plates and treated with IR. After indicated time points, the cells were fixed in cold methanol. Following blocking in 3% milk in PBS, the cells were incubated overnight at 4°C with the primary antibody NF-κB p65 (Santa Cruz Biotechnology C-20) diluted 1:100. The secondary antibody FITC-rabbit 1:700 was added for 1 hour at 37°C. After washing, DAPI diluted 1:1000 and antifade were added to the cover-slips.

4.3 Results

4.3.1 Native radiation-inducible promoter screening

4.3.1.1 BTG2 gene and promoter

Human B cell translocation gene 2 (BTG2, identified as PC3 and TIS21 in rats and mice, respectively) belongs to a family of structurally related proteins including BTG1, BTG3/ANA, PC3K/PC3B, TOB and TOB2. Although the precise functions of the B cell translocation (BTG) genes remain to be elucidated, they appear to act as antiproliferative proteins (Guehenneux *et al*, 1997; Matsuda *et al*, 1996; Rouault *et al*, 1992).

In response to genotoxic stresses including IR, BTG2 expression increases via a p53-dependent pathway. The expressed BTG2 protein may inhibit the cell cycle progression (Cortes *et al*, 2000; Rouault *et al*, 1996).

The main characteristics of the BTG2 promoter and gene were described by Duriez *et al* (Duriez *et al*, 2002) and are illustrated in Figure 4.1. BTG2 is composed of two exons separated by an intron. The 5'-upstream sequence contains a CAAT sequence located at the nucleotide -163 bp from the translational initiation site. Several GC-rich regions containing three Sp1 binding sites were identified. These features are commonly found in promoter regions of genes without a TATA box (Ji *et al*, 1996). The CpG island location was predicted from -554 to -80 with an average of GC content of 62%. Various potential binding sites of transcription factors such as Sp1, CREB, Gata-1, AP-1 and NF-κB were identified in the BTG2 promoter region. Furthermore, six highly related binding sites of p53 were revealed by sequencing (Duriez *et al*, 2002). Among them, two p53 binding sites were located in the intron and four p53 binding sites were recorded in the promoter region.

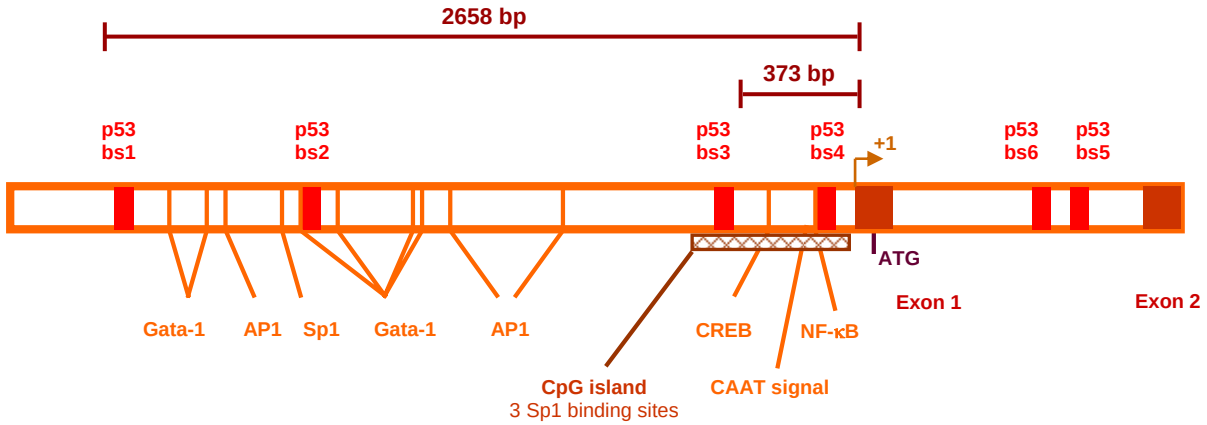

Figure 4.1 *Schematic representation of the human BTG2/PC3/TIS21 gene. The first nucleotide of the transcription start is indicated by an arrow and the number +1. The translational initiation site is indicated by ATG. The position of a CpG island is shown as a striped rectangle. The main transcription factor binding sites and the CAAT box, as well as the potential p53 binding sites (p53 bs1-6) are also indicated. The full length promoter of 2658 bp and the partial promoter long of 373 bp in lenght were cloned into a luciferase reporter by Duriez et al (Duriez et al, 2002), reported as pGL3-BTG2/p2658 and pGL3-BTG2/p373, respectively. The complete nucleotide sequence of BTG2 gene and promoter region is deposited with GeneBank (Accession number: AF361937) by Duriez et al (adapted from (Duriez et al, 2002)).*

BTG2 gene after ionizing radiation

In the cDNA microarray studies (Chapter 3), BTG2 (GeneBank accession number U72649) was induced by 3 Gy and 20 Gy in EA.hy 926 cells and by 3 Gy in HMEC. BTG2 gene was found to be significantly up-regulated after 3 Gy and 20 Gy at 1, 6 and 12 h post IR-treatment in EA.hy 926. The relative inductions from cDNA microarray analysis are reported in Table 4.6. To test the reliability of BTG2 transcript induction, quantitative RT-PCR analysis was performed. The lower panel of Figure 4.2 shows the RT-PCR amplification cycles of BTG2 gene in non-irradiated and irradiated EA.hy 926. The illustrated amplification cycles shown correspond to the cycle numbers where the DNA-incorporated fluorescence levels of all samples were identical. This specific cell cycle number is dependent on the starting amount of the target in the sample. Thus, more amplification cycles were needed for the mock-IR sample in comparison to the irradiated samples, suggesting that less starting RNA material was present in the non-irradiated sample than in the irradiated samples. The agarose gels of the RT-PCR products are shown in Figure 4.2 (upper panel) and the relative fold changes are shown in Table 4.6. In accordance to the cDNA microarray technology, the RT-PCR method confirms BTG2 induction by IR at a higher amplitude at 20 Gy in comparison to 3 Gy.

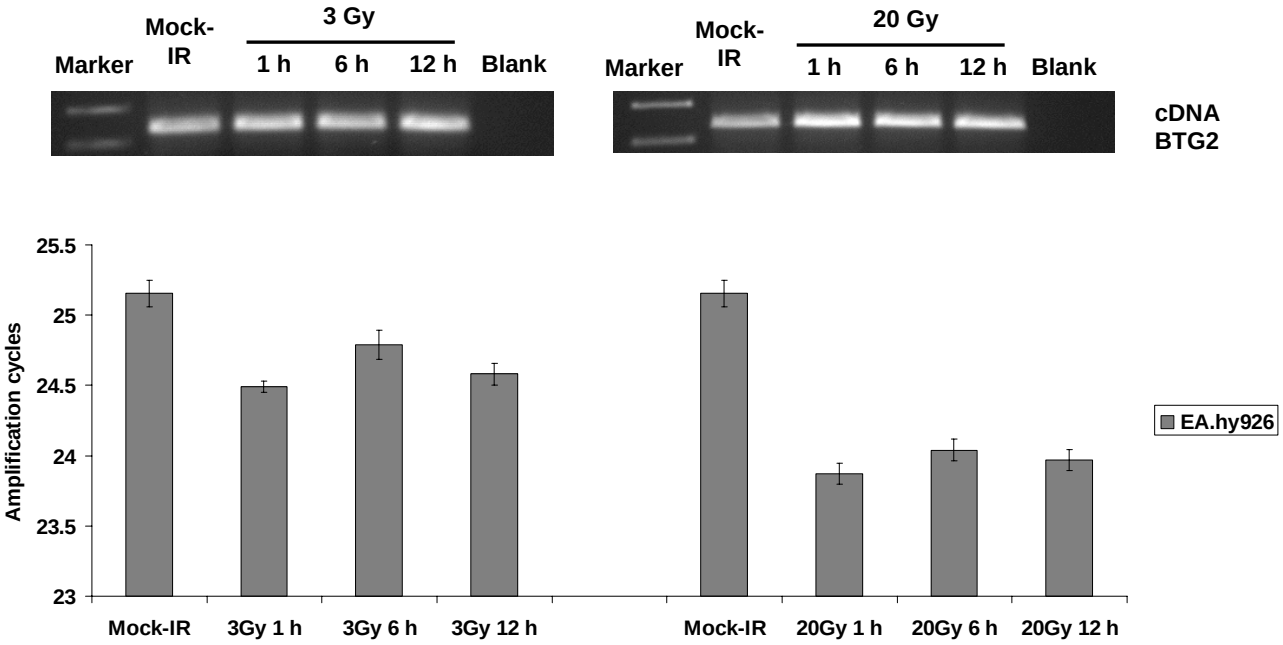

Figure 4.2 *Quantitative analysis of BTG2 transcript by RT-PCR in non-irradiated and irradiated EA.hy 926 cell line. Total RNA was extracted prior to IR (Mock-IR) or 1, 6 and 12 h post 3 Gy or 20 Gy. Upper panel: agarose gels illustrating RT-PCR products of amplified BTG2 using specific probes. Lower panel: BTG2 amplification cycles. The amplification cycles correspond to the number of cycles where the DNA-incorporated fluorescence was identical for all the samples. Larger numbers of cycles correspond to lower levels of starting RNA material present in the sample. Reactions were performed in duplicates using GAPDH as an endogenous control (not shown here).*

Table 4.6 *Fold inductions of BTG2 expression in irradiated EA.hy 926 obtained with cDNA microarray method and quantitative RT-PCR methods. RT-PCR values for irradiated and non-irradiated samples were normalized to the corresponding values of the internal control GAPDH. RT-PCR fold changes were calculated as described in Materials and Methods (Section 4.2).*

Irradiation dose	RT-PCR			cDNA microarray		
	Fold change			Fold change		
	1 h	6 h	12 h	1 h	6 h	12 h
3 Gy	1.58	0.98	1.4	1.84	1.94	1.61
20 Gy	2.82	2.48	2.62	3.26	3.07	2.73

As EA.hy 926 cells are particularly difficult to transfect, other cell lines such as HCT116 were used for the BTG2 promoter studies upon ionizing radiation due to their high transfection efficiency. BTG2 gene induction in HCT116 was assessed and revealed by RT-PCR at 1 h

post 3 Gy, 6 Gy and 9 Gy. The fold change at 1 h post 3 Gy was 1.77. The doses of 6 Gy and 9 Gy were indicative data to evaluate the response to higher doses. These amplitudes were 3.2 and 3.28, respectively.

BTG2 promoter after ionizing radiation

The human BTG2 promoter was cloned into a luciferase reporter plasmid by (Duriez *et al*, 2002). In this study, the full-length pGL3-BTG2/p2658 and a deletion mutant pGL3-BTG2/p373, kindly donated by Duriez (for details see (Duriez *et al*, 2002)), were utilized to investigate the BTG2 promoter following ionizing radiation exposures. Transient transfections of HCT116 with pGL3-BTG2/p2658 or pGL3-BTG2/p373, followed by luciferase assays were performed. Induction of luciferase activity upon IR was demonstrated using both constructs in an amount of 1000 ng (data not shown). However, different basal level activities were observed with higher repression of the pGL3-BTG2/p2658 in comparison to pGL3-BTG2/p373. The selection of pGL3-BTG2/p373 for further analysis was justified by the fact that a slightly higher amplitude of induction upon 3 Gy was observed in comparison to the full length promoter.

Different low quantities of pGL3-BTG2/p373 were transfected to reduce the non irradiated background and determine the optimum inductions in a reasonable background (Figure 4.3). The optimum induction upon 3 Gy occurs with 325 ng of pGL3-BTG2/p373. The corresponding fold change of 3-3.5 is shown in Figure 4.5. As a positive control, pGL3-BTG2/p373 was co-transfected with various amounts of pCMV-p53. Figure 4.4 shows induction of pGL3-BTG2/p373 at low levels of p53 and repression of pGL3-BTG2/p373 at higher levels of p53.

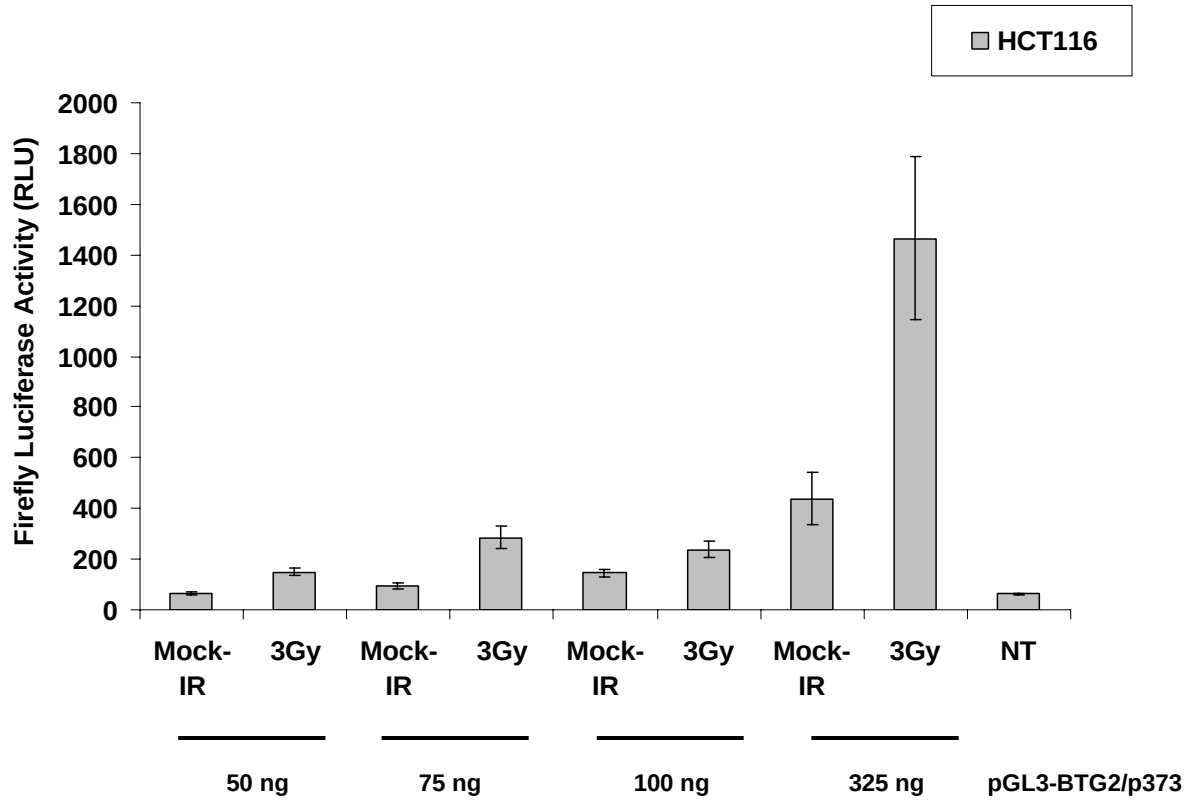

Figure 4.3 *Ionizing radiation-inducibility of the 5'-flanking region of BTG2 gene in a transient transfection assay. Firefly luciferase activity was measured in HCT116 cells transfected with the pGL3-BTG2/p373 in which the reporter Luciferase gene is under the control of the BTG2 partial promoter region. Cells were harvested 24 h post non-treatment or treatment. Columns: Mock-IR: transfected non irradiated cells; 3 Gy: transfected 3 Gy-irradiated cells; NT: non-transfected cells. RLU: Relative Light Unit.*

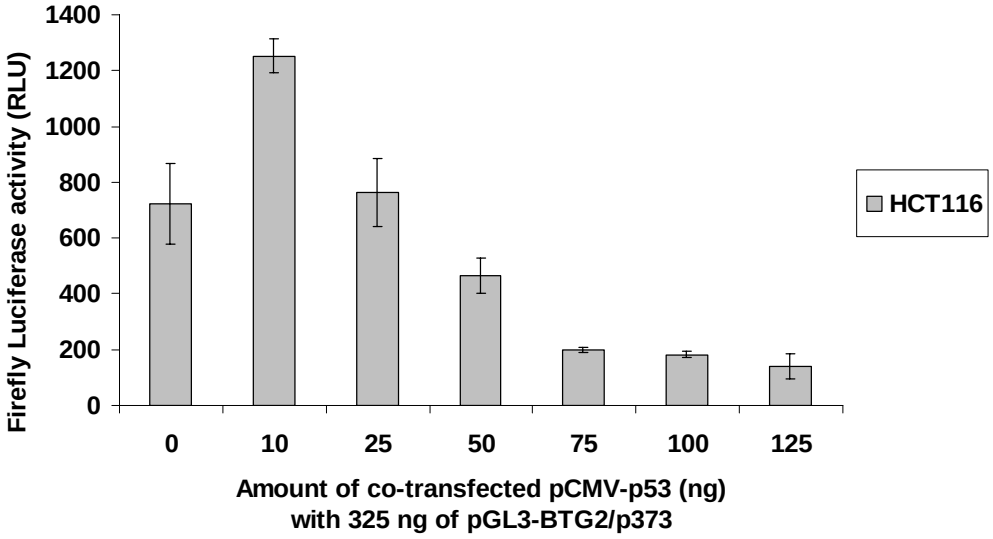

Figure 4.4 *Titration of pGL3-BTG2/p373 with increasing amounts of co-transfected pCMV-p53 in HCT116.*

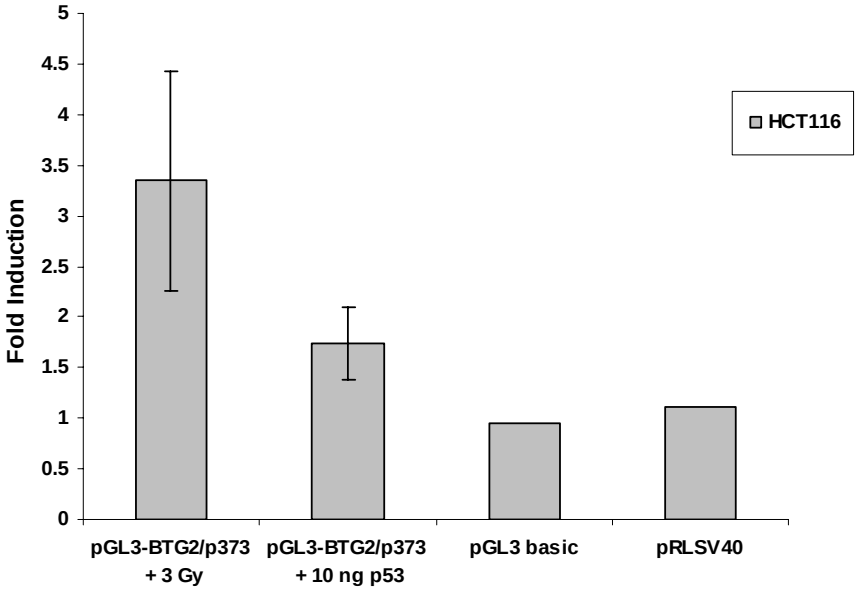

Figure 4.5 *Ionizing radiation fold induction of the 5'-flanking region of BTG2 gene expression in a transient transfection assay. Firefly luciferase activity was measured in HCT116 cells transfected with the pGL3-BTG2/p373 (325 ng), in which the reporter Luciferase gene is under the control of the BTG2 partial promoter region. Cells were harvested 24 h post treatments or non-treatment. Columns: Transfected cells with pGL3-BTG2/p373, irradiated cells (3 Gy) versus non-irradiated cells; co-transfected cells with pGL3-BTG2/p373 and 10 ng of pCMV-p53 versus transfected cells with pGL3-BTG2/p373; pGL3-basic, pGL3-SV40, cells transfected with pGL3-basic or pGL3-SV40 vectors that were used as negative controls (3 Gy irradiated cells versus non-irradiated cells).*

4.3.1.2 4-1BB gene and promoter

Human 4-1BB (CD137) is a member of the tumor necrosis factor receptor superfamily expressed on activated T cells, monocytes and natural killer (NK) cells. The interaction of 4-1BB and 4-1BB ligand was shown to provide a costimulatory signal leading to T-cell activation (DeBenedette *et al*, 1997; Schwarz *et al*, 1996). Signals delivered to the T cells can produce IL-2, proliferation, differentiation and protection of T-cells against activation-induced cell death (Hurtado *et al*, 1997; Saoulli *et al*, 1998).

Following DNA-damaging agent treatments such as mitomycin C, 4-1BB was interestingly found to have increased in human peripheral blood mononuclear cells (Kim *et al*, 2002). Its expression in the T-cells was also observed following doxorubicin, bleomycin and gamma-irradiation treatments (Kim *et al*, 2002).

A diagrammatic representation of the 4-1BB (CD137) gene is illustrated in Figure 4.6. The sequences proximal to the 4-1BB transcriptional start lack the conventional TATA box. Bindings of the transcription factors AP-1 and NF-κB to the indicated sites were illustrated by Kim *et al* (Kim *et al*, 2003). In the same region, putative binding sites for Gata-1 and Sp1 were predicted but the authors did not prove their bindings by electrophoretic mobility shift assay (EMSA) analysis.

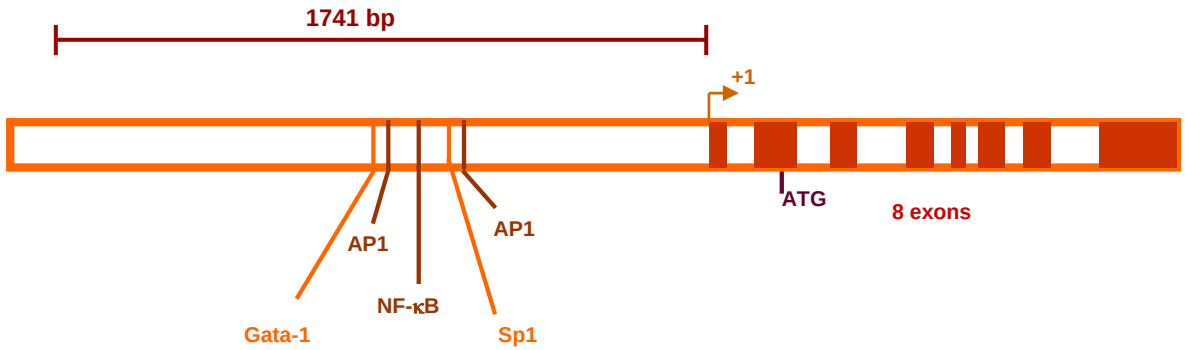

Figure 4.6 *Schematic representation of the human 4-1BB (CD137) gene and promoter region. The first nucleotide of the transcription start is indicated by an arrow and the number +1. The translational initiation site is indicated by ATG. The gene is composed of 8 exons. Putative binding sites for transcription factors are indicated. Binding of AP-1 at -1067 to -1048 and to -888 to -876 sites and of NF-κB to -915 to -894 sites (shown in brown color) were demonstrated by Kim et al by EMSA method (Kim et al, 2003). Here, a 1741 bp promoter region was cloned into a luciferase reporter gene. (GeneBank Accession number: U03397)*

4-1BB gene after ionizing radiation

In the microarray data studies (Chapter 3), 4-1BB receptor (GeneBank accession number U03397) was induced 10.66-fold at 6 h post 20 Gy. Its inducibility by IR was assessed by RT-PCR as shown in Figure 4.7 and Table 4.7. A transient expression occurred at 6 h post 20 Gy with a fold change of 8.68 and no expression was observed in the non-irradiated EA.hy 926. The induction of 4-1BB in 293-T cells was assessed by RT-PCR. A fold change of 6.14 was observed at 6 h post 20 Gy. 293-T cells were used in the 4-1BB promoter studies due to their high efficiency of transfection.

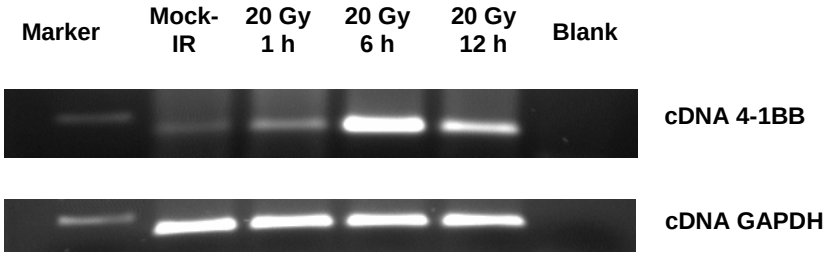

Figure 4.7 *Agarose gel illustrating 4-1BB amplified in non-irradiated and irradiated EA.hy 926 cell lines by quantitative RT-PCR. Total RNA was extracted prior to IR (Mock-IR) or 1, 6 and 12 h post 20 Gy. GAPDH was used as an endogenous control.*

Table 4.7 *Fold inductions of 4-1BB gene expression in irradiated EA.hy 926 obtained with cDNA microarray method and quantitative RT-PCR methods. RT-PCR values for irradiated and non-irradiated samples were normalized to the corresponding values of the internal control GAPDH. RT-PCR fold changes were calculated as described in Materials and Methods (Section 4.2). NC: no change in the 4-1BB expression upon IR.*

Irradiation dose	RT-PCR Fold change			cDNA microarray Fold change		
	1 h	6 h	12 h	1 h	6 h	12 h
20 Gy	NC	8.68	2.5	NC	10.66	NC

4-1BB promoter after ionizing radiation

A ~ 1.7 kb 5'-upstream region of the 4-1BB gene was cloned into a Firefly luciferase reporter (pGL3-4-1BB/p1741). Transfection into 293-T with this construct followed by luciferase measurement revealed a 1.5-2 fold induction at 6 h and 24 h post 20 Gy (data not shown). A basal activity in non-irradiated cells was detected in comparison to the empty vector (pGL3-basic), suggesting that regulatory sequences are present in this region. A ~ 1.5-2 fold induction after IR was observed following transfection of EA.hy 926 with this construct, RNA extraction and RT-PCR realized on the Firefly luciferase gene. However, due to low levels of these inductions, it could not be concluded that IR resulted in significantly increased 4-1BB promoter activity.

4.3.1.3 NK4 gene and the 5'-upstream region

The natural killer transcript 4 (NK4) gene was identified and mapped in the locus of disease genes responsible for the familial Mediterranean fever disorder. This region was shown to be located in the chromosome 16 (Bernot *et al*, 1998).

Prior to the work of Bernot *et al*, Dahl *et al* originally described the NK4 gene expressed in activated natural killer cells by interleukin 2 (IL-2) and in T cells by mitogens (Dahl *et al*, 1992). Bernot *et al* demonstrated that this gene was also expressed in most tested tissues (spleen, thymus, prostate, ovary, small intestine, colon, peripheral blood lymphocytes, heart, placenta, lung, liver, skeletal muscle, pancreas, stomach, thyroid, lymph nodem trachea and bone marrow). Due to the widespread expression of the NK4 gene, the elucidation of its precise function is of particular interest. This study is the first to report on NK4 induction by IR. Therefore, the isolation and characterization of the promoter region has been initiated. A schematic representation of NK4 gene and its 5'-upstream region is shown in Figure 4.8. The putative locations of transcription factors binding sites are represented in the transcriptional start region of NK4 gene (Figure 4.9).

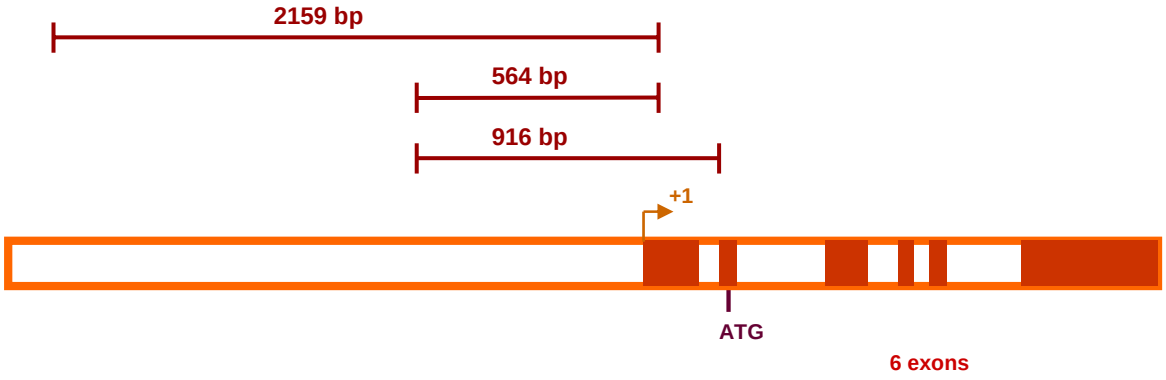

Figure 4.8 *Schematic representation of the human NK4 gene and 5'-upstream region. The first nucleotide of the transcription start is indicated by an arrow and the number +1. The translational initiation site is indicated by ATG. The gene is composed of 6 exons. In this study, 2159 bp, 564 bp and 916 bp regions were cloned into a luciferase reporter gene referred to as pGL3-NK4/p2159, pGL3-NK4/p564 and pGL3-NK4/p916, respectively. GeneBank (Accession number: AA631972).*

Figure 4.9 *The 5'-upstream sequence of the NK4 gene extracted from the Ensembl database (GeneBank accession number AA631972). The first nucleotide of the transcription start is*

indicated by an arrow and the number +1. The translational initiation site is indicated by ATG at position 501. In small green letters: part of the 5'-upstream sequence; in violet capital letters: exon of 183 bp; in small blue letters: intron of 289 bp; in violet capital letters: exon of 43 bp (only the sequence upstream of the translational starts ATG is shown here). In red bold letters: primers used for NK4 5'-upstream region cloning by PCR (P_FW1, P_FW2: forward primers; P_REV1, P_REV2: reverse primers). The region from the blue underlined bold nucleotide to the orange underlined bold nucleotide (2101 bp): promoter predicted by software developed by Oakley (Friedrich Miescher Institute, Basel Switzerland). The region from the pink underlined bold nucleotide to the orange underlined bold nucleotide (601 bp): promoter predicted by Genomatix software (www.genomatix.de). The main putative transcription factors binding sites in the transcriptional start region, generated by the software developed by Oakley, are illustrated in bold underlined letters.

NK4 gene after ionizing radiation

The natural killer transcript 4 was found to be the most significantly up-regulated gene following 20 Gy in EA.hy 926. Fold changes in NK4 gene values generated by Affymetrix microarray software were 85.41 and 92.06 at 6 h and 12 h post 20 Gy, respectively (see Chapter 3). No expression background of this gene could be detected without IR-treatment.

The confirmation of NK4s IR-inducibility in EA.hy 926 by RT-PCR is illustrated in Figure 4.10. The fold changes corresponding to the PCR products are given in Table 4.8. The differences in the fold changes are due to the different sensitivities and conditions of the applied methods, with a more precise sensitivity for the RT-PCR method.

Fractionated low doses of IR applied over several days result in additive induction (Figure 4.11). The corresponding fold changes are listed in Table 4.9. The NK4 gene was also shown to be induced by 20 Gy in other cells. Induction after IR was recorded in 293-T and HeLa with respective fold changes of 2.02 and 3.98 by using RT-PCR (data not shown). However, no induction was observed in HCT116 cells where a high background expression level was present in non-irradiated cells.

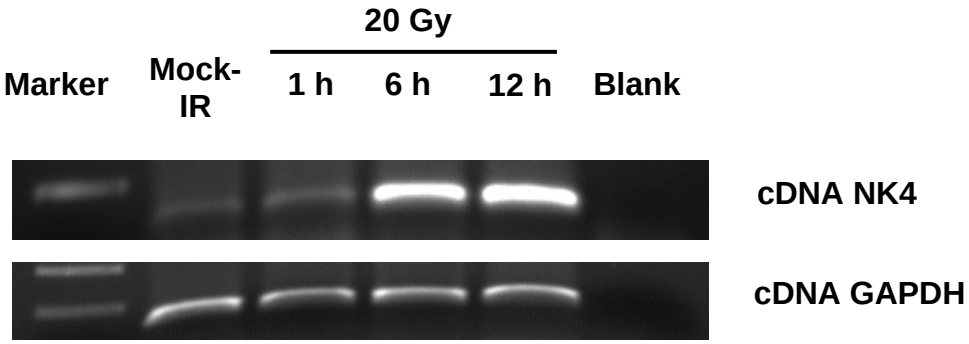

Figure 4.10 *Agarose gel illustrating NK4 amplified in non-irradiated and irradiated EA.hy 926 cell lines by quantitative RT-PCR. Total RNA was extracted prior to IR (Mock-IR) or 1, 6 and 12 h post 20 Gy. GAPDH was used as an endogenous control.*

Table 4.8 *Fold inductions of NK4 gene expression in irradiated EA.hy 926 obtained by cDNA microarray method and quantitative RT-PCR methods. RT-PCR values for irradiated and non-irradiated samples were normalized to the corresponding values of the internal control GAPDH. RT-PCR fold changes were calculated as described in Materials and Methods (Section 4.2). NC: no change in the NK4 expression following IR.*

Irradiation dose	RT-PCR			cDNA microarray		
	Fold change			Fold change		
	1 h	6 h	12 h	1 h	6 h	12 h
20 Gy	NC	5.14	5.94	NC	85.41	92.06

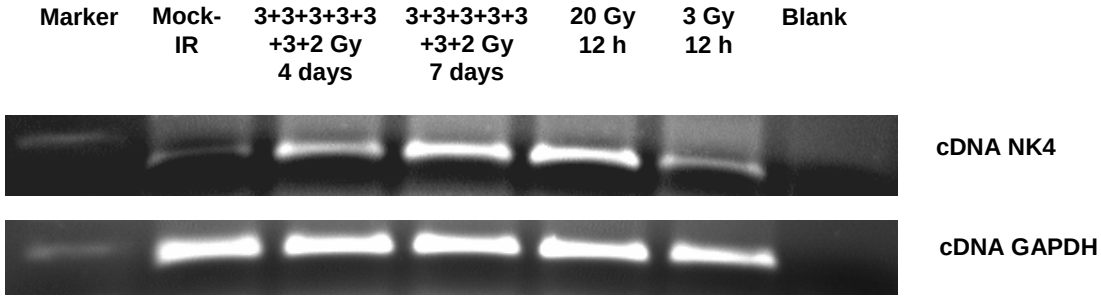

Figure 4.11 *Agarose gels illustrating RT-PCR product of the NK4 gene amplified with specific probes in EA.hy 926 cells. These were non-IR treated or treated with fractionated doses of a total of 20 Gy over 4 days or 7 days or treated with a single dose of 20 Gy harvested 12 h post 3 Gy or 20 Gy. GAPDH was used as an internal control.*

Table 4.9 *Fold inductions of NK4 gene expression in irradiated EA.hy 926 obtained by quantitative RT-PCR method. RT-PCR values for irradiated and non-irradiated samples were normalized to the corresponding values of the internal control GAPDH. RT-PCR fold changes were calculated as described in Materials and Methods (Section 4.2). NC: no change in the NK4 expression upon IR.*

Irradiation dose	RT-PCR Fold change
3+3+3+3+3+3+2 Gy over 4 days	2.26
3+3+3+3+3+3+2 Gy over 7 days	3.18
20 Gy 12 h	7.92
3 Gy 12 h	NC

Strategies to identify the NK4 promoter after ionizing radiation

Several strategies were used to characterize the regulatory elements region. A bacterial artificial chromosome (BAC) clone containing NK4 and large upstream and downstream regions was transfected into 293-T cells to assess NK4 inducibilily following ionizing radiation. As shown in Figure 4.12, the endogenous NK4 is induced by 20 Gy exposures whereas the transfected NK4 BAC displayed high background and slight induction levels.

Further experiments were conducted to understand the NK4 gene organization. RT-PCR was performed using different primer sets located in different exons (Figure 4.13). The results are illustrated by the agarose gels in Figure 4.14. The amplification at the 3'-end of NK4 mRNA using the forward (FW) and reverse (REV) primer set symbolized by FW1/REV1 resulted in one band occurring at the expected size. Amplifications in the 5'-end region of NK4 mRNA (primers FW2/REV1, FW3/REV1) led to several bands. In all cases induction of the endogenous NK4 gene was observed after 20 Gy. IR-inducibility on the transiently transfected NK4 BAC vector could not be detected due to the high background level in the non-irradiated sample.

In an attempt to characterize the size of the transcript induced by 20 Gy a northern blotting was performed (Figure 4.15). The resulting size of the NK4 transcript in the 20 Gy-lane was approximately 1 kb for EA.hy 926 cells. The same result was observed in 293-T cells (data not shown).

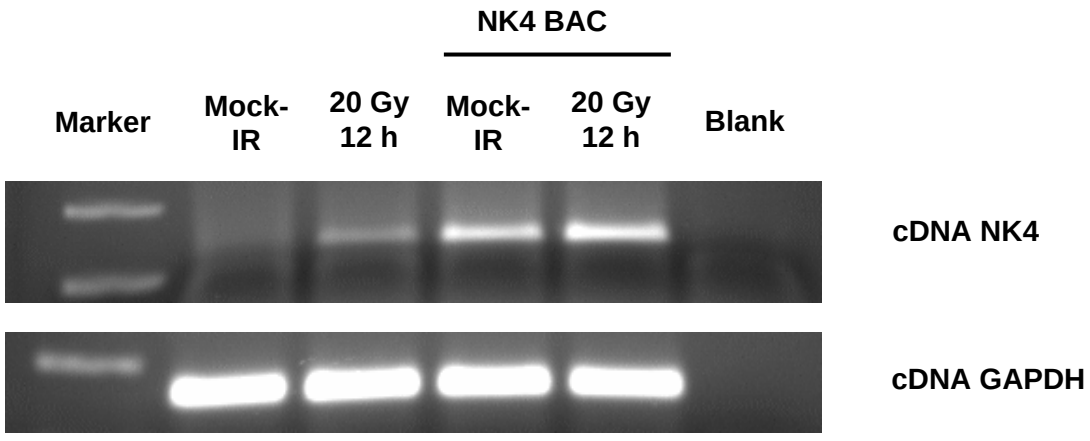

Figure 4.12 *Agarose gels illustrating RT-PCR product of the NK4 gene amplified with specific probes in 293-T cells. The cells were either non-transfected or transiently transfected with the* RP11-473M20 BAC-NK4 *vector, and either mock-IR treated or treated with 20 Gy 12 h post IR. GAPDH was used as an internal control.*

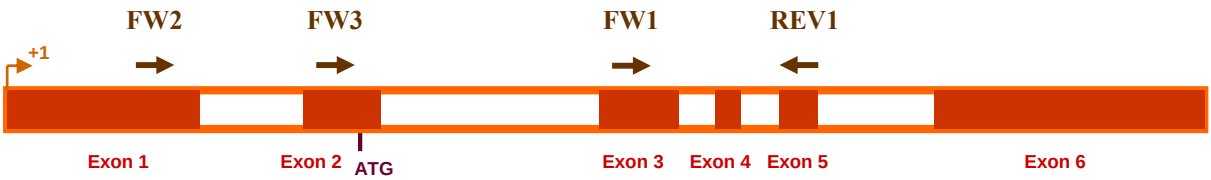

Figure 4.13 *Schematic representation of the human NK4 gene. The first nucleotide of the transcription start is indicated by an arrow and the number +1. The translational initiation site is indicated by ATG. Primers used for RT-PCR are represented by arrows in the corresponding exons. FW1-4: Forward primers; REV1: reverse primer. PCR products size: FW1-REV1: 143 bp; FW2-REV1: 394 bp; FW3-REV1: 335 bp.*

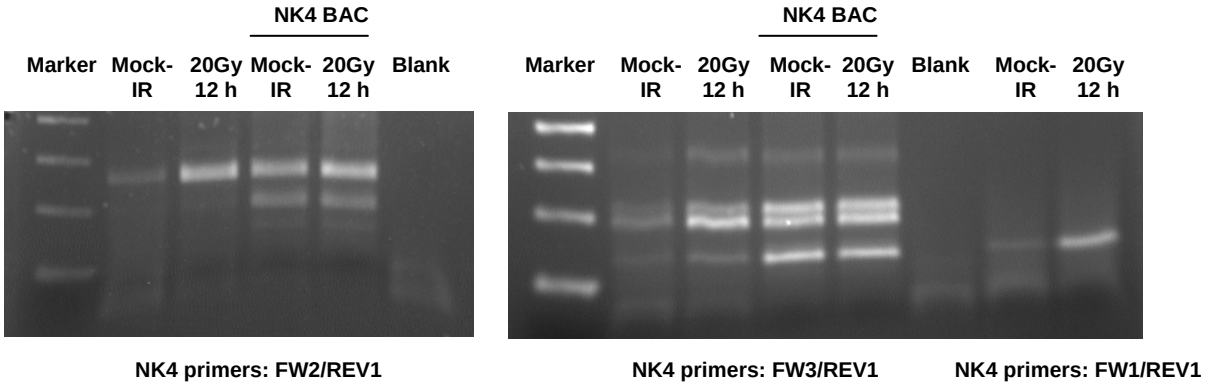

Figure 4.14 *Agarose gels illustrating RT-PCR product(s) of the NK4 gene using different specific primers in 293-T cells. The cells were either non-transfected or transfected with the RP11-473M20 BAC-NK4 vector, and either mock-IR treated or treated with 20 Gy 12 h post IR. GAPDH was used as an internal control (not shown here). Marker scale of the shown bands: 400, 300, 200 and 100 bp (top to the bottom). The primers and position in the NK4 gene used are described in Material and Methods in Section 4.2 and in Figure 4.13.*

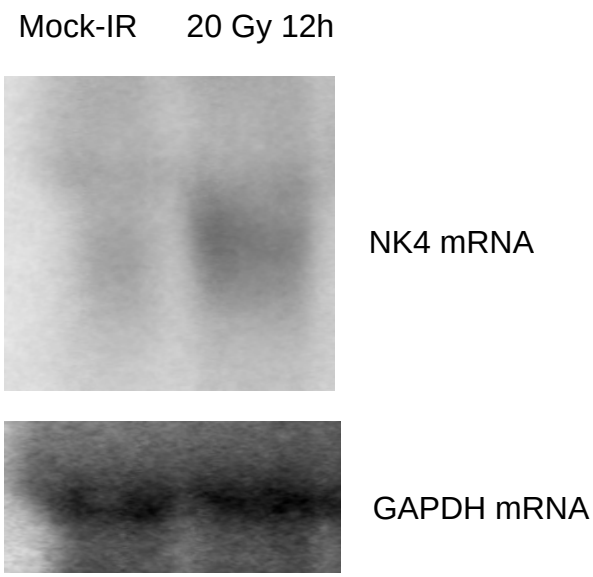

Figure 4.15 *Northern blotting illustrating NK4 gene expression in irradiated EA.hy 926 cells. The radioactive spot identified a transcript of approximately 1 kb. GAPDH was used as an internal control.*

5'-upstream region of NK4 after ionizing radiation

Three constructs of the 5'-upstream region (see Figure 4.8 and Figure 4.9) were transfected into 293-T and HeLa cells. The pGL3-NK4/p2159 and pGL3-NK4/p564 constructs did not exhibit any basal transcription of the luciferase gene. A slight basal activity was recorded in pGL3-NK4/p916 where the 5'-upstream region was cloned just upstream of the translation start. However, for the latter, only ~ 1.5-fold induction was measured in the HeLa cells.

4.3.2 Synthetic NF-κB binding sites to ionizing radiation exposure

The Nuclear Factor kappa B (NF-κB) is a transcription factor known to be induced by IR (Chapter 1). In non irradiated cells, NF-κB is located in the cytoplasm, bound to the inhibitor protein IκB. Ionizing radiation triggers an intracellular signal that results in the phosphorylation of IκB and its subsequent ubiquitin-dependent degradation by the proteasome. The free NF-κB translocates to the nucleus and activates the transcription target genes. The radiation-induced translocation of NF-κB to the nucleus was demonstrated by immunofluorescence in the endothelial EA.hy 926 cells (Figure 4.16). Translocation of NF-κB was assessed 1 h, 3h and 5h post 3 Gy and 20 Gy in EA.hy 926 cells. A maximum of positive cells (average of 40 %) was detected at 1 h post 20 Gy. After 3 Gy, no positive cells were detected, suggesting that translocation was too weak to be detected or non-existent. The same results were found in HeLa and 293-T cells (data not shown).

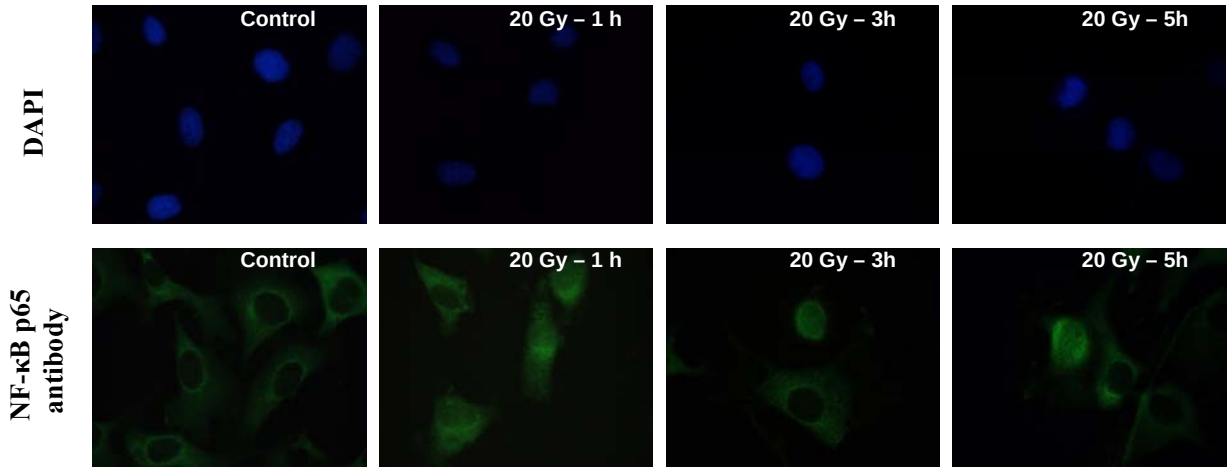

Figure 4.16 *Detection of the p65 subunit of the nuclear Factor κB in EA.hy 926 after 20 Gy. The cells were fixed 1 h, 3 and 5h after 3 Gy or non treatement and immunofluorescent labeling was performed with the rabbit polyclonal NF-κB p65 antibody coupled with FITC. Nuclei were stained with DAPI. The cells were subsequently examined by fluorescence microscopy.*

The activation of NF-κB transcription factor by IR can be exploited for improved gene therapy. A synthetic target region composed of five tandemly-repeated binding sites for NF-κB was studied following IR. The reporter vector contains the Firefly luciferase reporter gene driven by the upstream basic promoter elements (TATA box and the NF-κB *cis*-enhancer element). The sequence of the five tandemly positioned repeats of binding sites for NF-κB is as follows $(TGGGGACTTTCCGC)_5$. The NF-κB binding sites reporter plasmid, pNF-κB-Luc, was either transiently transfected into 293-T and EA.hy 926 cells (Figure 4.17) or stably transfected into 293-T cells (Figure 4.18).

As shown in Figure 4.17, the co-transfection of pNF-κB-Luc with pFC-MEKK leads to luciferase activity of the reporter plasmid. pFC-MEKK contains the MEKK gene that is driven by the CMV promoter. MEKK are mitogen-activated protein kinase kinases that are activated by extracellular stimuli. Three members of MEKK have been identified and can activate NF-κB transcription factor. They directly stimulate the IKK complex by phosphorylation of IκB, thereby allowing the nuclear translocation of NF-κB (Lee *et al*, 1997; Nemoto *et al*, 1998; Zhao and Lee, 1999). Here, the co-transfected pFC-MEKK, used as a positive control, induced the expression of the pNF-κB-Luc probably *via* NF-κB binding. Following IR, luciferase activity was increased in EA.hy 926 and 293-T. The reporter plasmid was shown to respond after the tested IR-doses of 3 Gy, 9 Gy and 20 Gy (Figure 4.17). Greater than 4-fold induction was observed in EA.hy 926 after 9 Gy. This result is particularly encouraging as these endothelial cells are very difficult to transfect (5% of transfected EA.hy 926). Therefore, 293-T cells were utilized for efficient transient transfection in the luciferase assay. Much higher levels of induction of 10-fold were observed in the easily-transfectable cell lines 293-T following 9 Gy.

As illustrated in Figure 4.18 an IR dose-response of the pNF-κB-Luc is observed in the stably transfected 293-T cells. A 16 fold-induction is recorded with the highest tested dose of 20 Gy. Following low doses a 1.5-fold induction and a 3-fold induction were shown after 1 Gy and 3 Gy, respectively. In addition, fractionated and repeated low IR doses revealed additive response to ionizing radiation. The exposure of 293-T cells to three doses of 3 Gy applied in 24h intervals resulted in 12-fold induction. These fractionated doses induce a greater effect in comparison to the single total dose of 9 Gy, which causes a 6-fold change. The same observation was made when fractionation was limited to two doses of 3 Gy. These results bode well for the use of this promoter system in fractionated radiotherapy.

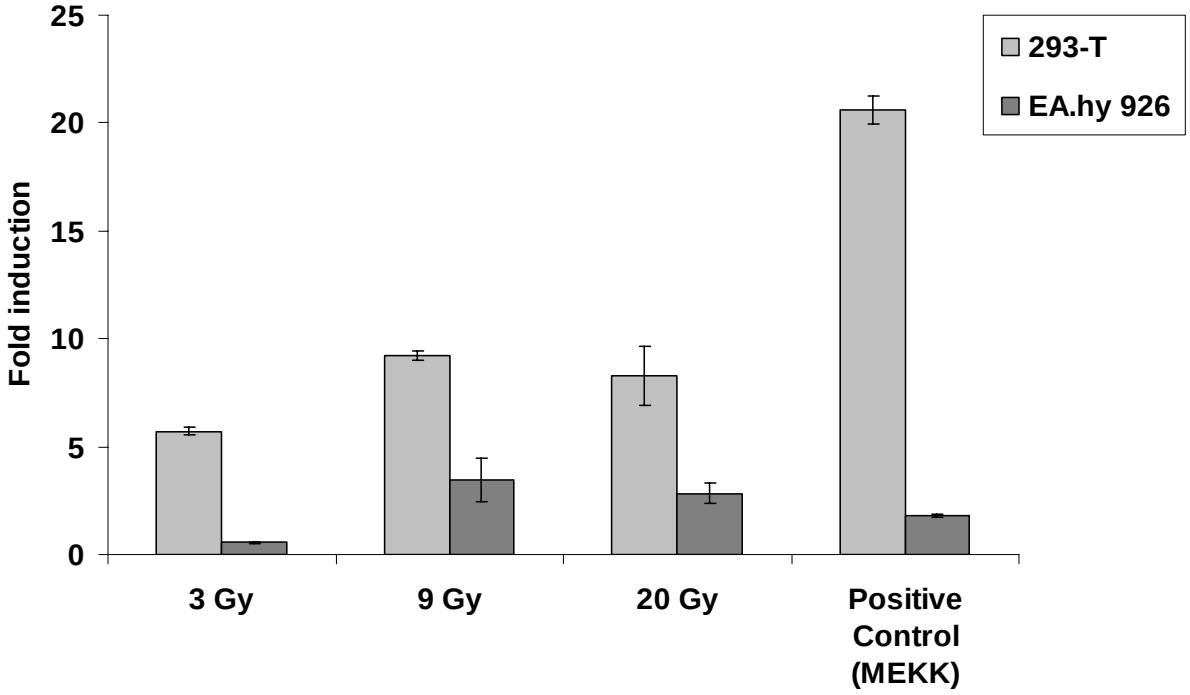

Figure 4.17 *Relative induction of the Firefly luciferase expression in the pNF-κB-Luciferase system by IR in EA.hy 926 and 293-T cells. Cells were transiently transfected with pNF-κB-Luciferase reporter and 24 hours post transfection the cells were either exposed to irradiation treatment or remained untreated. 24 hours post-IR cells were harvested and lysated in passive lysis buffer (PLB) and luciferase activity was measured. Co-transfection of pNF-κB-Luciferase with pFC-MEKK is illustrated here as a positive control.*

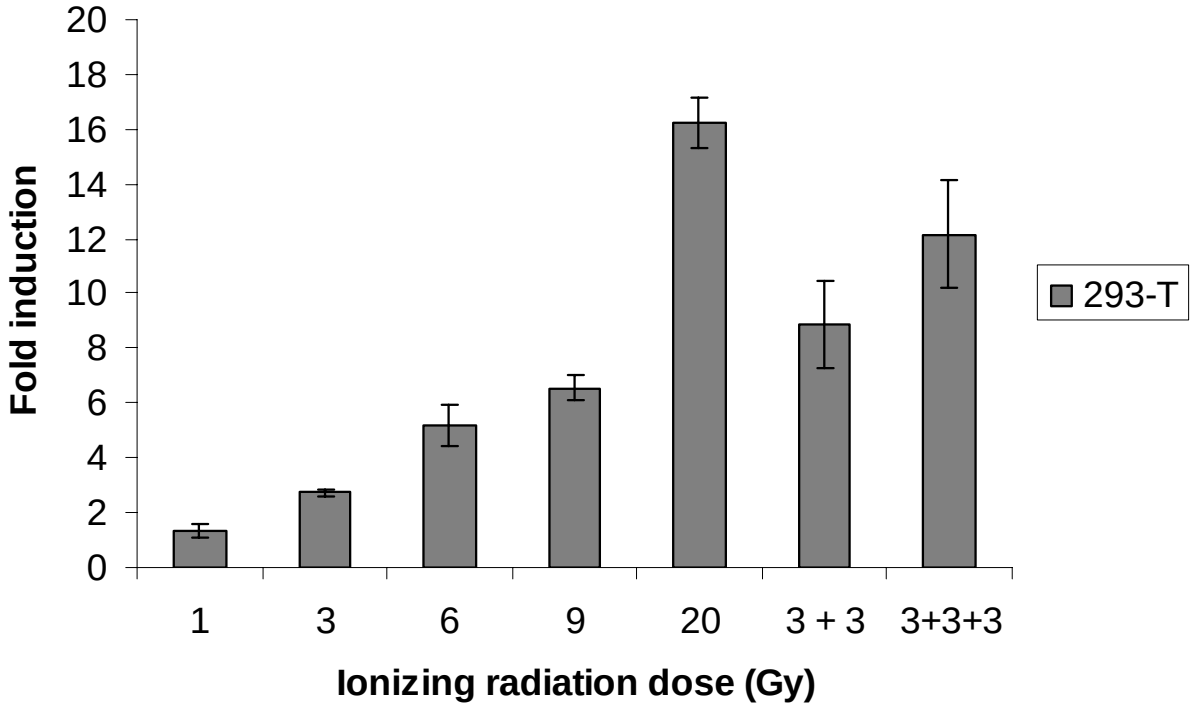

Figure 4.18 *Relative induction of the Firefly luciferase expression in the pNF-κB-Luciferase system by IR in 293-T cells. Cells were stably transfected with pNF-κB-Luciferase reporter. 24 h post IR treatment or non-treatment the cells were harvested and lysated in passive lysis buffer (PLB) and luciferase activity was measured.*

4.4 Discussion

Gene therapy is an emerging cancer treatment modality. The aim of gene therapy is to deliver specifically therapeutic genes to cancerous cells or normal tissues which contribute to tumor growth. In this study, we focused on developing a therapeutic gene expression system targeted by ionizing radiation. According to this concept, an expression system based on radiation-inducible promoters will drive the expression of anti-tumor genes in the tumor vasculature.

The identification of ionizing radiation-inducible promoters native to endothelial cells was investigated following analysis of irradiated gene expression profiles (Chapter 3). Genes induced by IR such as BTG2, 4-1BB and NK4 were selected and are discussed in the following sections.

The induction of the first gene studied namely the B cell translocation gene 2 (BTG2) was confirmed by RT-PCR in EA.hy 926 (Figure 4.2 and Table 4.6) and in HCT116 (data not shown). This gene was selected due to significant induction of this gene at the low dose of 3 Gy. Activation of the BTG2 promoter following 3 Gy was reported in HCT116 with induction amplitudes of 3-3.5 fold (Figure 4.5). The induction of BTG2 by p53-dependent mechanisms upon DNA damage was demonstrated by Rouault *et al* (Rouault *et al*, 1996). As a positive control, a plasmid overexpressing p53 was co-transfected with BTG2 promoter. The results revealed either induction or repression of the BTG2 promoter according to the amount of p53 present (Figure 4.4).

Basal expression of the endogenous BTG2 gene was observed in non-irradiated EA.hy 926 (Figure 4.2) and in HCT116 (data not shown). This expression could be a drawback for gene therapy application as activity of the corresponding promoter could lead to the expression of toxic genes in the non-irradiated tissues. To prove the possibility of decreasing the background levels while retaining the IR-inducibility characteristic, different low amounts of BTG2 promoter were transfected into HCT116 cells. The results shown in Figure 4.3 confirmed that activity of the BTG2 promoter remained even when its basal activity was approximating that of the non-transfected cells. With the aim of lowering the basal activity, Scott *et al* engineered chimeric constructs. These constructs were of particular benefit when reducing the radiation-inducible early growth factor 1 (egr-1) promoter basal level activity ((Scott *et al*, 2002)). The authors engineered a “molecular switch” based on the recombination system of the bacteriophage P1. In the presence of ionizing radiation the synthetic egr-1 enhancer/promoter induces the expression of the recombinase Cre which in turn activates the

herpes simplex virus-thymidine kinase (HSV-TK) by loxP site-mediated recombination. Therefore, a single dose of radiation as low as 1 Gy could induce the HSV-TK gene expression via the strong constitutive CMV promoter, thereby producing a significant amplification of the radiation-response. According to these developed strategies the BTG2 promoter should be investigated further to optimize its potential utilization in cancer gene therapy.

Another gene activated by IR is the 4-1BB (CD137) member of the tumor necrosis factor receptor superfamily. The 4-1BB gene was demonstrated to be transiently activated by IR and its very low endogenous background makes this gene a good candidate for the promoter studies (Figure 4.7). However, the 4-1BB promoter system resulted only in a slight induction by IR, which did not allow considering 4-1BB as a candidate for cancer gene therapy.

The natural killer transcript 4 (NK4) is a very interesting candidate due to its low background in non-irradiated cells and the high induction levels (Figure 4.10 and Table 4.8). In addition, its additional inducibility following fractionated low IR doses corresponds to the criteria of radiotherapy as it is applied in clinics (Figure 4.11 and Table 4.9). The bioinformatic softwares available from Genomatix (www.genomatix.com) and developed by Oakley (Friedrich Miescher Institute, Basel Switzerland) were utilized in an attempt to characterize the promoter in the 5'-upstream region. These softwares are based on the identification of TATA-box sequences which are often located ~30 bp upstream of a transcription start site. However, the analyzed sequence was not predicted to be a core promoter, as supported by the absence of the canonical TATA-box or regulatory elements such as a GC box or a CAAT located upstream of the transcriptional start. However, to verify whether the 5'-upstream region could correspond to a promoter, three different cloning procedures were performed (Figure 4.8 and Figure 4.9). A slight IR-induction was observed for the construct containing the 5' region upstream of the translational start, but this could not be significantly confirmed due to the low response to IR.

In an attempt to characterize the NK4 promoter, several strategies were utilized. First, a BAC clone containing NK4 gene and large upstream and downstream segments was used to demonstrate the presence of the NK4 promoter in the proximity of the gene. Constitutive activation of the transiently transfected NK4 BAC vector was observed in the non-irradiated cells probably due to the toxic effects of transfection. The non significant IR-induction (Figure 4.12) observed could be explained either by the high background levels that might hinder any signal or by the absence of IR enhancers in the NK4 BAC. The second

characterization strategy aimed at studying the NK4 gene organization. RT-PCR amplifications in different exons were performed. The results in Figure 4.14 showed that the NK4 gene was differentially spliced. The recent work of Kim *et al* showed that alternative splicing of NK4, referred as interleukin-32 (IL-32), also occurred (Kim *et al*, 2005). The authors showed that four splice variants of IL-32 gene are involved in the pathways of NF-κB and p38 MAPK. In this study, all the amplified variants were proven to be induced by IR. These results suggested that the NK4 promoter might not be localized in any introns but might be localized upstream of the exon 1 instead. Indeed, the use of the primer set in exon 1 and exon 5 (FW2/REV1) revealed IR-inducibility of NK4 (Figure 4.13 and Figure 4.14). In this respect, the candidate regulatory regions of NK4 might be localized upstream of exon 1, in the proximity region or even at large distances of several kilobases.

The answer was revealed by the third strategy through the use of a northern blotting. A transcript of ~ 1 kb was identified following IR, suggesting that the promoter might be located in the proximity region of exon 1. However, this hypothesis remains to be elucidated and further characterization studies are needed to better understand the mechanism of transcriptional regulation of the NK4 gene in response to IR.

To conclude this section of the study, promoters in their native form might not be useful candidates for gene therapy. One example, in the literature, is provided by the native promoter of the radiation-inducible egr-1 gene. This promoter, used in suicide gene therapy, demonstrated greater background activities than its artificial counterpart. A synthetic promoter containing four cArG elements was shown to respond to radiation doses as low as 1 Gy and was more radiation-responsive than the wild type egr-1 counterpart at an optimal 3 Gy dose (Scott *et al*, 2000). Recently, this construct composed of radiation-inducible cArG elements that drive the toxin tumor necrosis factor α (TNF-α), is the only radiation-induced suicide vector being used in phase I clinical trials (Weichselbaum *et al*, 2002).

Examination of the literature indicates that NF-κB transcription factor is reproducibly responsive to clinically relevant doses of ionizing radiation (reviewed by Criswell *et al* (Criswell *et al*, 2003)). In this respect, *cis*-regulated elements of NF-κB may be useful for IR-inducible expression in gene therapy. In this study, a synthetic target region composed of five tandemly-repeated binding sites for NF-κB was studied following IR. As a control, NF-κB activation was illustrated following IR in EA.hy 926 (Figure 4.16), HeLa and 293-T cells (data not shown). Five tandemly repeated TGGGGACTTTCCGC elements for NF-κB binding were cloned into a luciferase reporter. Transient transfection of this construct into

EA.hy 926 and 293-T revealed a dose-dependent increase in luciferase activity (Figure 4.17). This observation was confirmed in the stably transfected 293-T cell line (Figure 4.18). Interestingly, the response to fractionated therapeutically low doses was improved in comparison to the total single dose in stably transfected 293-T cells (Figure 4.18). As substantial improvements in the response induction to low doses of radiation could be achieved, studies increasing the number of tandemly repeated TGGGGACTTTCCGC elements may be required. Recently, Marples *et al* investigated the radiation-response of promoters containing different numbers, sequences and arrangements of elements after transfection into adenocarcinoma and glioblastoma cell lines (Marples *et al*, 2000). They demonstrated that increasing the number from four to nine tandemly repeated cArG elements of the synthetic egr-1 promoter improved the induction to low doses of radiation. They suggested that by providing more target sequences, the cArG elements would be presented in a suitably accessible configuration, which enables efficient binding of specific transcription factor complexes, thus driving gene expression. Their results also revealed that increasing the number of cArG elements in synthetic promoters did not lead to a corresponding increase in non-specific gene expression. Conversely, synthetic enhancers with more IR responsive units exhibited progressively less basal activity under non irradiated conditions. This phenomenon was also observed with the native egr-1 enhancer, which demonstrates more background than any of the engineered constructs.

The described characteristics of artificial promoters might be suitable to drive the gene expression of toxic molecules in the vicinity of tumor cells. Ueda *et al* used the NF-κB-responsive c-IAP2 promoter to drive the expression of the proaoptotic BAX gene to induce cell death at 2 Gy (Ueda *et al*, 2001). Their results and the present data confirm the possibility of NF-κB-directed promoter use following low IR doses. Here, investigations aiming at exploiting NF-κB repeated binding sites for toxin expression after IR are underway.

5 CONCLUSIONS AND PERSPECTIVES

Ionizing radiation can elicit a variety of cellular responses including cell cycle arrest, DNA repair, cell death and transcriptional responses. The identification of global transcriptional changes induced by ionizing radiation can be analyzed by the modern integrative cDNA microarray technology. The cDNA microarray was utilized to gain further insights into the molecular and cellular processes underlying responses to IR in various cell types (reviewed by (Snyder and Morgan, 2004)).

In this study, cDNA microarray technology was utilized to analyze the profiles of irradiated endothelial cells. Different doses of IR were tested to determine how the cells are affected at a molecular level. Among the common modulated genes at low and higher doses a majority of genes was found to be involved in the DNA repair, cell cycle regulation or apoptosis.

The next step was to isolate from the cDNA microarray studies the native radiation-inducible promoters in endothelial cells. Identification of radiation-inducible promoters was aimed at developing them as tools in the radio-inducible gene therapy delivery of anti-cancer molecules to the tumor vasculature endothelium. Investigating promoters such as BTG2 or 4-1BB revealed that authentic promoters cloned onto a plasmid are not suitable for cancer gene therapy, because of their limitions by their too low induction following ionizing radiation.

Further investigations were oriented around synthetic promoters containing repeated sequence-specific binding sites for IR-activated transcription factors such as NF-κB. The activity of five tandemly repeated TGGGGACTTTCCGC elements for NF-κB binding in a luciferase reporter was increased in a dose-dependent manner. Interestingly, the response to fractionated therapeutically low doses of IR was improved in comparison to the total single dose, rendering this system of particular interest for clinical applications. The repetition of specific binding site elements may probably represent a suitably accessible configuration for NF-κB binding. Thus, investigations which increase the number of tandemly repeated TGGGGACTTTCCGC elements may further improve the induction levels to low doses of radiation.

Endothelial cells represent a very promising target since angiogenesis was identified as a key process in tumor development. A stable cell line of the EA.hy 926 cells with the construct containing the NF-κB binding sites-Luciferase is currently being established by using a lentivirus transduction vector system.

Finally, it is of interest to investigate whether a molecule such as a therapeutic herpes simplex virus-thymidine kinase (HSV-TK) under the control of the artificial promoter for NF-κB binding and in the presence of ganciclovir might improve the cell killing rate of endothelial cells exposed to IR. This will bring the answer of the possible use of the artificial promoter for NF-κB binding alsongside the ionizing radiation administration to destroy the tumor dependent blood vasculature.

6 REFERENCES

Abraham, R.T. (2001) Cell cycle checkpoint signaling through the ATM and ATR kinases. *Genes Dev*, **15**, 2177-2196.

Amorino, G.P., Hamilton, V.M., Valerie, K., Dent, P., Lammering, G. and Schmidt-Ullrich, R.K. (2002) Epidermal growth factor receptor dependence of radiation-induced transcription factor activation in human breast carcinoma cells. *Mol Biol Cell*, **13**, 2233-2244.

Amundson, S.A., Bittner, M., Chen, Y., Trent, J., Meltzer, P. and Fornace, A.J., Jr. (1999a) Fluorescent cDNA microarray hybridization reveals complexity and heterogeneity of cellular genotoxic stress responses. *Oncogene*, **18**, 3666-3672.

Amundson, S.A., Do, K.T. and Fornace, A.J., Jr. (1999b) Induction of stress genes by low doses of gamma rays. *Radiat Res*, **152**, 225-231.

Amundson, S.A., Do, K.T., Shahab, S., Bittner, M., Meltzer, P., Trent, J. and Fornace, A.J., Jr. (2000) Identification of potential mRNA biomarkers in peripheral blood lymphocytes for human exposure to ionizing radiation. *Radiat Res*, **154**, 342-346.

Amundson, S.A., Lee, R.A., Koch-Paiz, C.A., Bittner, M.L., Meltzer, P., Trent, J.M. and Fornace, A.J., Jr. (2003) Differential responses of stress genes to low dose-rate gamma irradiation. *Mol Cancer Res*, **1**, 445-452.

Amundson, S.A., Patterson, A., Do, K.T. and Fornace, A.J., Jr. (2002) A nucleotide excision repair master-switch: p53 regulated coordinate induction of global genomic repair genes. *Cancer Biol Ther*, **1**, 145-149.

Arap, W., Pasqualini, R. and Ruoslahti, E. (1998) Chemotherapy targeted to tumor vasculature. *Curr Opin Oncol*, **10**, 560-565.

Arora, N., Masood, R., Zheng, T., Cai, J., Smith, D.L. and Gill, P.S. (1999) Vascular endothelial growth factor chimeric toxin is highly active against endothelial cells. *Cancer Res*, **59**, 183-188.

Balcer-Kubiczek, E.K., Zhang, X.F., Harrison, G.H., Zhou, X.J., Vigneulle, R.M., Ove, R., McCready, W.A. and Xu, J.F. (1999) Delayed expression of hpS2 and prolonged expression of CIP1/WAF1/SDI1 in human tumour cells irradiated with X-rays, fission neutrons or 1 GeV/nucleon Fe ions. *Int J Radiat Biol*, **75**, 529-541.

Banin, S., Moyal, L., Shieh, S., Taya, Y., Anderson, C.W., Chessa, L., Smorodinsky, N.I., Prives, C., Reiss, Y., Shiloh, Y. and Ziv, Y. (1998) Enhanced phosphorylation of p53 by ATM in response to DNA damage. *Science*, **281**, 1674-1677.

Bartek, J., Falck, J. and Lukas, J. (2001) CHK2 kinase--a busy messenger. *Nat Rev Mol Cell Biol*, **2**, 877-886.

Basu, S., Rosenzweig, K.R., Youmell, M. and Price, B.D. (1998) The DNA-dependent protein kinase participates in the activation of NF kappa B following DNA damage. *Biochem Biophys Res Commun*, **247**, 79-83.

Beetz, A., Peter, R.U., Oppel, T., Kaffenberger, W., Rupec, R.A., Meyer, M., van Beuningen, D., Kind, P. and Messer, G. (2000) NF-kappaB and AP-1 are responsible for inducibility of the IL-6 promoter by ionizing radiation in HeLa cells. *Int J Radiat Biol*, **76**, 1443-1453.

Bentires, M. (2001) [Kappa-B nuclear factor and apoptosis of cancerous cells]. *Bull Mem Acad R Med Belg*, **156**, 329-337.

Bernot, A., Heilig, R., Clepet, C., Smaoui, N., Da Silva, C., Petit, J.L., Devaud, C., Chiannilkulchai, N., Fizames, C., Samson, D., Cruaud, C., Caloustian, C., Gyapay, G.,

Delpech, M. and Weissenbach, J. (1998) A transcriptional Map of the FMF region. *Genomics*, **50**, 147-160.

Bode, A.M. and Dong, Z. (2004) Post-translational modification of p53 in tumorigenesis. *Nat Rev Cancer*, **4**, 793-805.

Brach, M.A., Hass, R., Sherman, M.L., Gunji, H., Weichselbaum, R. and Kufe, D. (1991) Ionizing radiation induces expression and binding activity of the nuclear factor kappa B. *J Clin Invest*, **88**, 691-695.

Budihardjo, I., Oliver, H., Lutter, M., Luo, X. and Wang, X. (1999) Biochemical pathways of caspase activation during apoptosis. *Annu Rev Cell Dev Biol*, **15**, 269-290.

Bulavin, D.V., Demidov, O.N., Saito, S., Kauraniemi, P., Phillips, C., Amundson, S.A., Ambrosino, C., Sauter, G., Nebreda, A.R., Anderson, C.W., Kallioniemi, A., Fornace, A.J., Jr. and Appella, E. (2002) Amplification of PPM1D in human tumors abrogates p53 tumor-suppressor activity. *Nat Genet*, **31**, 210-215.

Bulavin, D.V., Phillips, C., Nannenga, B., Timofeev, O., Donehower, L.A., Anderson, C.W., Appella, E. and Fornace, A.J., Jr. (2004) Inactivation of the Wip1 phosphatase inhibits mammary tumorigenesis through p38 MAPK-mediated activation of the p16(Ink4a)-p19(Arf) pathway. *Nat Genet*, **36**, 343-350.

Burns, T.F. and El-Deiry, W.S. (2003) Microarray analysis of p53 target gene expression patterns in the spleen and thymus in response to ionizing radiation. *Cancer Biol Ther*, **2**, 431-443.

Cai, H., Smola, U., Wixler, V., Eisenmann-Tappe, I., Diaz-Meco, M.T., Moscat, J., Rapp, U. and Cooper, G.M. (1997) Role of diacylglycerol-regulated protein kinase C isotypes in growth factor activation of the Raf-1 protein kinase. *Mol Cell Biol*, **17**, 732-741.

Cao, X., Mahendran, R., Guy, G.R. and Tan, Y.H. (1993) Detection and characterization of cellular EGR-1 binding to its recognition site. *J Biol Chem*, **268**, 16949-16957.

Carmeliet, P. and Jain, R.K. (2000) Angiogenesis in cancer and other diseases. *Nature*, **407**, 249-256.

Chastel, C., Jiricny, J. and Jaussi, R. (2004) Activation of stress-responsive promoters by ionizing radiation for deployment in targeted gene therapy. *DNA Repair (Amst)*, **3**, 201-215.

Chen, X., Ko, L.J., Jayaraman, L. and Prives, C. (1996) p53 levels, functional domains, and DNA damage determine the extent of the apoptotic response of tumor cells. *Genes Dev*, **10**, 2438-2451.

Chmura, S.J., Nodzenski, E., Beckett, M.A., Kufe, D.W., Quintans, J. and Weichselbaum, R.R. (1997) Loss of ceramide production confers resistance to radiation-induced apoptosis. *Cancer Res*, **57**, 1270-1275.

Choi, J., Appella, E. and Donehower, L.A. (2000) The structure and expression of the murine wildtype p53-induced phosphatase 1 (Wip1) gene. *Genomics*, **64**, 298-306.

Choi, J., Nannenga, B., Demidov, O.N., Bulavin, D.V., Cooney, A., Brayton, C., Zhang, Y., Mbawuike, I.N., Bradley, A., Appella, E. and Donehower, L.A. (2002) Mice deficient for the wild-type p53-induced phosphatase gene (Wip1) exhibit defects in reproductive organs, immune function, and cell cycle control. *Mol Cell Biol*, **22**, 1094-1105.

Contessa, J.N., Reardon, D.B., Todd, D., Dent, P., Mikkelsen, R.B., Valerie, K., Bowers, G.D. and Schmidt-Ullrich, R.K. (1999) The inducible expression of dominant-negative epidermal growth factor receptor-CD533 results in radiosensitization of human mammary carcinoma cells. *Clin Cancer Res*, **5**, 405-411.

Cortes, U., Moyret-Lalle, C., Falette, N., Duriez, C., Ghissassi, F.E., Barnas, C., Morel, A.P., Hainaut, P., Magaud, J.P. and Puisieux, A. (2000) BTG gene expression in the p53-

dependent and -independent cellular response to DNA damage. *Mol Carcinog*, **27**, 57-64.

Criswell, T., Leskov, K., Miyamoto, S., Luo, G. and Boothman, D.A. (2003) Transcription factors activated in mammalian cells after clinically relevant doses of ionizing radiation. *Oncogene*, **22**, 5813-5827.

Dahl, C.A., Schall, R.P., He, H.L. and Cairns, J.S. (1992) Identification of a novel gene expressed in activated natural killer cells and T cells. *J Immunol*, **148**, 597-603.

Datta, R., Hallahan, D.E., Kharbanda, S.M., Rubin, E., Sherman, M.L., Huberman, E., Weichselbaum, R.R. and Kufe, D.W. (1992a) Involvement of reactive oxygen intermediates in the induction of c-jun gene transcription by ionizing radiation. *Biochemistry*, **31**, 8300-8306.

Datta, R., Rubin, E., Sukhatme, V.P., Qureshi, S., Hallahan, D., Weichselbaum, R.R. and Kufe, D. (1992b) Ionizing radiation activates transcription of the *EGR1* gene via CArG elements. *Proc. Natl. Acad. Sci. USA*, **89**, 10149-10153.

Datta, R., Taneja, N., Sukhatme, V.P., Qureshi, S.A., Weichselbaum, R. and Kufe, D.W. (1993) Reactive oxygen intermediates target CC(A/T)6GG sequences to mediate activation of the early growth response 1 transcription factor gene by ionizing radiation. *Proc Natl Acad Sci U S A*, **90**, 2419-2422.

DeBenedette, M.A., Shahinian, A., Mak, T.W. and Watts, T.H. (1997) Costimulation of CD28- T lymphocytes by 4-1BB ligand. *J Immunol*, **158**, 551-559.

Dent, P., Yacoub, A., Fisher, P.B., Hagan, M.P. and Grant, S. (2003) MAPK pathways in radiation responses. *Oncogene*, **22**, 5885-5896.

Ding, G.R., Honda, N., Nakahara, T., Tian, F., Yoshida, M., Hirose, H. and Miyakoshi, J. (2003) Radiosensitization by inhibition of IkappaB-alpha phosphorylation in human glioma cells. *Radiat Res*, **160**, 232-237.

Donehower, L.A. (1996) The p53-deficient mouse: a model for basic and applied cancer studies. *Semin Cancer Biol*, **7**, 269-278.

Dulic, V., Stein, G.H., Far, D.F. and Reed, S.I. (1998) Nuclear accumulation of p21Cip1 at the onset of mitosis: a role at the G2/M-phase transition. *Mol Cell Biol*, **18**, 546-557.

Duriez, C., Falette, N., Audoynaud, C., Moyret-Lalle, C., Bensaad, K., Courtois, S., Wang, Q., Soussi, T. and Puisieux, A. (2002) The human BTG2/TIS21/PC3 gene: genomic structure, transcriptional regulation and evaluation as a candidate tumor suppressor gene. *Gene*, **282**, 207-214.

Edgell, C.-J.S., McDonald, C.C. and Graham, J.B. (1983) Permanent cell line expressing human factor VIII-related antigen established by hybridization. *Proc. Natl. Acad. Sci. USA*, **80**, 3734-3737.

el-Deiry, W.S., Kern, S.E., Pietenpol, J.A., Kinzler, K.W. and Vogelstein, B. (1992) Definition of a consensus binding site for p53. *Nat Genet*, **1**, 45-49.

Embree-Ku, M., Venturini, D. and Boekelheide, K. (2002) Fas is involved in the p53-dependent apoptotic response to ionizing radiation in mouse testis. *Biol Reprod*, **66**, 1456-1461.

Fei, P., Bernhard, E.J. and El-Deiry, W.S. (2002) Tissue-specific induction of p53 targets in vivo. *Cancer Res*, **62**, 7316-7327.

Fei, P. and El-Deiry, W.S. (2003) P53 and radiation responses. *Oncogene*, **22**, 5774-5783.

Folkman, J. (1971) Tumor angiogenesis: therapeutic implications. *N.Engl.J Med.*, **285**, 1182-1186.

Folkman, J. (2001) Angiogenesis. In Braunwald, E., Fauci, A., Kasper, D., Hauser, S., Longo, D. and Jameson, J. (eds.), *Harrison's Textbook of Internal Medicine*. McGraw-Hill, pp. 517-530.

Folkman, J. and Camphausen, K. (2001) Cancer. What does radiotherapy do to endothelial cells? *Science*, **293**, 227-228.

Gault, N., Vozenin-Brotons, M.C., Calenda, A., Lefaix, J.L. and Martin, M.T. (2002) Promoter sequences involved in transforming growth factor beta1 gene induction in HaCaT keratinocytes after gamma irradiation. *Radiat Res*, **157**, 249-255.

Gerber, H.P., Condorelli, F., Park, J. and Ferrara, N. (1997) Differential transcriptional regulation of the two vascular endothelial growth factor receptor genes. Flt-1, but not Flk-1/KDR, is up-regulated by hypoxia. *J Biol Chem*, **272**, 23659-23667.

Gong, B. and Almasan, A. (2000) Apo2 ligand/TNF-related apoptosis-inducing ligand and death receptor 5 mediate the apoptotic signaling induced by ionizing radiation in leukemic cells. *Cancer Res*, **60**, 5754-5760.

Gorski, D.H., Beckett, M.A., Jaskowiak, N.T., Calvin, D.A., Mauceri, H.J., Salloum, R.M., Seetharam, S., Koons, A., Hari, D.M., Kufe, D. and Weichselbaum, R.R. (1999) Blockade of the Vascular Endothelial Growth Factor Stress Response Increases the Antitumor Effects of Ionizing Radiation. *Cancer Research*, **59**, 3374-3378.

Gorski, D.H., Mauceri, H.J., Salloum, R.M., Gately, S., Hellman, S., Beckett, M.A., Sukhatme, V.P., Soff, G.A., Kufe, D.W. and Weichselbaum, R.R. (1998) Potentiation of the antitumor effect of ionizing radiation by brief concomitant exposures to angiostatin. *Cancer Res*, **58**, 5686-5689.

Graubert, M.D., Ortega, M.A., Kessel, B., Mortola, J.F. and Iruela-Arispe, M.L. (2001) Vascular repair after menstruation involves regulation of vascular endothelial growth factor-receptor phosphorylation by sFLT-1. *Am J Pathol*, **158**, 1399-1410.

Greenblatt, M.S., Bennett, W.P., Hollstein, M. and Harris, C.C. (1994) Mutations in the p53 tumor suppressor gene: clues to cancer etiology and molecular pathogenesis. *Cancer Res*, **54**, 4855-4878.

Groth, A., Lukas, J., Nigg, E.A., Sillje, H.H., Wernstedt, C., Bartek, J. and Hansen, K. (2003) Human Tousled like kinases are targeted by an ATM- and Chk1-dependent DNA damage checkpoint. *Embo J*, **22**, 1676-1687.

Guehenneux, F., Duret, L., Callanan, M.B., Bouhas, R., Hayette, S., Berthet, C., Samarut, C., Rimokh, R., Birot, A.M., Wang, Q., Magaud, J.P. and Rouault, J.P. (1997) Cloning of the mouse BTG3 gene and definition of a new gene family (the BTG family) involved in the negative control of the cell cycle. *Leukemia*, **11**, 370-375.

Guo, G., Wang, T., Gao, Q., Tamae, D., Wong, P., Chen, T., Chen, W.C., Shively, J.E., Wong, J.Y. and Li, J.J. (2004) Expression of ErbB2 enhances radiation-induced NF-kappaB activation. *Oncogene*, **23**, 535-545.

Gupta, V.K., Jaskowiak, N.T., Beckett, M.A., Mauceri, H.J., Grunstein, J., Johnson, R.S., Calvin, D.A., Nodzenski, E., Pejovic, M., Kufe, D.W., Posner, M.C. and Weichselbaum, R.R. (2002) Vascular endothelial growth factor enhances endothelial cell survival and tumor radioresistance. *Cancer J*, **8**, 47-54.

Hagedorn, M. and Bikfalvi, A. (2000) Target molecules for anti-angiogenic therapy: from basic research to clinical trials. *Critical Reviews in Oncology/Hematology*, **34**, 89-110.

Haimovitz-Friedman, A., Kan, C.C., Ehleiter, D., Persaud, R.S., McLoughlin, M., Fuks, Z. and Kolesnick, R.N. (1994) Ionizing radiation acts on cellular membranes to generate ceramide and initiate apoptosis. *J Exp Med*, **180**, 525-535.

Halin, C., Rondini, S., Nilsson, F., Berndt, A., Kosmehl, H., Zardi, L. and Neri, D. (2002) Enhancement of the antitumor activity of interleukin-12 by targeted delivery to neovasculature. *Nature biotechnology*, **20**, 264-269.

Hall, E.J. (1994) Molecular biology in radiation therapy: the potential impact of recombinant technology on clinical practice. *Int J Radiat Oncol Biol Phys*, **30**, 1019-1028.

Hallahan, D.E., Chen, A.Y., Teng, M. and Cmelak, A.J. (1999) Drug-radiation interactions in tumor blood vessels. *Oncology (Williston Park)*, **13**, 71-77.

Hallahan, D.E., Dunphy, E., Kuchibhotla, J., Kraft, A., Unlap, T. and Weichselbaum, R.R. (1996) Prolonged c-jun expression in irradiated ataxia telangiectasia fibroblasts. *Int J Radiat Oncol Biol Phys*, **36**, 355-360.

Hallahan, D.E., Sukhatme, V.P., Sherman, M.L., Virudachalam, S., Kufe, D. and Weichselbaum, R.R. (1991) Protein kinase C mediates x-ray inducibility of nuclear signal transducers EGR1 and JUN. *Proc Natl Acad Sci U S A*, **88**, 2156-2160.

Hanahan, D. and Folkman, J. (1996) Patterns and emerging mechanisms of the angiogenic switch during tumorigenesis. *Cell*, **86**, 353-364.

Hari, D., Beckett, M.A., Sukhatme, V.P., Dhanabal, M., Nodzenski, E., Lu, H., Mauceri, H.J., Kufe, D.W. and Weichselbaum, R.R. (2000) Angiostatin induces mitotic cell death of proliferating endothelial cells. *Mol Cell Biol Res Commun*, **3**, 277-282.

Haupt, S., Berger, M., Goldberg, Z. and Haupt, Y. (2003) Apoptosis - the p53 network. *J Cell Sci*, **116**, 4077-4085.

Heinloth, A.N., Shackelford, R.E., Innes, C.L., Bennett, L., Li, L., Amin, R.P., Sieber, S.O., Flores, K.G., Bushel, P.R. and Paules, R.S. (2003a) ATM-dependent and -independent gene expression changes in response to oxidative stress, gamma irradiation, and UV irradiation. *Radiat Res*, **160**, 273-290.

Heinloth, A.N., Shackelford, R.E., Innes, C.L., Bennett, L., Li, L., Amin, R.P., Sieber, S.O., Flores, K.G., Bushel, P.R. and Paules, R.S. (2003b) Identification of distinct and common gene expression changes after oxidative stress and gamma and ultraviolet radiation. *Mol Carcinog*, **37**, 65-82.

Helmlinger, G., Dellian, M. and Jain, R.K. (1997) Interstitial pH and pO2 gradients in solid tumors in vivo: high-resolution measurements reveal a lack of correlation. *Nat Med.*, **3**, 177-182.

Hengartner, M.O. (2000) The biochemistry of apoptosis. *Nature*, **407**, 770-776.

Hermeking, H., Lengauer, C., Polyak, K., He, T.C., Zhang, L., Thiagalingam, S., Kinzler, K.W. and Vogelstein, B. (1997) 14-3-3 sigma is a p53-regulated inhibitor of G2/M progression. *Mol Cell*, **1**, 3-11.

Hirao, A., Cheung, A., Duncan, G., Girard, P.M., Elia, A.J., Wakeham, A., Okada, H., Sarkissian, T., Wong, J.A., Sakai, T., De Stanchina, E., Bristow, R.G., Suda, T., Lowe, S.W., Jeggo, P.A., Elledge, S.J. and Mak, T.W. (2002) Chk2 is a tumor suppressor that regulates apoptosis in both an ataxia telangiectasia mutated (ATM)-dependent and an ATM-independent manner. *Mol Cell Biol*, **22**, 6521-6532.

Holmgren, L., O'Reilly, M.S. and Folkman, J. (1995) Dormancy of micrometastases: balanced proliferation and apoptosis in the presence of angiogenesis suppression. *Nat Med*, **1**, 149-153.

Honda, N., Yagi, K., Ding, G.R. and Miyakoshi, J. (2002) Radiosensitization by overexpression of the nonphosphorylation form of IkappaB-alpha in human glioma cells. *J Radiat Res (Tokyo)*, **43**, 283-292.

Hurtado, J.C., Kim, Y.J. and Kwon, B.S. (1997) Signals through 4-1BB are costimulatory to previously activated splenic T cells and inhibit activation-induced cell death. *J Immunol*, **158**, 2600-2609.

Iliakis, G., Wang, Y., Guan, J. and Wang, H. (2003) DNA damage checkpoint control in cells exposed to ionizing radiation. *Oncogene*, **22**, 5834-5847.

Jen, K.Y. and Cheung, V.G. (2003) Transcriptional response of lymphoblastoid cells to ionizing radiation. *Genome Res*, **13**, 2092-2100.

Ji, C., Casinghino, S., McCarthy, T.L. and Centrella, M. (1996) Cloning, characterization, and expression of the transforming growth factor-beta type I receptor promoter in fetal rat bone cells. *J Cell Biochem*, **63**, 478-490.

Jung, M. and Dritschilo, A. (2001) NF-kappa B signaling pathway as a target for human tumor radiosensitization. *Semin Radiat Oncol*, **11**, 346-351.

Jung, M., Kondratyev, A., Lee, S.A., Dimtchev, A. and Dritschilo, A. (1997) ATM gene product phosphorylates I kappa B-alpha. *Cancer Res*, **57**, 24-27.

Jung, M., Zhang, Y., Lee, S. and Dritschilo, A. (1995) Correction of radiation sensitivity in ataxia telangiectasia cells by a truncated I kappa B-alpha. *Science*, **268**, 1619-1621.

Karin, M. (1995) The regulation of AP-1 activity by mitogen-activated protein kinases. *J Biol Chem*, **270**, 16483-16486.

Karin, M. and Ben-Neriah, Y. (2000) Phosphorylation meets ubiquitination: the control of NF-[kappa]B activity. *Annu Rev Immunol*, **18**, 621-663.

Karreman, C. (1998) A new set of positive/negative selectable markers for mammalian cells. *Gene*, **218**, 57-61.

Kastan, M.B. (2001) Cell cycle. Checking two steps. *Nature*, **410**, 766-767.

Kastan, M.B., Onyekwere, O., Sidransky, D., Vogelstein, B. and Craig, R.W. (1991) Participation of p53 protein in the cellular response to DNA damage. *Cancer Res*, **51**, 6304-6311.

Kerbel, R.S. (2001) Clinical Trials of Antiangiogenic Drugs: Opportunities, Problems, and Assessment of Initial Results. *Journal of Clinical Oncology*, **19**, 45-51.

Keshet, E. and Ben-Sasson, S.A. (1999) Anticancer drug targets: approaching angiogenesis. *The Journal of Clinical Investigation*, **104**, 1497-1501.

Khosravi, R., Maya, R., Gottlieb, T., Oren, M., Shiloh, Y. and Shkedy, D. (1999) Rapid ATM-dependent phosphorylation of MDM2 precedes p53 accumulation in response to DNA damage. *Proc Natl Acad Sci U S A*, **96**, 14973-14977.

Kim, J.O., Kim, H.W., Baek, K.M. and Kang, C.Y. (2003) NF-kappaB and AP-1 regulate activation-dependent CD137 (4-1BB) expression in T cells. *FEBS Lett*, **541**, 163-170.

Kim, K.M., Kim, H.W., Kim, J.O., Baek, K.M., Kim, J.G. and Kang, C.Y. (2002) Induction of 4-1BB (CD137) expression by DNA damaging agents in human T lymphocytes. *Immunology*, **107**, 472-479.

Kim, M.R., Lee, J.Y., Park, M.T., Chun, Y.J., Jang, Y.J., Kang, C.M., Kim, H.S., Cho, C.K., Lee, Y.S., Jeong, H.Y. and Lee, S.J. (2001) Ionizing radiation can overcome resistance to TRAIL in TRAIL-resistant cancer cells. *FEBS Lett*, **505**, 179-184.

Kim, S.H., Han, S.Y., Azam, T., Yoon, D.Y. and Dinarello, C.A. (2005) Interleukin-32: a cytokine and inducer of TNFalpha. *Immunity*, **22**, 131-142.

Kim, S.H., Kim, J.H. and Djordjevic, B. (1970) Effects of X-irradiation on RNA and protein synthesis in HeLa cells. *Radiat Res*, **42**, 577-589.

Kozin, S.V., Boucher, Y., Hicklin, D.J., Bohlen, P., Jain, R.K. and Suit, H.D. (2001) Vascular endothelial growth factor receptor-2-blocking antibody potentiates radiation-induced long-term control of human tumor xenografts. *Cancer Res*, **61**, 39-44.

Kunimoto, B.T. (1999) Growth factors in wound healing: the next great innovation? *Ostomy Wound Manage*, **45**, 56-64; quiz 65-56.

Kyriakis, J.M. and Avruch, J. (1996) Protein kinase cascades activated by stress and inflammatory cytokines. *Bioessays*, **18**, 567-577.

Lane, D.P. (1992) Cancer. p53, guardian of the genome. *Nature*, **358**, 15-16.

Lee, C.G., Heijn, M., di Tomaso, E., Griffon-Etienne, G., Ancukiewicz, M., Koike, C., Park, K.R., Ferrara, N., Jain, R.K., Suit, H.D. and Boucher, Y. (2000) Anti-Vascular endothelial growth factor treatment augments tumor radiation response under normoxic or hypoxic conditions. *Cancer Res*, **60**, 5565-5570.

Lee, F.S., Hagler, J., Chen, Z.J. and Maniatis, T. (1997) Activation of the IkappaB alpha kinase complex by MEKK1, a kinase of the JNK pathway. *Cell*, **88**, 213-222.

Lee, S.J., Dimtchev, A., Lavin, M.F., Dritschilo, A. and Jung, M. (1998) A novel ionizing radiation-induced signaling pathway that activates the transcription factor NF-kappaB. *Oncogene*, **17**, 1821-1826.

Lee, W., Haslinger, A., Karin, M. and Tjian, R. (1987) Activation of transcription by two factors that bind promoter and enhancer sequences of the human metallothionein gene and SV40. *Nature*, **325**, 368-372.

Li, N. and Karin, M. (1998) Ionizing radiation and short wavelength UV activate NF-kappaB through two distinct mechanisms. *Proc Natl Acad Sci U S A*, **95**, 13012-13017.

Li, Z., Xia, L., Lee, L.M., Khaletskiy, A., Wang, J., Wong, J.Y. and Li, J.J. (2001) Effector genes altered in MCF-7 human breast cancer cells after exposure to fractionated ionizing radiation. *Radiat Res*, **155**, 543-553.

Liu, Q., Guntuku, S., Cui, X.S., Matsuoka, S., Cortez, D., Tamai, K., Luo, G., Carattini-Rivera, S., DeMayo, F., Bradley, A., Donehower, L.A. and Elledge, S.J. (2000) Chk1 is an essential kinase that is regulated by Atr and required for the G(2)/M DNA damage checkpoint. *Genes Dev*, **14**, 1448-1459.

Lu, Y. and Settleman, J. (1999) The Drosophila Pkn protein kinase is a Rho/Rac effector target required for dorsal closure during embryogenesis. *Genes Dev*, **13**, 1168-1180.

Magne, N., Didelot, C., Toillon, R.A., Van Houtte, P. and Peyron, J.F. (2004) [Biomodulation of transcriptional factor NF-kappa B by ionizing radiation]. *Cancer Radiother*, **8**, 315-321.

Marini, P., Schmid, A., Jendrossek, V., Faltin, H., Daniel, P.T., Budach, W. and Belka, C. (2005) Irradiation specifically sensitises solid tumour cell lines to TRAIL mediated apoptosis. *BMC Cancer*, **5**, 5.

Marko, N.F., Dieffenbach, P.B., Yan, G., Ceryak, S., Howell, R.W., McCaffrey, T.A. and Hu, V.W. (2003) Does metabolic radiolabeling stimulate the stress response? Gene expression profiling reveals differential cellular responses to internal beta vs. external gamma radiation. *Faseb J*, **17**, 1470-1486.

Marples, B., Scott, S.D., Hendry, J.H., Embleton, M.J., Lashford, L.S. and Margison, G.P. (2000) Development of synthetic promoters for radiation-mediated gene therapy. *Gene Ther*, **7**, 511-517.

Martin, M., Vozenin, M.C., Gault, N., Crechet, F., Pfarr, C.M. and Lefaix, J.L. (1997) Coactivation of AP-1 activity and TGF-beta1 gene expression in the stress response of normal skin cells to ionizing radiation. *Oncogene*, **15**, 981-989.

Matsuda, S., Kawamura-Tsuzuku, J., Ohsugi, M., Yoshida, M., Emi, M., Nakamura, Y., Onda, M., Yoshida, Y., Nishiyama, A. and Yamamoto, T. (1996) Tob, a novel protein that interacts with p185erbB2, is associated with anti-proliferative activity. *Oncogene*, **12**, 705-713.

Matsuoka, S., Huang, M. and Elledge, S.J. (1998) Linkage of ATM to cell cycle regulation by the Chk2 protein kinase. *Science*, **282**, 1893-1897.

Matsuoka, S., Rotman, G., Ogawa, A., Shiloh, Y., Tamai, K. and Elledge, S.J. (2000) Ataxia telangiectasia-mutated phosphorylates Chk2 in vivo and in vitro. *Proc Natl Acad Sci U S A*, **97**, 10389-10394.

Mauceri, H.J., Hanna, N.N., Beckett, M.A., Gorski, D.H., Staba, M.J., Stellato, K.A., Bigelow, K., Heimann, R., Gately, S., Dhanabal, M., Soff, G.A., Sukhatme, V.P., Kufe, D.W. and Weichselbaum, R.R. (1998) Combined effects of angiostatin and ionizing radiation in antitumour therapy. *Nature*, **394**, 287-291.

Mauceri, H.J., Hanna, N.N., Wayne, J.D., Hallahan, D.E., Hellman, S. and Weichselbaum, R.R. (1996) Tumor necrosis factor alpha (TNF-alpha) gene therapy targeted by ionizing radiation selectively damages tumor vasculature. *Cancer Res*, **56**, 4311-4314.

Maya, R., Balass, M., Kim, S.T., Shkedy, D., Leal, J.F., Shifman, O., Moas, M., Buschmann, T., Ronai, Z., Shiloh, Y., Kastan, M.B., Katzir, E. and Oren, M. (2001) ATM-dependent phosphorylation of Mdm2 on serine 395: role in p53 activation by DNA damage. *Genes Dev*, **15**, 1067-1077.

McGowan, C.H. (2002) Checking in on Cds1 (Chk2): A checkpoint kinase and tumor suppressor. *Bioessays*, **24**, 502-511.

Mendelsohn, J. and Baselga, J. (2000) The EGF receptor family as targets for cancer therapy. *Oncogene*, **19**, 6550-6565.

Meyer, R.G., Kupper, J.H., Kandolf, R. and Rodemann, H.P. (2002) Early growth response-1 gene (Egr-1) promoter induction by ionizing radiation in U87 malignant glioma cells in vitro. *Eur J Biochem*, **269**, 337-346.

Minet, E., Michel, G., Mottet, D., Piret, J.P., Barbieux, A., Raes, M. and Michiels, C. (2001) c-JUN gene induction and AP-1 activity is regulated by a JNK-dependent pathway in hypoxic HepG2 cells. *Exp Cell Res*, **265**, 114-124.

Mohan, N. and Meltz, M.L. (1994) Induction of nuclear factor kappa B after low-dose ionizing radiation involves a reactive oxygen intermediate signaling pathway. *Radiat Res*, **140**, 97-104.

Nakano, K. and Vousden, K.H. (2001) PUMA, a novel proapoptotic gene, is induced by p53. *Mol Cell*, **7**, 683-694.

Nemoto, S., DiDonato, J.A. and Lin, A. (1998) Coordinate regulation of IkappaB kinases by mitogen-activated protein kinase kinase kinase 1 and NF-kappaB-inducing kinase. *Mol Cell Biol*, **18**, 7336-7343.

Oda, K., Arakawa, H., Tanaka, T., Matsuda, K., Tanikawa, C., Mori, T., Nishimori, H., Tamai, K., Tokino, T., Nakamura, Y. and Taya, Y. (2000) p53AIP1, a potential mediator of p53-dependent apoptosis, and its regulation by Ser-46-phosphorylated p53. *Cell*, **102**, 849-862.

Offer, H., Erez, N., Zurer, I., Tang, X., Milyavsky, M., Goldfinger, N. and Rotter, V. (2002) The onset of p53-dependent DNA repair or apoptosis is determined by the level of accumulated damaged DNA. *Carcinogenesis*, **23**, 1025-1032.

O'Reilly, M.S., Holmgren, L., Chen, C. and Folkman, J. (1996) Angiostatin induces and sustains dormancy of human primary tumors in mice. *Nat Med.*, **2**, 689-692.

Oren, M., Damalas, A., Gottlieb, T., Michael, D., Taplick, J., Leal, J.F., Maya, R., Moas, M., Seger, R., Taya, Y. and Ben-Ze'Ev, A. (2002) Regulation of p53: intricate loops and delicate balances. *Ann N Y Acad Sci*, **973**, 374-383.

Owen-Schaub, L.B., Zhang, W., Cusack, J.C., Angelo, L.S., Santee, S.M., Fujiwara, T., Roth, J.A., Deisseroth, A.B., Zhang, W.W., Kruzel, E. and et al. (1995) Wild-type human p53 and a temperature-sensitive mutant induce Fas/APO-1 expression. *Mol Cell Biol*, **15**, 3032-3040.

Painter, R.B. and Young, B.R. (1980) Radiosensitivity in ataxia-telangiectasia: a new explanation. *Proc Natl Acad Sci U S A*, **77**, 7315-7317.

Park, J.S., Qiao, L., Su, Z.Z., Hinman, D., Willoughby, K., McKinstry, R., Yacoub, A., Duigou, G.J., Young, C.S., Grant, S., Hagan, M.P., Ellis, E., Fisher, P.B. and Dent, P. (2001) Ionizing radiation modulates vascular endothelial growth factor (VEGF) expression through multiple mitogen activated protein kinase dependent pathways. *Oncogene*, **20**, 3266-3280.

Prasad, A.V., Mohan, N., Chandrasekar, B. and Meltz, M.L. (1994) Activation of nuclear factor kappa B in human lymphoblastoid cells by low-dose ionizing radiation. *Radiat Res*, **138**, 367-372.

Raju, U., Gumin, G.J. and Tofilon, P.J. (1999) NF kappa B activity and target gene expression in the rat brain after one and two exposures to ionizing radiation. *Radiat Oncol Investig*, **7**, 145-152.

Reap, E.A., Roof, K., Maynor, K., Borrero, M., Booker, J. and Cohen, P.L. (1997) Radiation and stress-induced apoptosis: a role for Fas/Fas ligand interactions. *Proc Natl Acad Sci U S A*, **94**, 5750-5755.

Risau, W. (1997) Mechanisms of angiogenesis. *Nature*, **386**, 671-674.

Robles, A.I., Bemmels, N.A., Foraker, A.B. and Harris, C.C. (2001) *APAF-1* Is a Transcriptional Target of p53 in DNA Damage-induced Apoptosis. *Cancer Research*, **61**, 6660-6664.

Rouault, J.P., Falette, N., Guehenneux, F., Guillot, C., Rimokh, R., Wang, Q., Berthet, C., Moyret-Lalle, C., Savatier, P., Pain, B., Shaw, P., Berger, R., Samarut, J., Magaud, J.P., Ozturk, M., Samarut, C. and Puisieux, A. (1996) Identification of BTG2, an antiproliferative p53-dependent component of the DNA damage cellular response pathway. *Nat Genet*, **14**, 482-486.

Rouault, J.P., Rimokh, R., Tessa, C., Paranhos, G., Ffrench, M., Duret, L., Garoccio, M., Germain, D., Samarut, J. and Magaud, J.P. (1992) BTG1, a member of a new family of antiproliferative genes. *Embo J*, **11**, 1663-1670.

Russell, J.S. and Tofilon, P.J. (2002) Radiation-induced activation of nuclear factor-kappaB involves selective degradation of plasma membrane-associated I(kappa)B(alpha). *Mol Biol Cell*, **13**, 3431-3440.

Sahijdak, W.M., Yang, C.R., Zuckerman, J.S., Meyers, M. and Boothman, D.A. (1994) Alterations in transcription factor binding in radioresistant human melanoma cells after ionizing radiation. *Radiat Res*, **138**, S47-51.

Sanchez, Y., Wong, C., Thoma, R.S., Richman, R., Wu, Z., Piwnica-Worms, H. and Elledge, S.J. (1997) Conservation of the Chk1 checkpoint pathway in mammals: linkage of DNA damage to Cdk regulation through Cdc25. *Science*, **277**, 1497-1501.

Santana, P., Pena, L.A., Haimovitz-Friedman, A., Martin, S., Green, D., McLoughlin, M., Cordon-Cardo, C., Schuchman, E.H., Fuks, Z. and Kolesnick, R. (1996) Acid sphingomyelinase-deficient human lymphoblasts and mice are defective in radiation-induced apoptosis. *Cell*, **86**, 189-199.

Saoulli, K., Lee, S.Y., Cannons, J.L., Yeh, W.C., Santana, A., Goldstein, M.D., Bangia, N., DeBenedette, M.A., Mak, T.W., Choi, Y. and Watts, T.H. (1998) CD28-independent, TRAF2-dependent costimulation of resting T cells by 4-1BB ligand. *J Exp Med*, **187**, 1849-1862.

Schmidt-Ullrich, R.K., Mikkelsen, R.B., Dent, P., Todd, D.G., Valerie, K., Kavanagh, B.D., Contessa, J.N., Rorrer, W.K. and Chen, P.B. (1997) Radiation-induced proliferation of the human A431 squamous carcinoma cells is dependent on EGFR tyrosine phosphorylation. *Oncogene*, **15**, 1191-1197.

Schreck, R., Albermann, K. and Baeuerle, P.A. (1992) Nuclear factor kappa B: an oxidative stress-responsive transcription factor of eukaryotic cells (a review). *Free Radic Res Commun*, **17**, 221-237.

Schwachtgen, J.L., Campbell, C.J. and Braddock, M. (2000) Full promoter sequence of human early growth response factor-1 (Egr-1): demonstration of the fifth functional serum response element. *DNA Seq.*, **10**, 429-432.

Schwarz, H., Blanco, F.J., von Kempis, J., Valbracht, J. and Lotz, M. (1996) ILA, a member of the human nerve growth factor/tumor necrosis factor receptor family, regulates T-lymphocyte proliferation and survival. *Blood*, **87**, 2839-2845.

Scott, S.D., Joiner, M.C. and Marples, B. (2002) Optimizing radiation-responsive gene promoters for radiogenetic cancer therapy. *Gene Ther*, **9**, 1396-1402.

Scott, S.D., Marples, B., Hendry, J.H., Lashford, L.S., Embleton, M.J., Hunter, R.D., Howell, A. and Margison, G.P. (2000) A radiation-controlled molecular switch for use in gene therapy of cancer. *Gene Ther*, **7**, 1121-1125.

Senzer, N., Mani, S., Rosemurgy, A., Nemunaitis, J., Cunningham, C., Guha, C., Bayol, N., Gillen, M., Chu, K., Rasmussen, C., Rasmussen, H., Kufe, D., Weichselbaum, R. and Hanna, N. (2004) TNFerade biologic, an adenovector with a radiation-inducible promoter, carrying the human tumor necrosis factor alpha gene: a phase I study in patients with solid tumors. *J Clin Oncol*, **22**, 592-601.

Sherman, M.L., Datta, R., Hallahan, D.E., Weichselbaum, R.R. and Kufe, D.W. (1990) Ionizing radiation regulates expression of the c-*jun* protooncogene. *Proc. Natl. Acad. Sci. USA*, **87**, 5663-5666.

Shi, W., Teschendorf, C., Muzyczka, N. and Siemann, D.W. (2003) Gene Therapy delivery of endostatin enhances the treatment efficacy of radiation. *Radiotherapy and Oncology*, **66**, 1-9.

Shibue, T., Takeda, K., Oda, E., Tanaka, H., Murasawa, H., Takaoka, A., Morishita, Y., Akira, S., Taniguchi, T. and Tanaka, N. (2003) Integral role of Noxa in p53-mediated apoptotic response. *Genes Dev*, **17**, 2233-2238.

Shieh, S.Y., Ahn, J., Tamai, K., Taya, Y. and Prives, C. (2000) The human homologs of checkpoint kinases Chk1 and Cds1 (Chk2) phosphorylate p53 at multiple DNA damage-inducible sites. *Genes Dev*, **14**, 289-300.

Shieh, S.Y., Taya, Y. and Prives, C. (1999) DNA damage-inducible phosphorylation of p53 at N-terminal sites including a novel site, Ser20, requires tetramerization. *Embo J*, **18**, 1815-1823.

Shweiki, D., Itin, A., Soffer, D. and Keshet, E. (1992) Vascular endothelial growth factor induced by hypoxia may mediate hypoxia-initiated angiogenesis. *Nature*, **359**, 843-845.

Siemann, D.W., Chaplin, D.J. and Horsman, M.R. (2004) Vascular-targeting therapies for treatment of malignant disease. *Cancer*, **100**, 2491-2499.

Siliciano, J.D., Canman, C.E., Taya, Y., Sakaguchi, K., Appella, E. and Kastan, M.B. (1997) DNA damage induces phosphorylation of the amino terminus of p53. *Genes Dev*, **11**, 3471-3481.

Slee, E.A. and Lu, X. (2003) The ASPP family: deciding between life and death after DNA damage. *Toxicol Lett*, **139**, 81-87.

Snyder, A.R. and Morgan, W.F. (2004) Gene expression profiling after irradiation: clues to understanding acute and persistent responses? *Cancer Metastasis Rev*, **23**, 259-268.

Somosy, Z. (2000) Radiation response of cell organelles. *Micron*, **31**, 165-181.

Stassen, T., Port, M., Nuyken, I. and Abend, M. (2003) Radiation-induced gene expression in MCF-7 cells. *Int J Radiat Biol*, **79**, 319-331.

Stewart, Z.A. and Pietenpol, J.A. (2001) p53 Signaling and cell cycle checkpoints. *Chem Res Toxicol*, **14**, 243-263.

Takimoto, R. and El-Deiry, W.S. (2000) Wild-type p53 transactivates the KILLER/DR5 gene through an intronic sequence-specific DNA-binding site. *Oncogene*, **19**, 1735-1743.

Tanner, F.C., Carr, D.P., Nabel, G.J. and Nabel, E.G. (1997) Transfection of human endothelial cells. *Cardiovascular Research*, **35**, 522-528.

Taraboletti, G. and Margosio, B. (2001) Antiangiogenic and antivascular therapy for cancer. *Curr Opin Pharmacol*, **1**, 378-384.

Treisman, R. (1985) Transient accumulation of c-fos RNA following serum stimulation requires a conserved 5' element and c-fos 3' sequences. *Cell*, **42**, 889-902.

Tusher, V.G., Tibshirani, R. and Chu, G. (2001) Significance analysis of microarrays applied to the ionizing radiation response. *Proc Natl Acad Sci U S A*, **98**, 5116-5121.

Ueda, T., Akiyama, N., Sai, H., Oya, N., Noda, M., Hiraoka, M. and Kizaka-Kondoh, S. (2001) c-IAP2 is induced by ionizing radiation through NF-kappaB binding sites. *FEBS Lett*, **491**, 40-44.

Verheij, M., Bose, R., Lin, X.H., Yao, B., Jarvis, W.D., Grant, S., Birrer, M.J., Szabo, E., Zon, L.I., Kyriakis, J.M., Haimovitz-Friedman, A., Fuks, Z. and Kolesnick, R.N. (1996) Requirement for ceramide-initiated SAPK/JNK signalling in stress-induced apoptosis. *Nature*, **380**, 75-79.

Vit, J.P. and Rosselli, F. (2003) Role of the ceramide-signaling pathways in ionizing radiation-induced apoptosis. *Oncogene*, **22**, 8645-8652.

Vogelstein, B., Lane, D. and Levine, A.J. (2000) Surfing the p53 network. *Nature*, **408**, 307-310.

Wachsberger, P., Burd, R. and Dicker, A.P. (2003) Tumor Response to Ionizing Radiation Combined with Antiangiogenesis or Vascular Targeting Agents: Exploring Mechanisms of Interaction. *Clinical Cancer Research*, **9**, 1957-1971.

Wachsberger, P.R., Burd, R., Marero, N., Daskalakis, C., Ryan, A., McCue, P. and Dicker, A.P. (2005) Effect of the tumor vascular-damaging agent, ZD6126, on the radioresponse of U87 glioblastoma. *Clin Cancer Res*, **11**, 835-842.

Waldman, T., Lengauer, C., Kinzler, K.W. and Vogelstein, B. (1996) Uncoupling of S phase and mitosis induced by anticancer agents in cells lacking p21. *Nature*, **381**, 713-716.

Wang, P., Reed, M., Wang, Y., Mayr, G., Stenger, J.E., Anderson, M.E., Schwedes, J.F. and Tegtmeyer, P. (1994) p53 domains: structure, oligomerization, and transformation. *Mol Cell Biol*, **14**, 5182-5191.

Wang, T., Zhang, X. and Li, J.J. (2002) The role of NF-kappaB in the regulation of cell stress responses. *Int Immunopharmacol*, **2**, 1509-1520.

Wang, X.W., Zhan, Q., Coursen, J.D., Khan, M.A., Kontny, H.U., Yu, L., Hollander, M.C., O'Connor, P.M., Fornace, A.J., Jr. and Harris, C.C. (1999) GADD45 induction of a G2/M cell cycle checkpoint. *Proc Natl Acad Sci U S A*, **96**, 3706-3711.

Weichselbaum, R.R., Hallahan, D., Fuks, Z. and Kufe, D. (1994) Radiation induction of immediate early genes: effectors of the radiation-stress response. *Int J Radiat Oncol Biol Phys*, **30**, 229-234.

Weichselbaum, R.R., Kufe, D.W., Hellman, S., Rasmussen, H.S., King, C.R., Fischer, P.H. and Mauceri, H.J. (2002) Radiation-induced tumour necrosis factor-α expression: clinical application of transcriptional and physical targeting of gene therapy. *The Lancet Oncology*, **3**, 665-671.

Witte, L., Fuks, Z., Haimovitz-Friedman, A., Vlodavsky, I., Goodman, D.S. and Eldor, A. (1989) Effects of irradiation on the release of growth factors from cultured bovine, porcine, and human endothelial cells. *Cancer Res*, **49**, 5066-5072.

World Health Organization. (2004) http://www.who.int/cancer/en/.

Wu, G.S., Burns, T.F., McDonald, E.R., 3rd, Jiang, W., Meng, R., Krantz, I.D., Kao, G., Gan, D.D., Zhou, J.Y., Muschel, R., Hamilton, S.R., Spinner, N.B., Markowitz, S., Wu, G. and el-Deiry, W.S. (1997) KILLER/DR5 is a DNA damage-inducible p53-regulated death receptor gene. *Nat Genet*, **17**, 141-143.

Yancopoulos, G.D., Davis, S., Gale, N.W., Rudge, J.S., Wiegand, S.J. and Holash, J. (2000) Vascular-specific growth factors and blood vessel formation. *Nature*, **407**, 242-248.

Zhan, Q., Fan, S., Bae, I., Guillouf, C., Liebermann, D.A., O'Connor, P.M. and Fornace, A.J., Jr. (1994) Induction of bax by genotoxic stress in human cells correlates with normal p53 status and apoptosis. *Oncogene*, **9**, 3743-3751.

Zhao, Q. and Lee, F.S. (1999) Mitogen-activated protein kinase/ERK kinase kinases 2 and 3 activate nuclear factor-kappaB through IkappaB kinase-alpha and IkappaB kinase-beta. *J Biol Chem*, **274**, 8355-8358.

Zhou, B.B. and Bartek, J. (2004) Targeting the checkpoint kinases: chemosensitization versus chemoprotection. *Nat Rev Cancer*, **4**, 216-225.

Zhou, B.B. and Elledge, S.J. (2000) The DNA damage response: putting checkpoints in perspective. *Nature*, **408**, 433-439.

Zundel, W. and Giaccia, A. (1998) Inhibition of the anti-apoptotic PI(3)K/Akt/Bad pathway by stress. *Genes Dev*, **12**, 1941-1946.

ACKNOWLEDGEMENTS

The present research work was realized at the Institute for Medical Radiobiology from Paul Scherrer Institute (PSI, Villigen Switzerland) and at the Institute of Molecular Cancer Research (IMCR, Zurich Switzerland). It was financed by the "Bundessamt für Energiewirtschaft, Hauptabteilung für die Sicherheit der Kernanlagen".
During my PhD experience, I met along the way number of people who helped me in the completion of this work. Today, I would like to address them my profound gratitude.

I would like to gratefully thank Prof. Dr. Josef Jiricny, who gave me the opportunity to start my PhD thesis at PSI and then to have welcomed me in his team at IMCR. I benefited greatly from his expertise and I am very grateful for his continuous support, encouragement, scientific thinking throughout the thesis.

I especially thank PD. Dr. Rolf Jaussi for his supervision and support at PSI, his immense scientific help, and his trust.

I am very grateful to Prof. Dr. Kurt Ballmer-Hofer for advices and for the fruitful scientific discussions regarding the project during the first part of my thesis.

Ma très sincère gratitude s'adresse également aux membres du jury, Prof. Jean-Pierre Cazenave, directeur de thèse, Dr. Pierre Bischoff, rapporteur, qui ont accepté de juger ce travail. My gratitude is also expressed to Dr. Stefano Ferrari for accepting to review my thesis manuscript.

I am grateful to the bioinformaticians and technicians of the Functional Genomics Center Zurich, Ulrich Wagner and Andrea Patrignani for their immense help and advice. Thank you also to Massimiliano Di Pietro and Giancarlo Marra for teaching me all the secrets of cDNA microarray and to Jacob Sabates for sharing his Genespring expertise with me.

I kindly acknowledge Suzanne Fournier for participating to the project works during 5 months and for her great help.

A big thank to all my friends and colleagues in both laboratories for their help and for creating a nice working atmosphere. To Alma, Silvia, Kai, Patrick, Steffen, Stéphanie, Elda, Petr, Lovorka, Nina, Betta, Ludovic, Farah, Milica, Fransiska, Katja, Conni, Carine, Ann, Jasna, Sandie, … and all the people from the long list I don't enumerate here. Thank you all for the non-scientific and scientific advices, for motivating me, for the nice coffee breaks and lunches, lab-events, unforgettable trip to Marseille and everything that helped towards having great time in and outside the institutes.

Un merci du fond du coeur à mes parents, ma famille et mes amis pour leurs encouragements et continuel support moral.

And finally, my very special thank goes to Martin, for your inexhaustible support and patience throughout the thesis, and simply for the time we share together.